Electronic Supplementary Information

Extended cavity pyrene-based iptycenes for the turn-off fluorescence detection of RDX and common nitroaromatic explosives

Albert F. Khasanov,[a] Dmitry S. Kopchuk,[a, b] Igor S. Kovalev,[a] Olga S. Taniya,[a] Kousik Giri,[c] Pavel A. Slepukhin,[a,b] Sougata Santra,*[a] Matiur Rahman,[a] Adinath Majee,[d] Valery N. Charushin[a,b] and Oleg N. Chupakhin[a,b]

[a] *Department of Organic and Biomolecular Chemistry, Chemical Engineering Institute, Ural Federal University, 19 Mira Street, Yekaterinburg, K-2, 620002, Russian Federation. Email: sougatasantra85@gmail.com; ssantra@urfu.ru*

[b] *I. Ya. Postovskiy Institute of Organic Synthesis, Ural Division of the Russian Academy of Sciences, 22 S. Kovalevskoy Str., Yekaterinburg, 620219, Russian Federation*

[c] *Centre for Computational Sciences, School of Basic and Applied Sciences, Central University of Punjab, City Campus, Mansa Road, Bathinda-151001, India*

[d] *Department of Chemistry, Visva-Bharati (A Central University), Santiniketan-731235, India.*

Table of Contents

Chemical structures of fluorophores (2,3,4a,4b,4c)

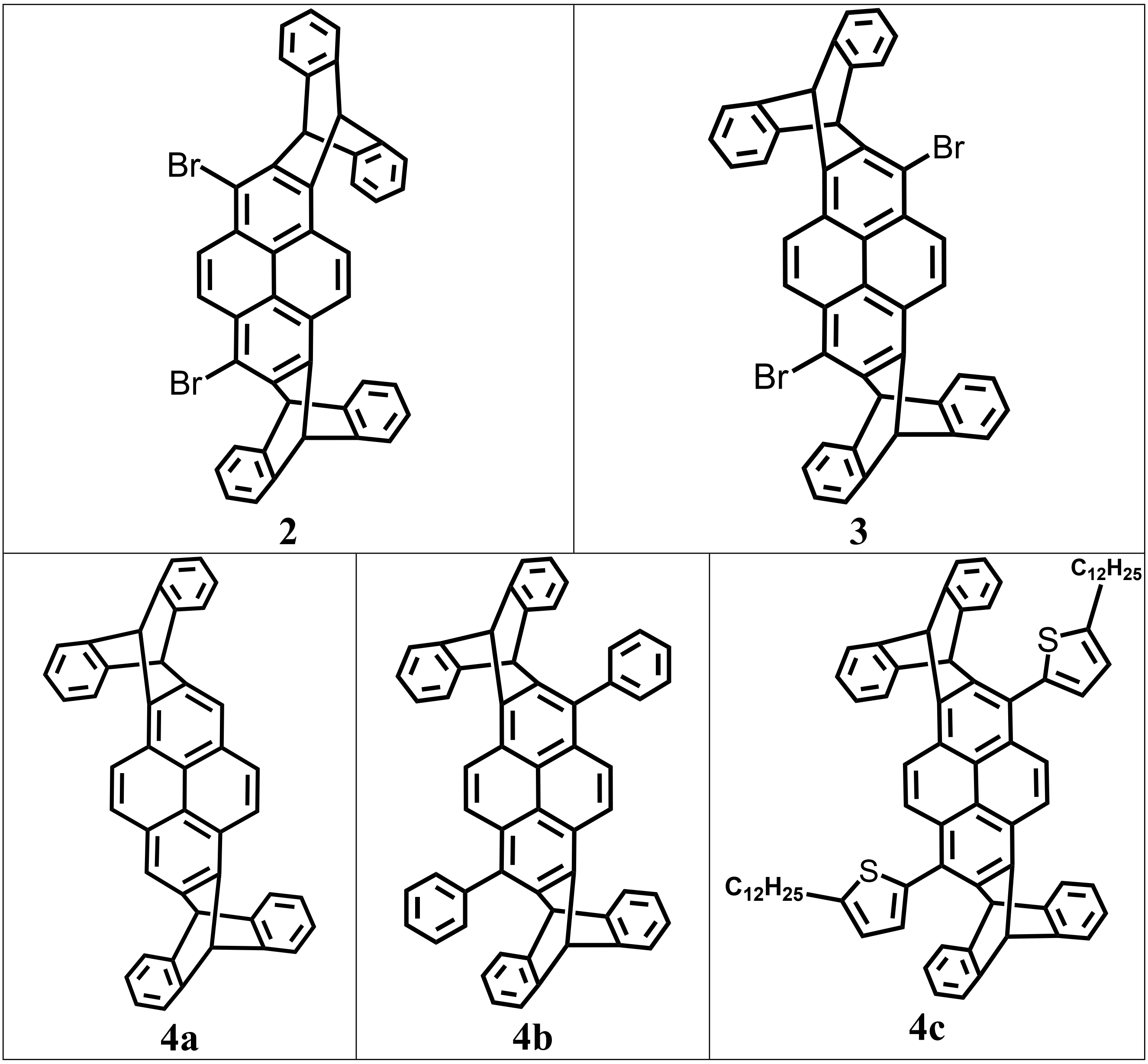

Fig. S1 Chemical structures of fluorophores **(2,3,4a,4b,4c)**

Fluorescence titration experiments

Experiments were carried out by using the Horiba-Fluoromax-4. Solutions of fluorophores were prepared by dissolving the sample in THF.

In a typical titration experiment 1 mL of the solution of sensors (10^{-6} M) were placed in a quartz cell, followed by adding there to 10 aliquots of 0.1 molar equivalent of each analyte (NACs).

The fluorescence emission spectra were measured (298 K) under λ_{ex} = 375 nm. The fluorescent quenching experiments were carried out by means of the titration of solutions (10^{-6} M) of sensors.

There were no changes in the shape of the emission spectrum by gradually putting the initial fluorescence emission during titration nitroaromatic quencher.

Analysis of fluorescence emission intensity ($(I_0/I)-1$), as a function of the concentration of the quencher ([Q]) describes a Stern-Volmer equation

$$I_0/ I = 1 + Ksv [Q].$$

The binding constant was calculated as the slope of the graph.

Compound 2

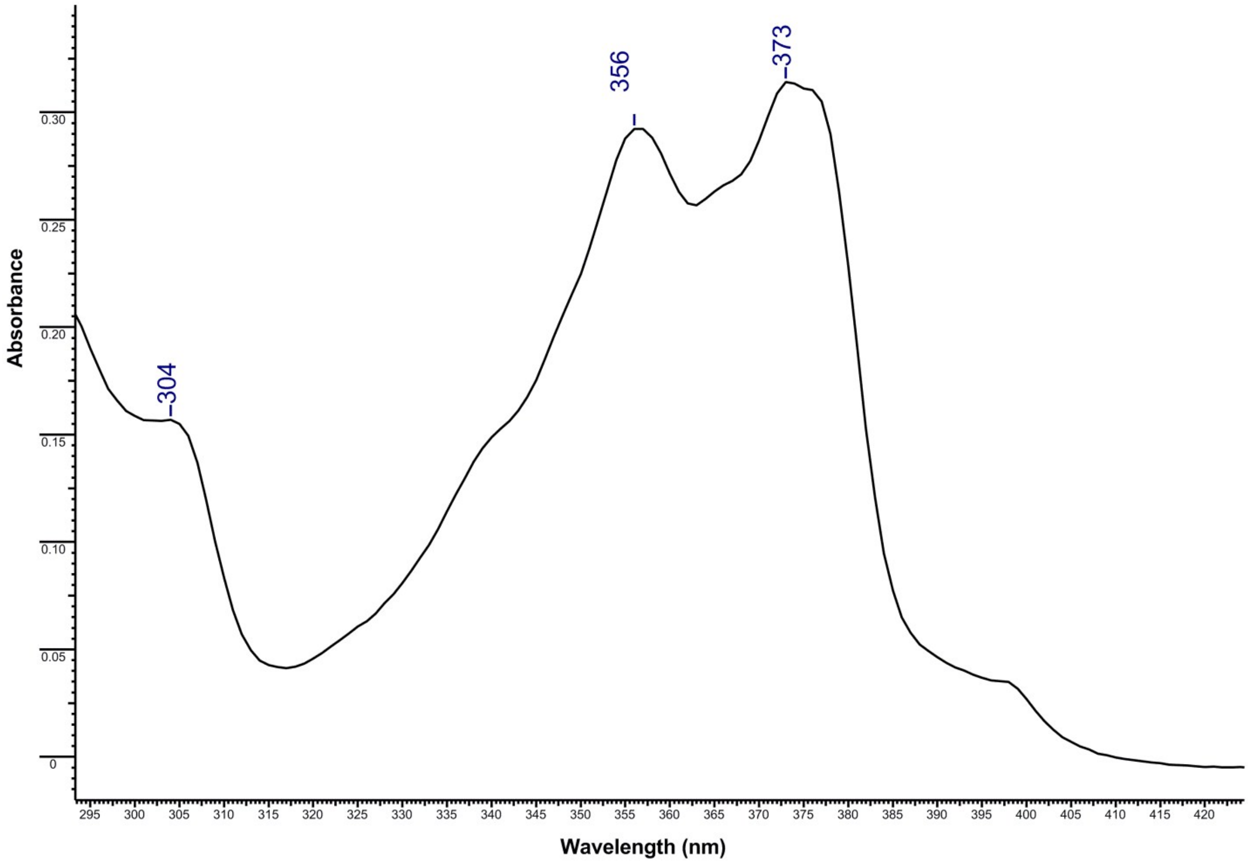

Fig. S2 Electronic absorption spectrum of compound **2**

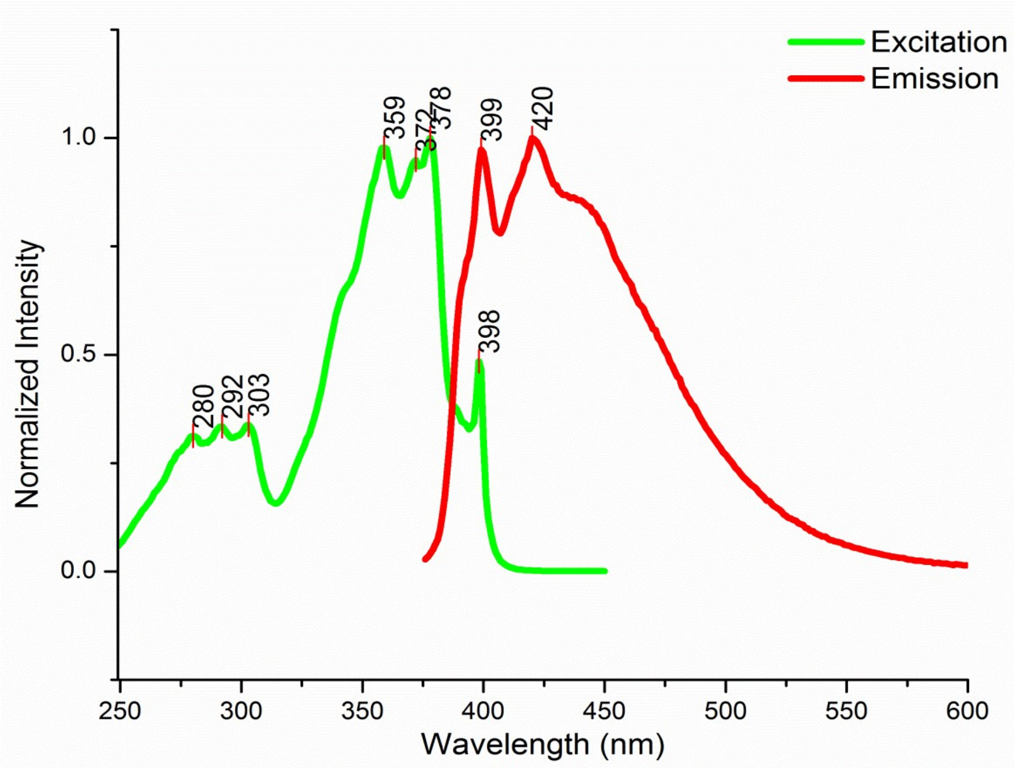

Fig. S3 Fluorescence excitation and emission spectrum of compound **2**

Fluorescence quenching with nitrobenzene (NB) in THF

The fluorescence quenching of the fluorophore **2** (1.0×10^{-5} M) with nitrobenzene (2.0×10^{-2} M) was carried out in THF.

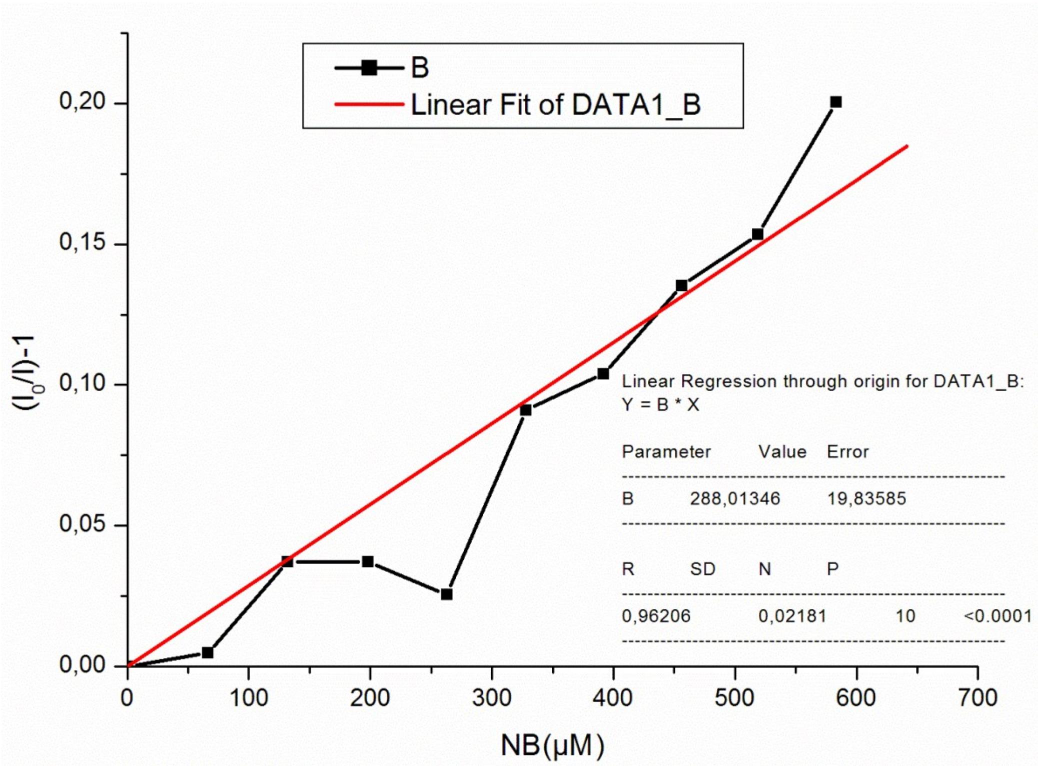

Fig.S4 Stern-Volmer plot

Fluorescence quenching with 2,4-dinitrotoluene (DNT) in THF

The fluorescence quenching of the fluorophore **2** (1.0×10^{-5} M) with 2,4-dinitrotoluene (2.0×10^{-2} M) was carried out in THF.

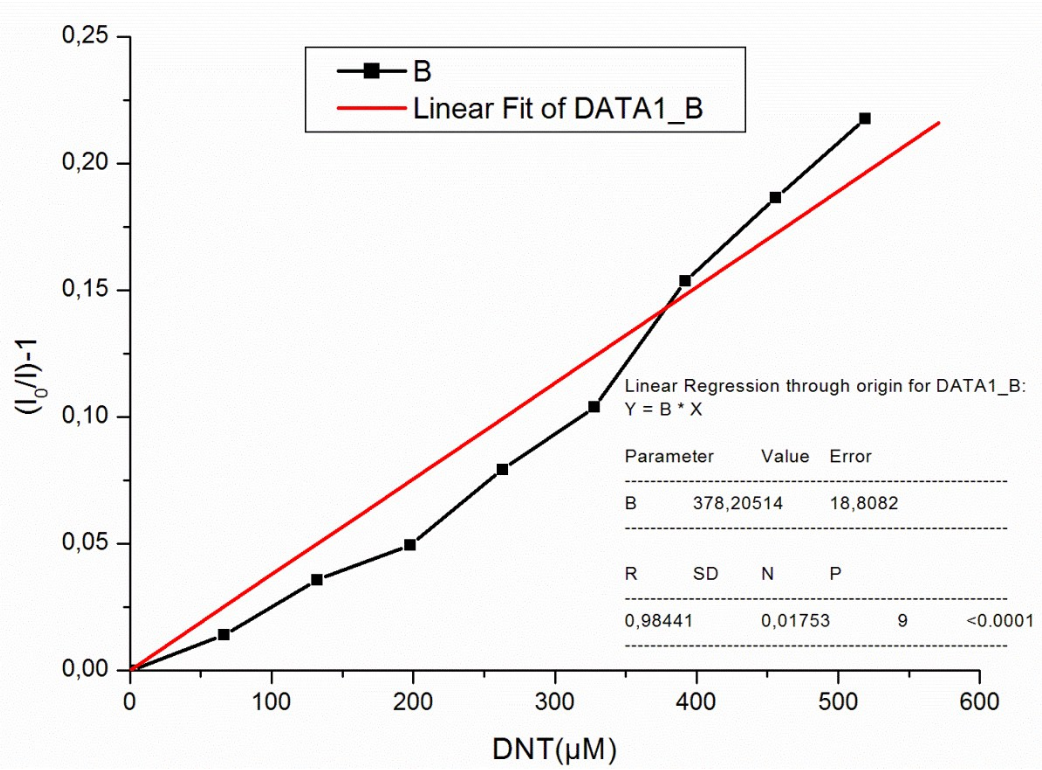

Fig.S5 Stern-Volmer plot

Fluorescence quenching with trinitrotoluene (TNT) in THF

The fluorescence quenching of the fluorophore **2** (1.0×10^{-5} M) with trinitrotoluene (2.0×10^{-2} M) was carried out in THF.

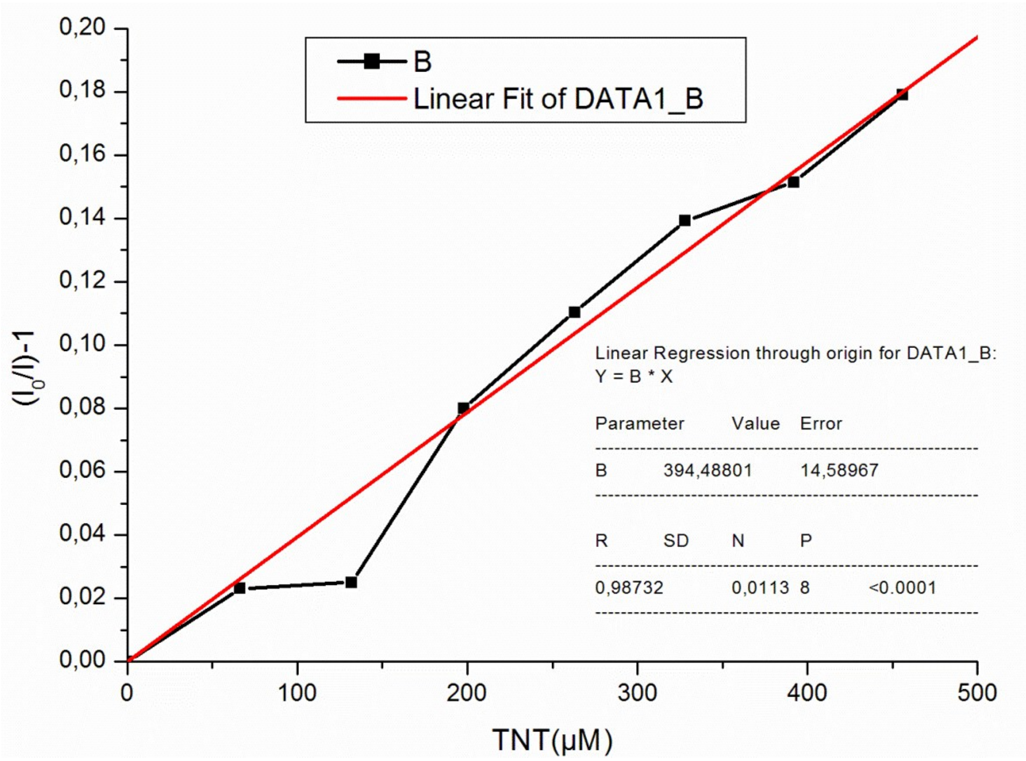

Fig.S6 Stern-Volmer plot

Estimation of the detection limit for sensor 2

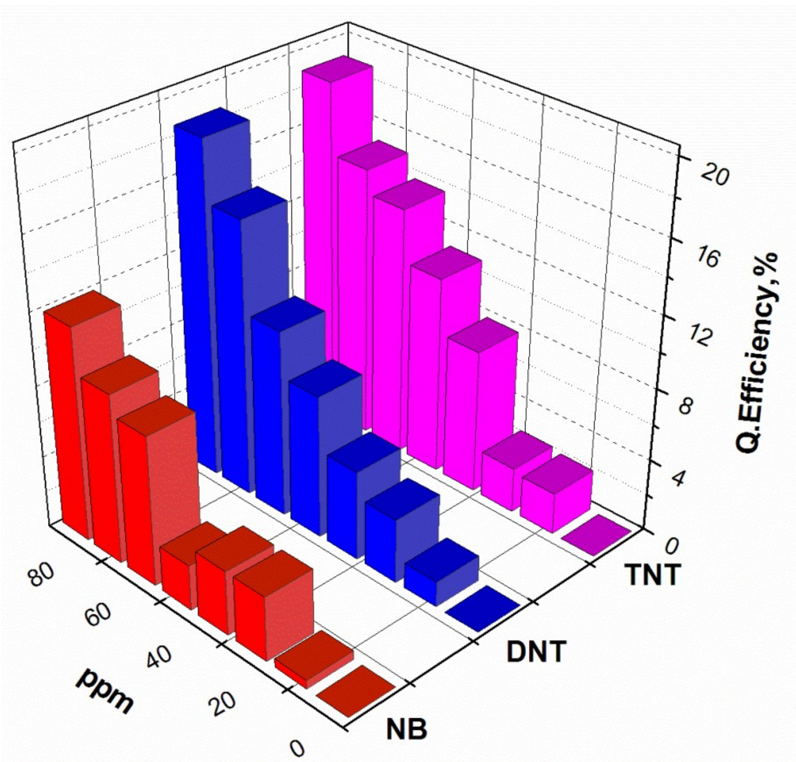

Fig.S7. Estimation of the detection limit for sensor **2**

PLQY

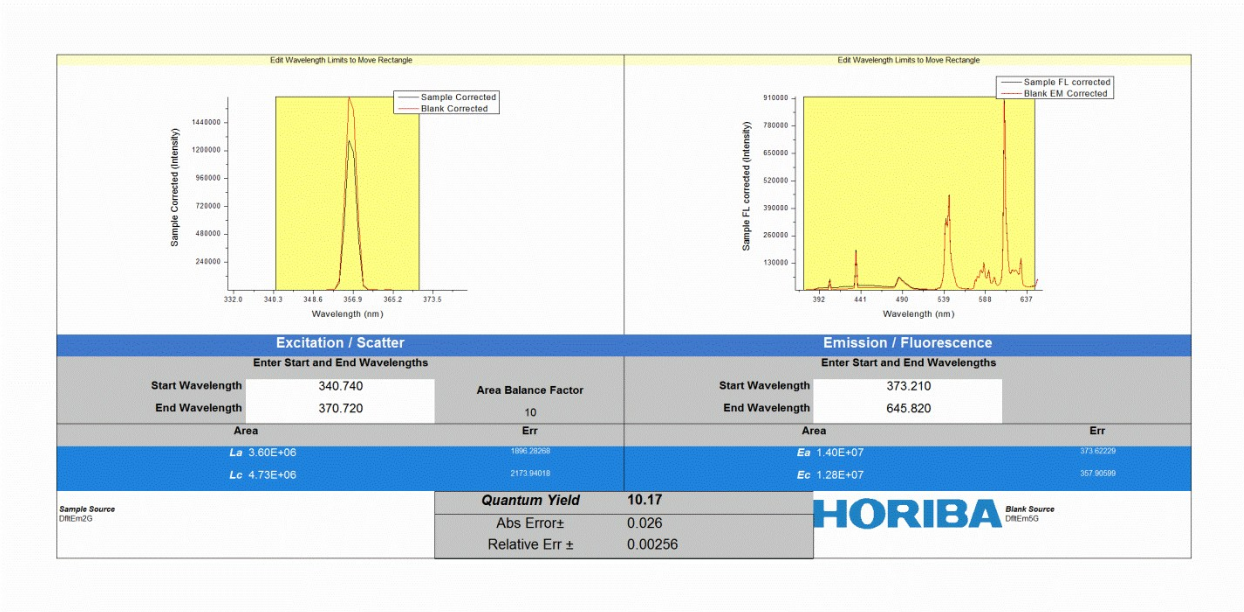

	Ksv (R) in THF
NB	288 (R=0.9621)
DNT	378 (R=0.9844)
TNT	394 (R=0.9873)

Compound 3

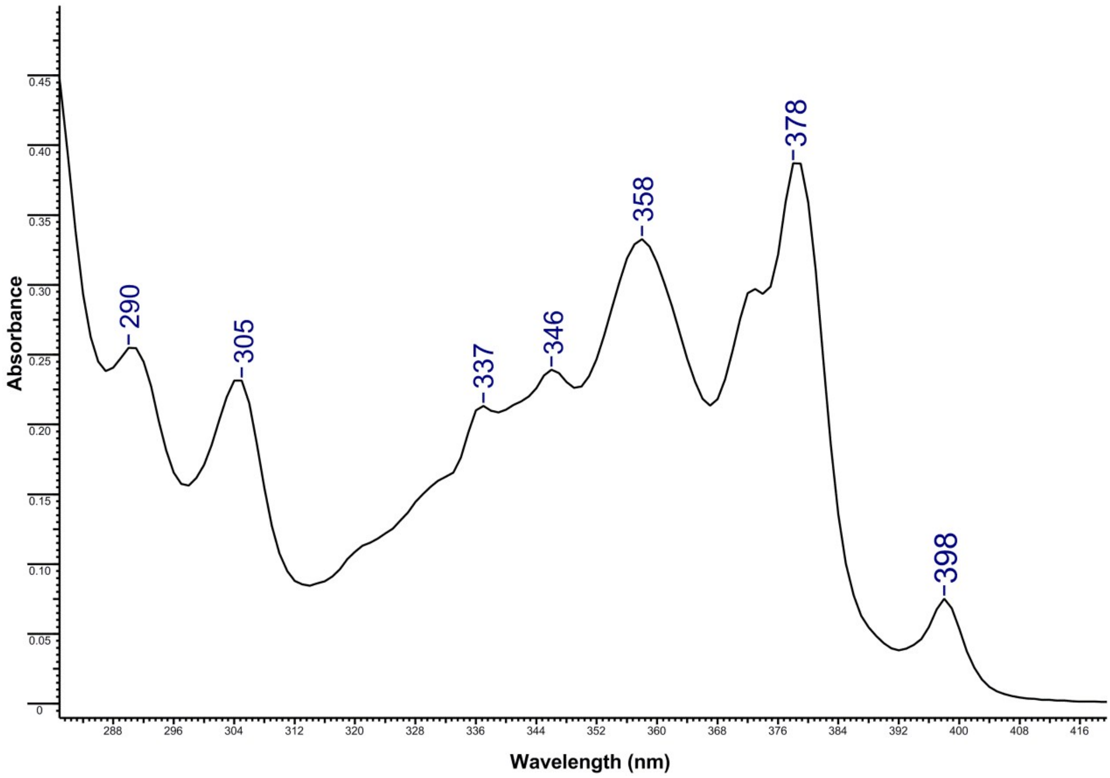

Fig.S8 Electronic absorption spectrum of compound **3**

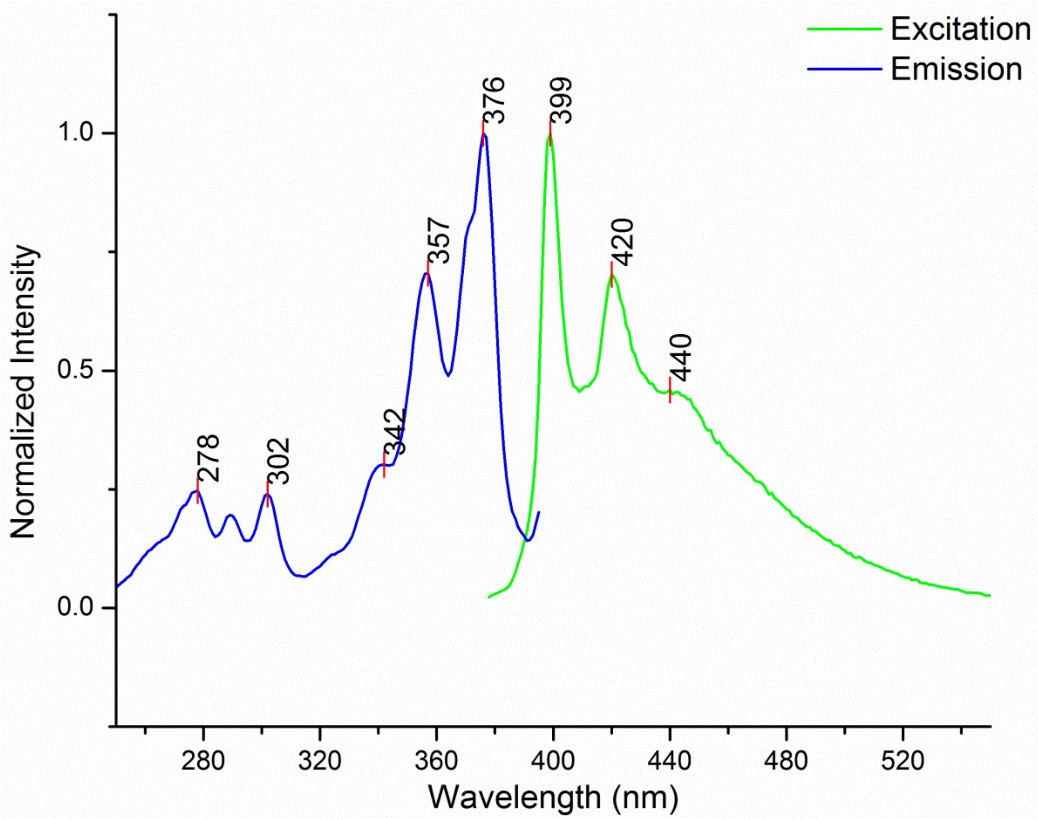

Fig.S9 Fluorescence excitation and emission spectrum of compound **3**

Fluorescence quenching with 2, 4-dinitritoluene in THF

The fluorescence quenching of the fluorophore **3** (1.0×10^{-5} M) with 2, 4-dinitrotoluene (2.0×10^{-3} M) was carried out in THF.

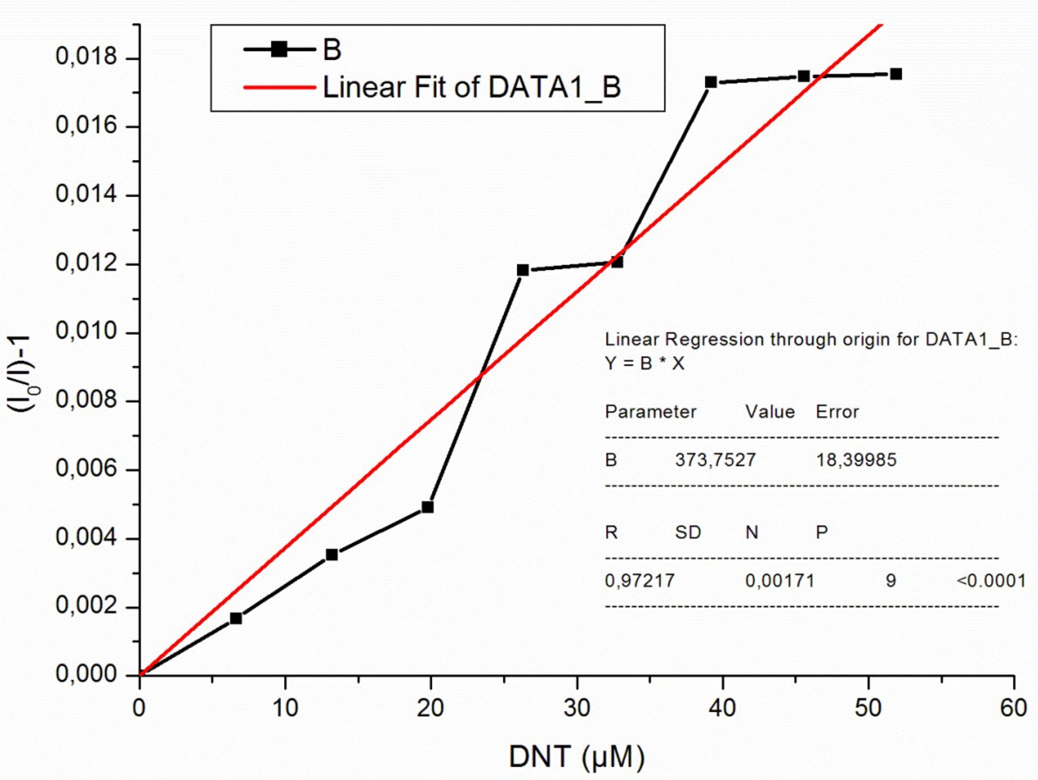

Fig.S10 Stern-Volmer plot

2,4-DNT (μM)	$(I_0/I)-1$
0,00E+00	0,00000
6,64E+00	0,00168
1,32E+01	0,00352
1,98E+01	0,00491
2,63E+01	0,01183
3,28E+01	0,01207
3,92E+01	0,01730
4,56E+01	0,01747
5,19E+01	0,01754

Fig.S11 Fluorescence quenching of the fluorophore **3** with DNT in THF

Fluorescence quenching with trinitrotoluene in THF

The fluorescence quenching of the fluorophore **3** (1.0×10^{-5} M) with trinitrotoluene (2.0×10^{-3} M) was carried out in THF.

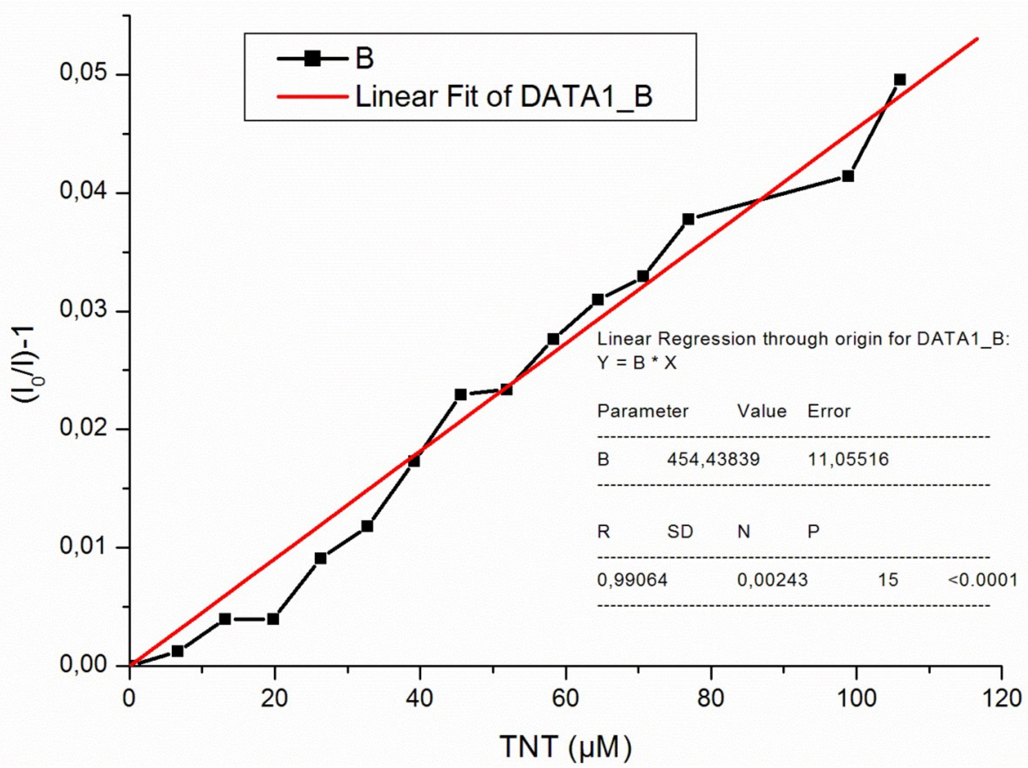

Fig.S12 Stern-Volmer plot

TNT (μM)	(I_0/I)-1
0,00E+00	0,00000
6,64E+00	0,00124
1,32E+01	0,00398
1,98E+01	0,00398
2,63E+01	0,00911
3,28E+01	0,01179
3,92E+01	0,01730
4,56E+01	0,02296
5,19E+01	0,02337
5,83E+01	0,02765
6,45E+01	0,03093
7,07E+01	0,03291

Fig.S13 Fluorescence quenching of the fluorophore **3** with TNT in THF

Fluorescence quenching with picric acid in THF

The fluorescence quenching of the fluorophore **3** (1.0×10^{-5} M) with picric acid (2.0×10^{-3} M) was carried out in THF.

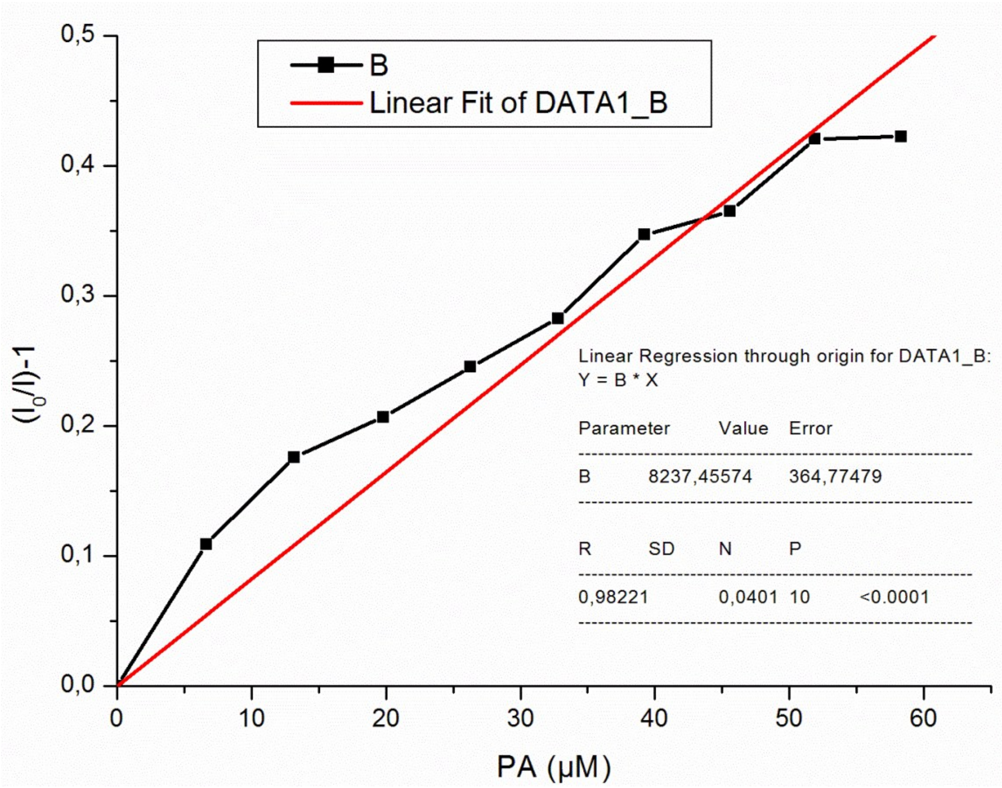

Fig.S14 Stern-Volmer plot

TNP(PA) (μM)	(I_0/I)-1
0,00E+00	0,00000
6,64E+00	0,10917
1,32E+01	0,17614
1,98E+01	0,20689
2,63E+01	0,24524
3,28E+01	0,28265
3,92E+01	0,34692
4,56E+01	0,36497
5,19E+01	0,42041

Fig.S15 Fluorescence quenching of the fluorophore **3** with TNP(PA) in THF

Fluorescence quenching with nitrobenzene in THF

The fluorescence quenching of the fluorophore **3** (1.0×10^{-5} M) with nitrobenzene (2.0×10^{-2} M) was carried out in THF.

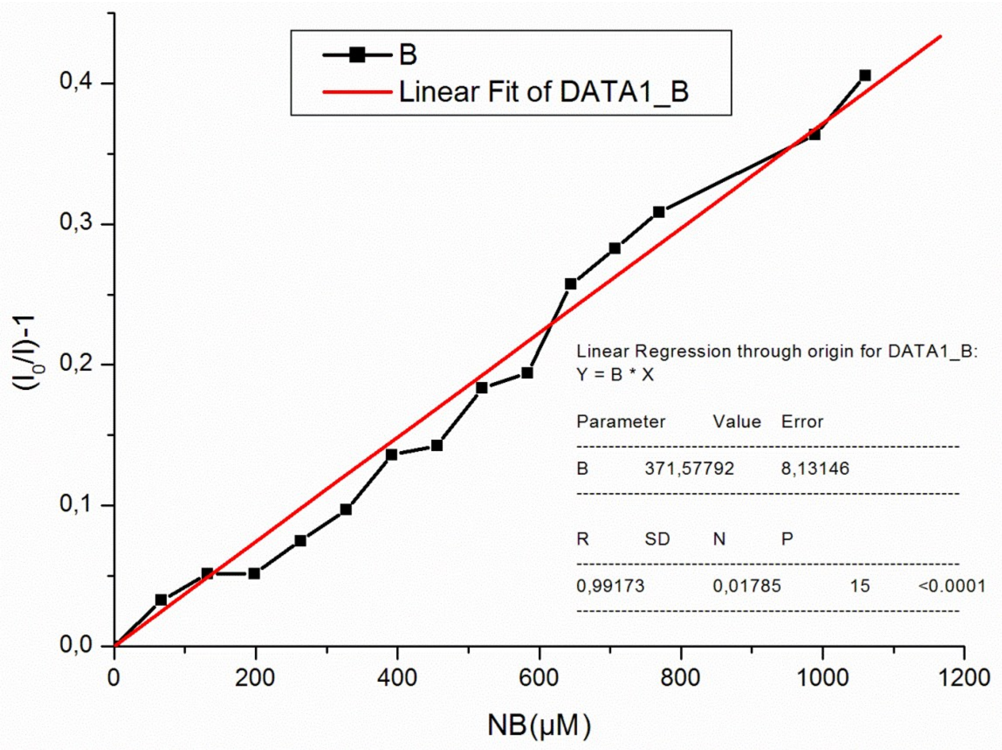

Fig.S16 Stern-Volmer plot

NB (μM)	(I_0/I)-1
0,00E+00	0,00000
6,64E+01	0,03290
1,32E+02	0,05177
1,98E+02	0,05177
2,63E+02	0,07520
3,28E+02	0,09695
3,92E+02	0,13618
4,56E+02	0,14262
5,19E+02	0,18358
5,83E+02	0,19416
6,45E+02	0,25716
7,07E+02	0,28274

Fig.S17 Fluorescence quenching of the fluorophore **3** with NB in THF

	Ksv (R) in THF
NB	372 (R=0.9917)
DNT	374 (R=0.9722)
TNT	454 (R=0.9906)
TNP(PA)	8237 (R=0.9822)

Estimation of the detection limit for sensor 3

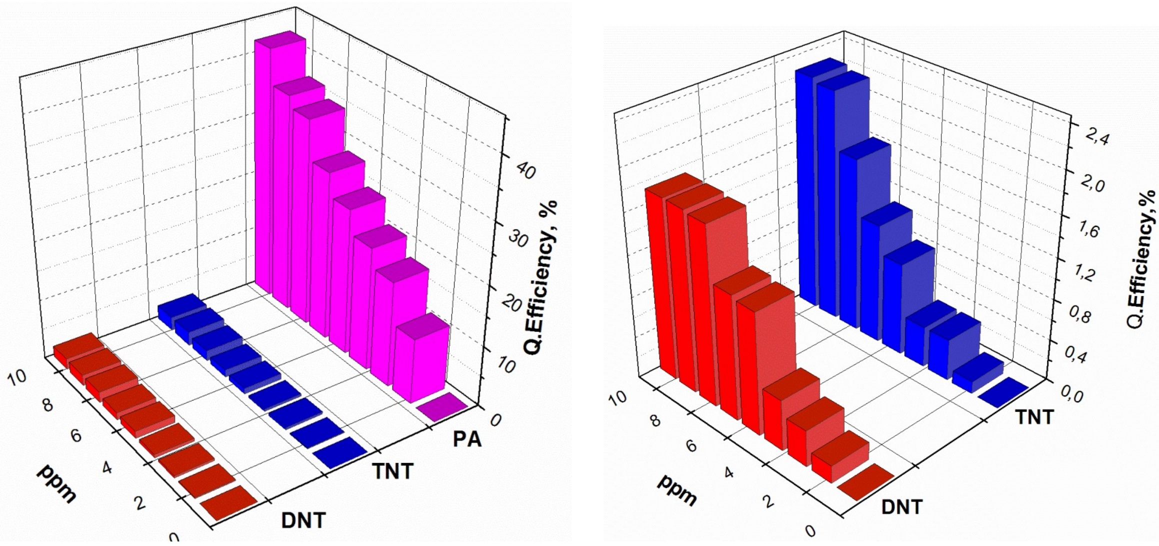

Fig.S18 Estimation of the detection limit for sensor **3**

PLQY

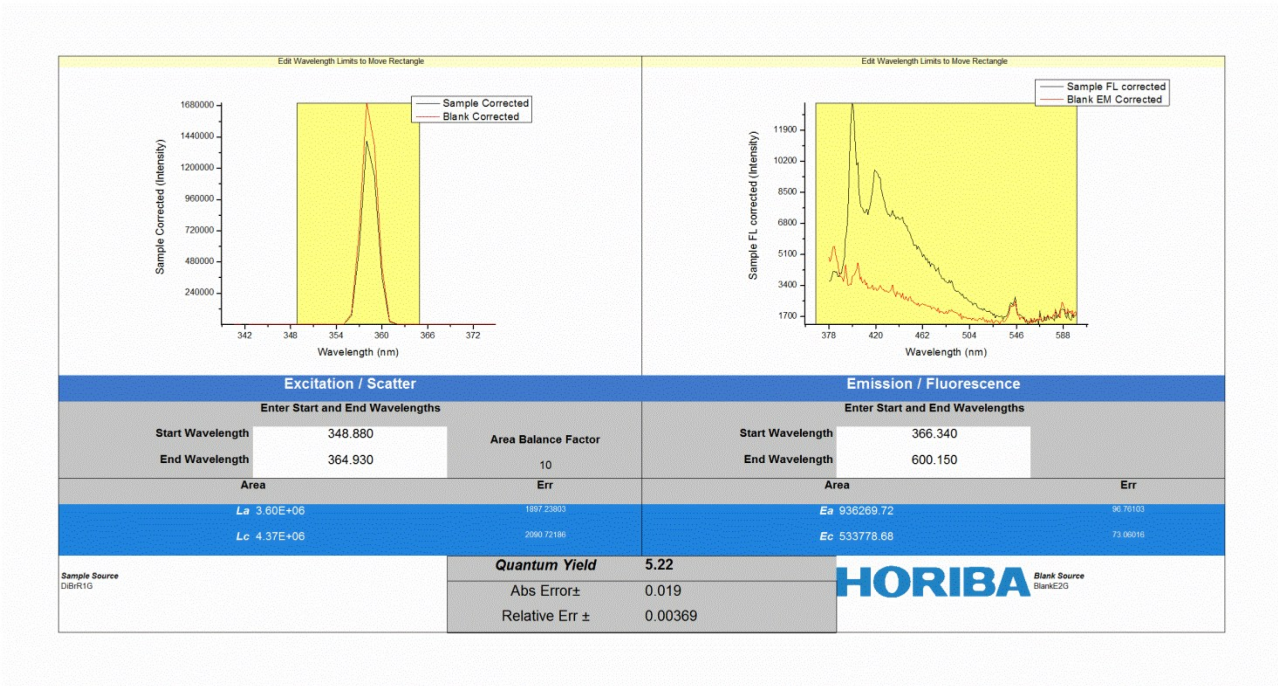

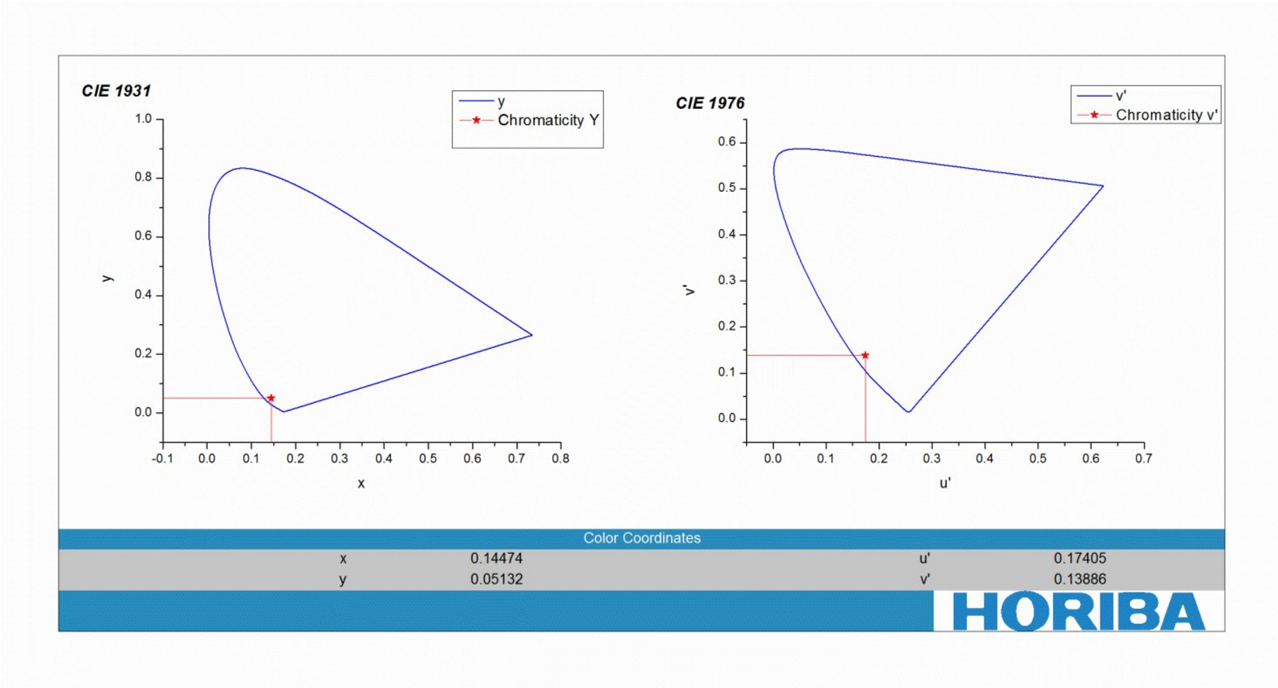

Compound 4a

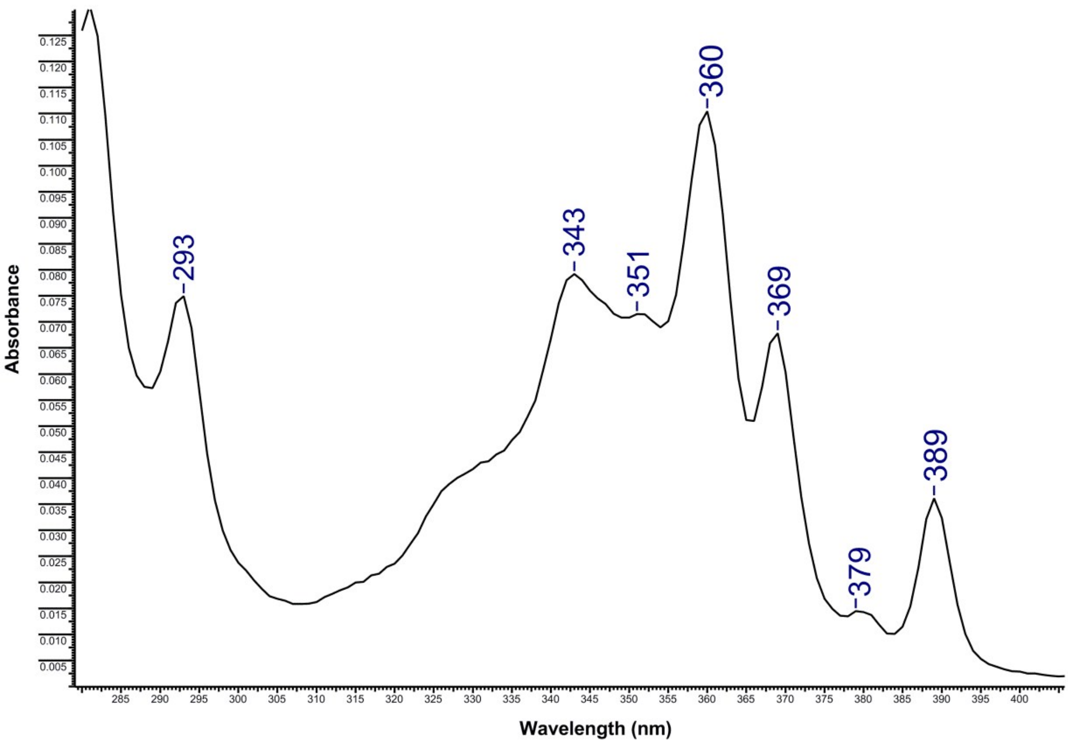

Fig.S19 Electronic absorption spectrum of compound **4a**

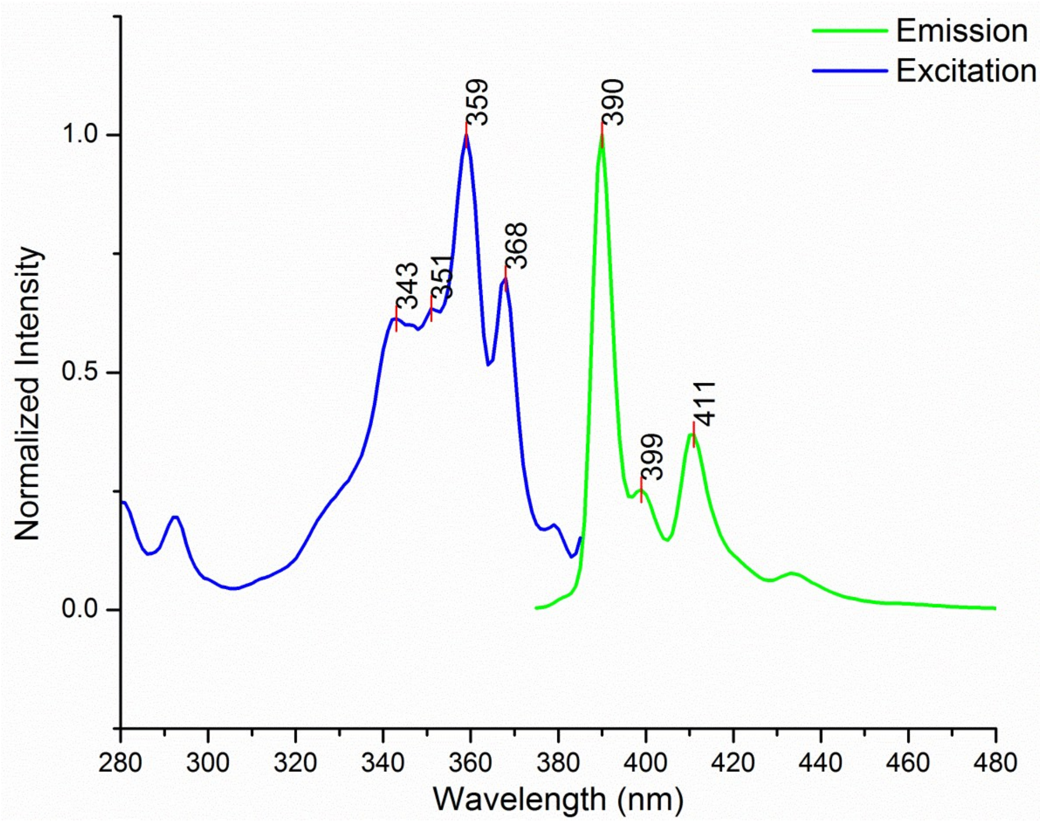

Fig.S20 Fluorescence excitation and emission spectrum of compound **4a**

Fluorescence quenching with 2, 4-dinitritoluene in THF

The fluorescence quenching of the fluorophore **4a** (1.0×10^{-5} M) with 2, 4-dinitrotoluene (2.0×10^{-3} M) was carried out in THF.

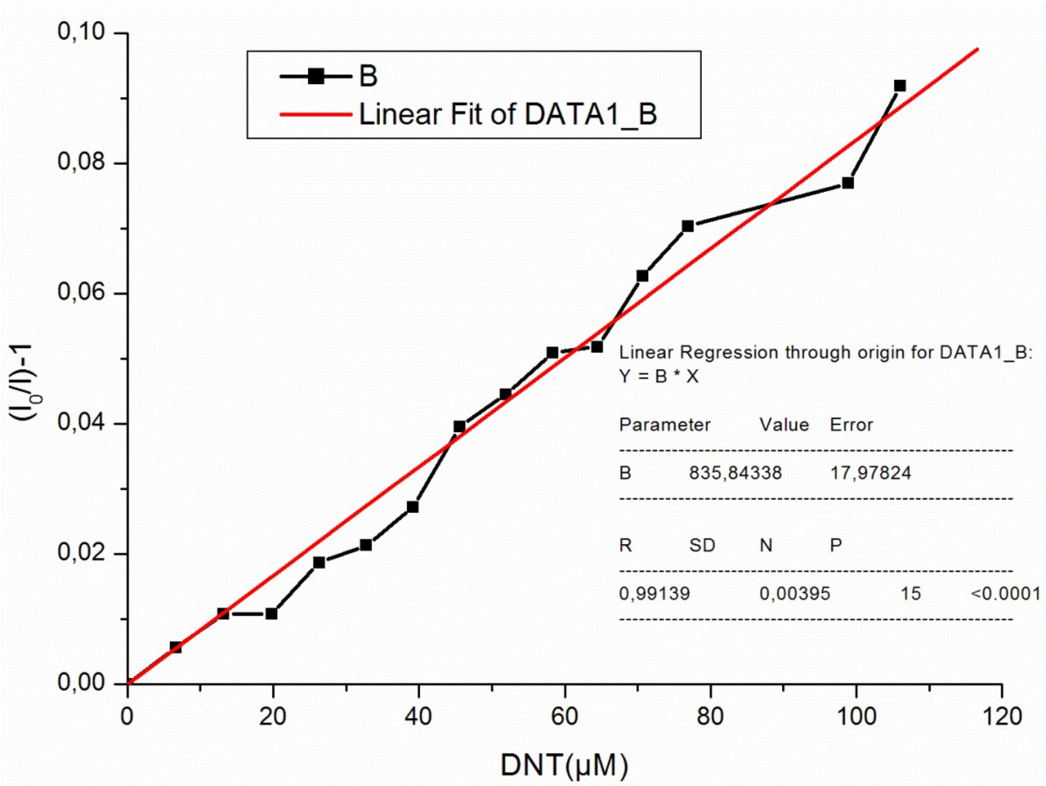

Fig.S21 Stern-Volmer plot

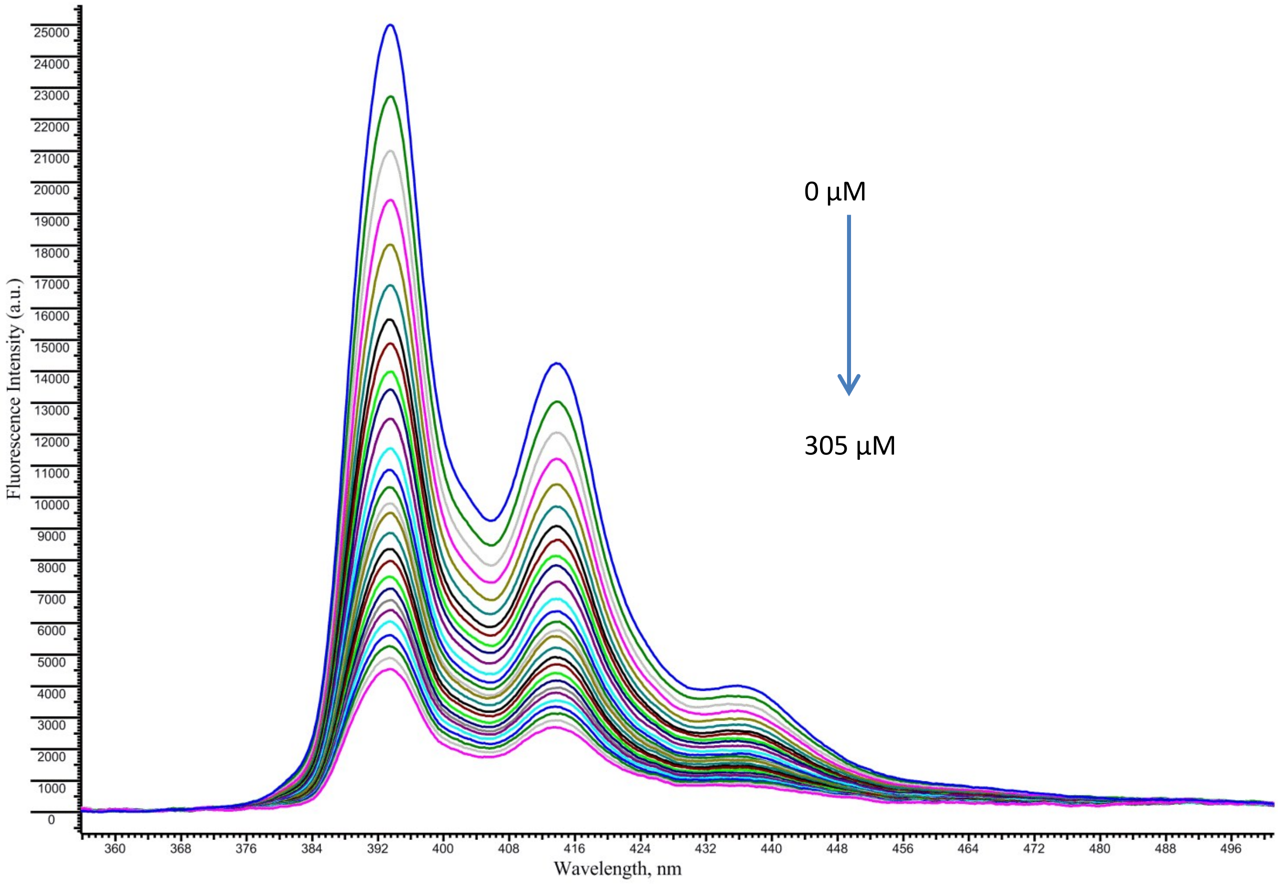

Fig.S22 Fluorescence quenching of the fluorophore **4a** with DNT in THF

Fluorescence quenching with trinitrotoluene in THF

The fluorescence quenching of the fluorophore **4a** (1.0×10^{-5} M) with trinitrotoluene (2.0×10^{-3} M) was carried out in THF.

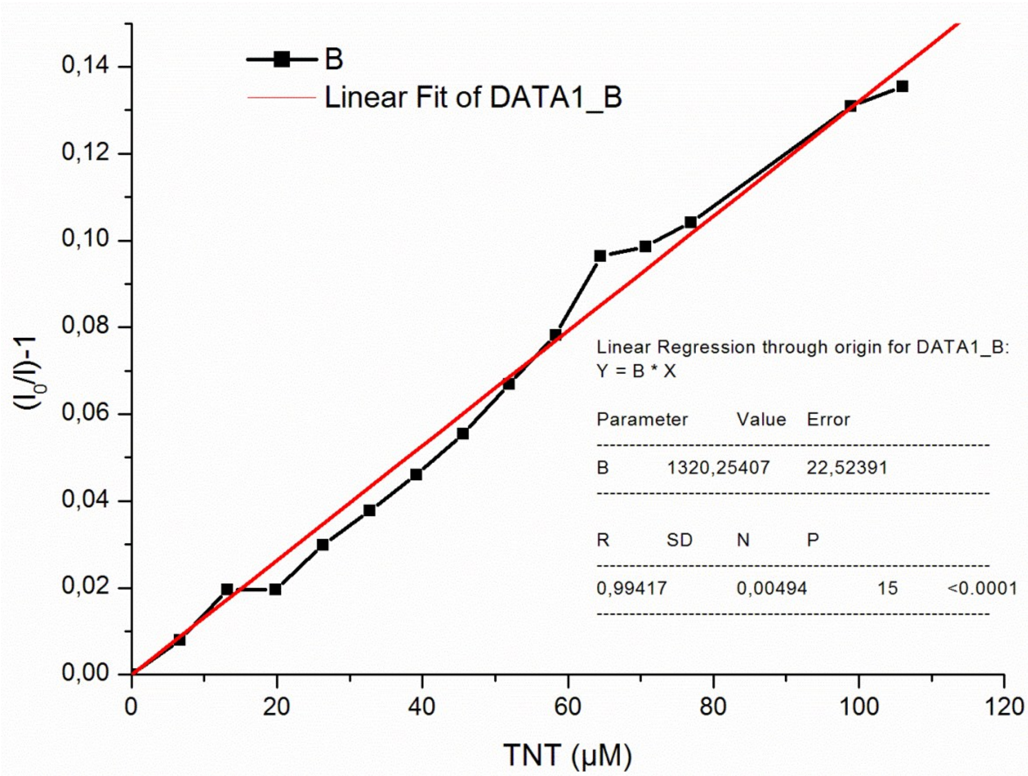

Fig.S23 Stern-Volmer plot

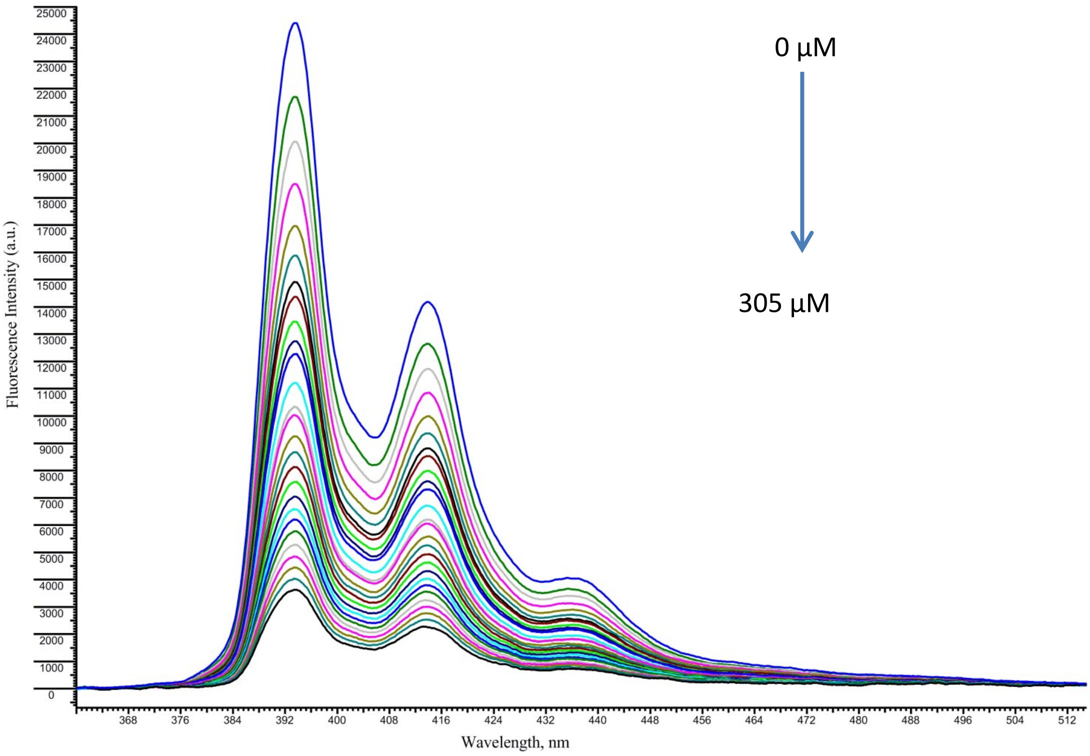

Fig.S24 Fluorescence quenching of the fluorophore **4a** with TNT in THF

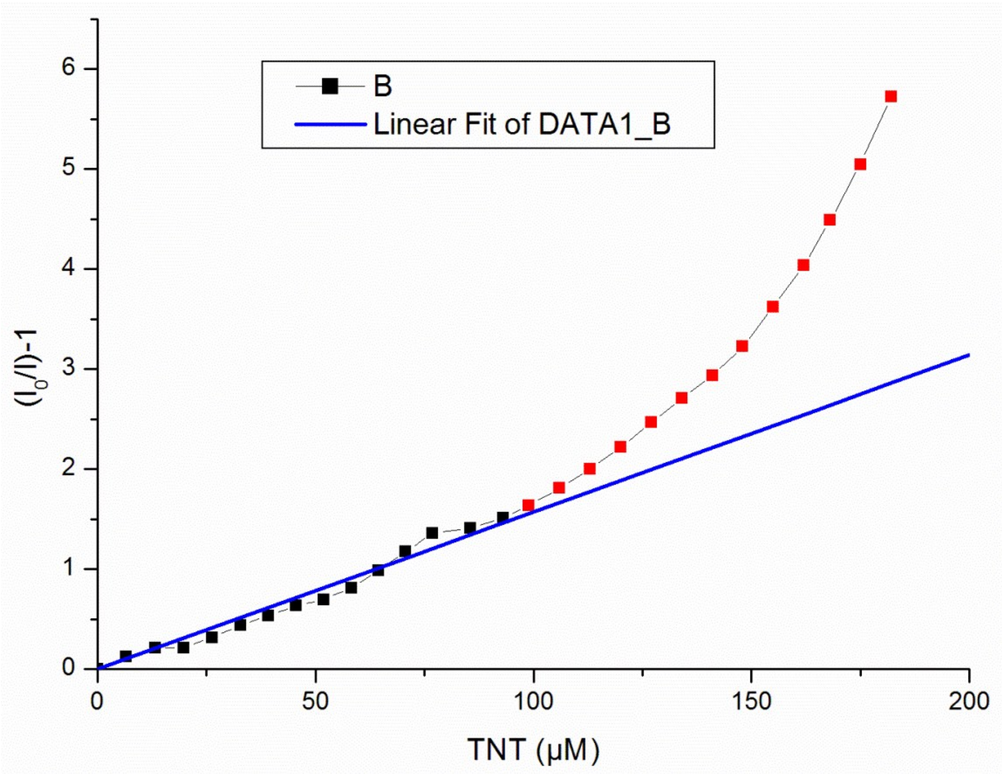

Fig.S25 Stern-Volmer plot of **4a** sensor at different concentration of TNT (28 points)

Fluorescence quenching with 2,4,6-trinitrophenol (picric acid) in THF

The fluorescence quenching of the fluorophore **4a** (1.0×10^{-5} M) with picric acid (2.0×10^{-3} M) was carried out in THF.

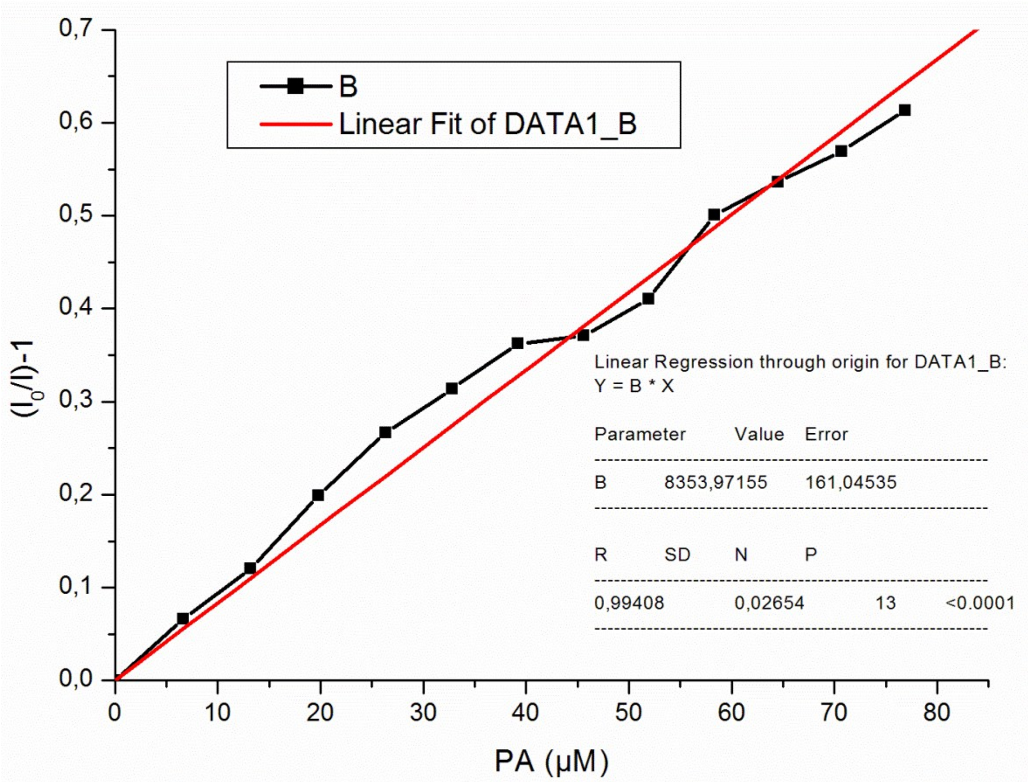

Fig. S26 Stern-Volmer plot

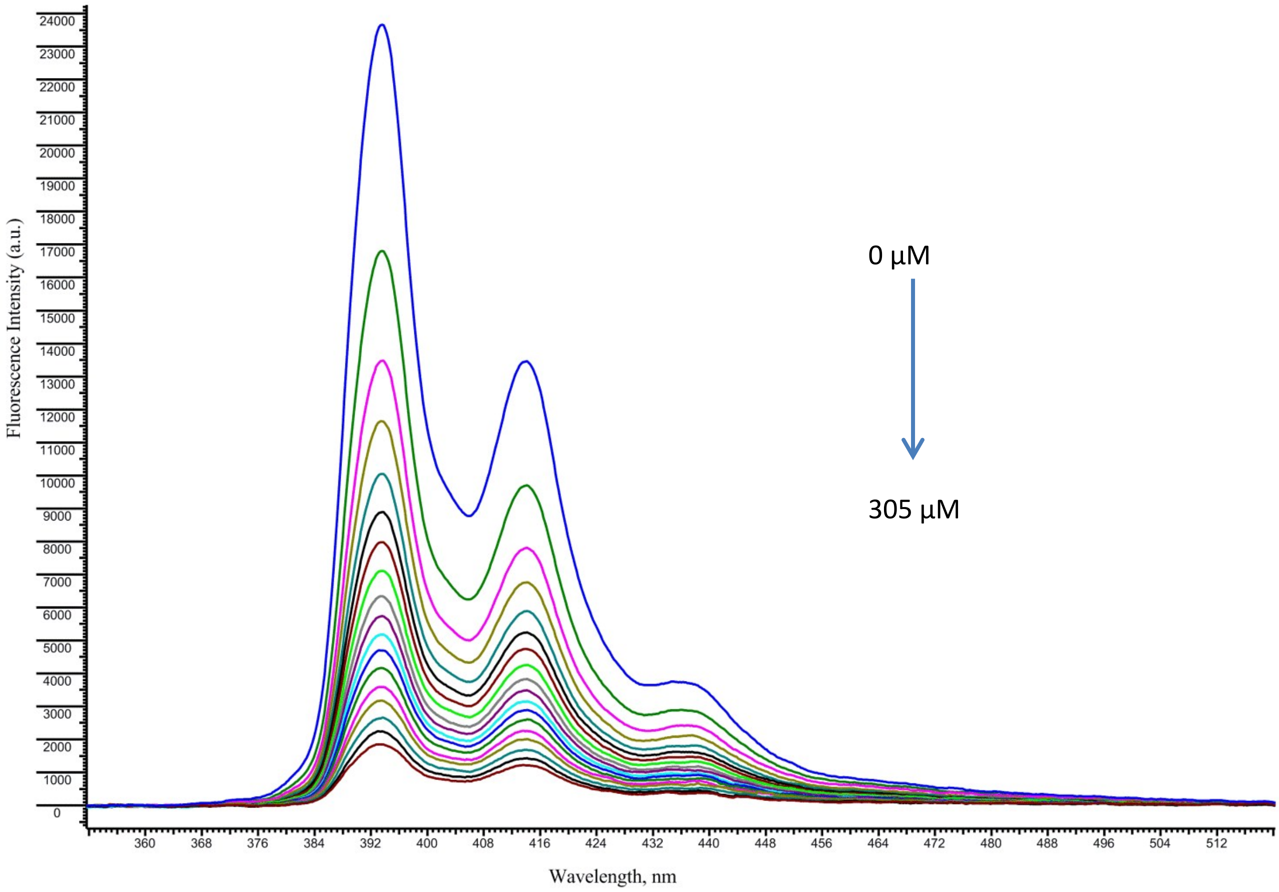

Fig.S27 Fluorescence quenching of the fluorophore **4a** with TNP(PA) in THF

Fluorescence quenching with nitrobenzene in THF

The fluorescence quenching of the fluorophore **4a** (1.0×10^{-5} M) with nitrobenzene (2.0×10^{-2} M) was carried out in THF.

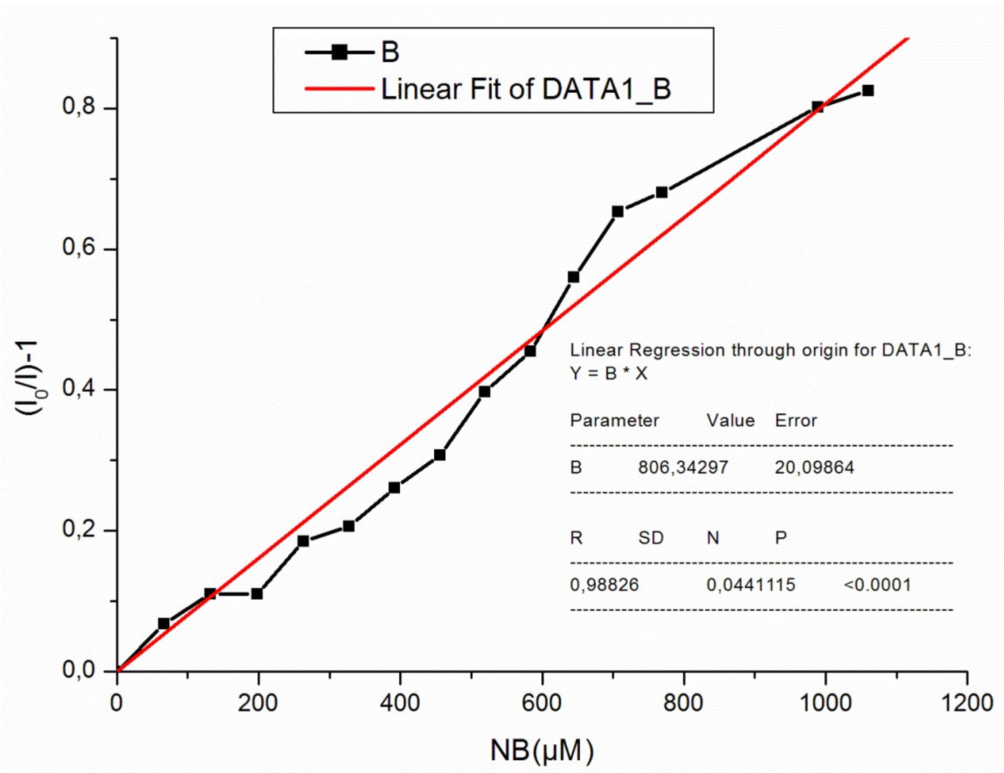

Fig.S28 Stern-Volmer plot

Fluorescence quenching with RDX in THF

The fluorescence quenching of the fluorophore **4a** (1.0×10^{-5} M) with RDX (2.0×10^{-3} M) was carried out in THF.

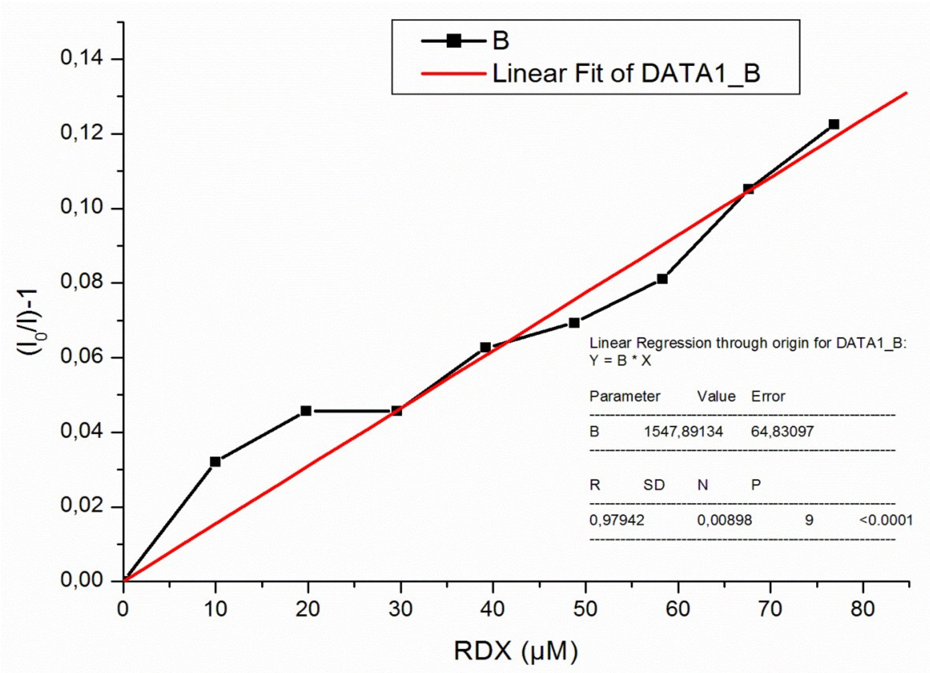

Fig.S29 Stern-Volmer plot

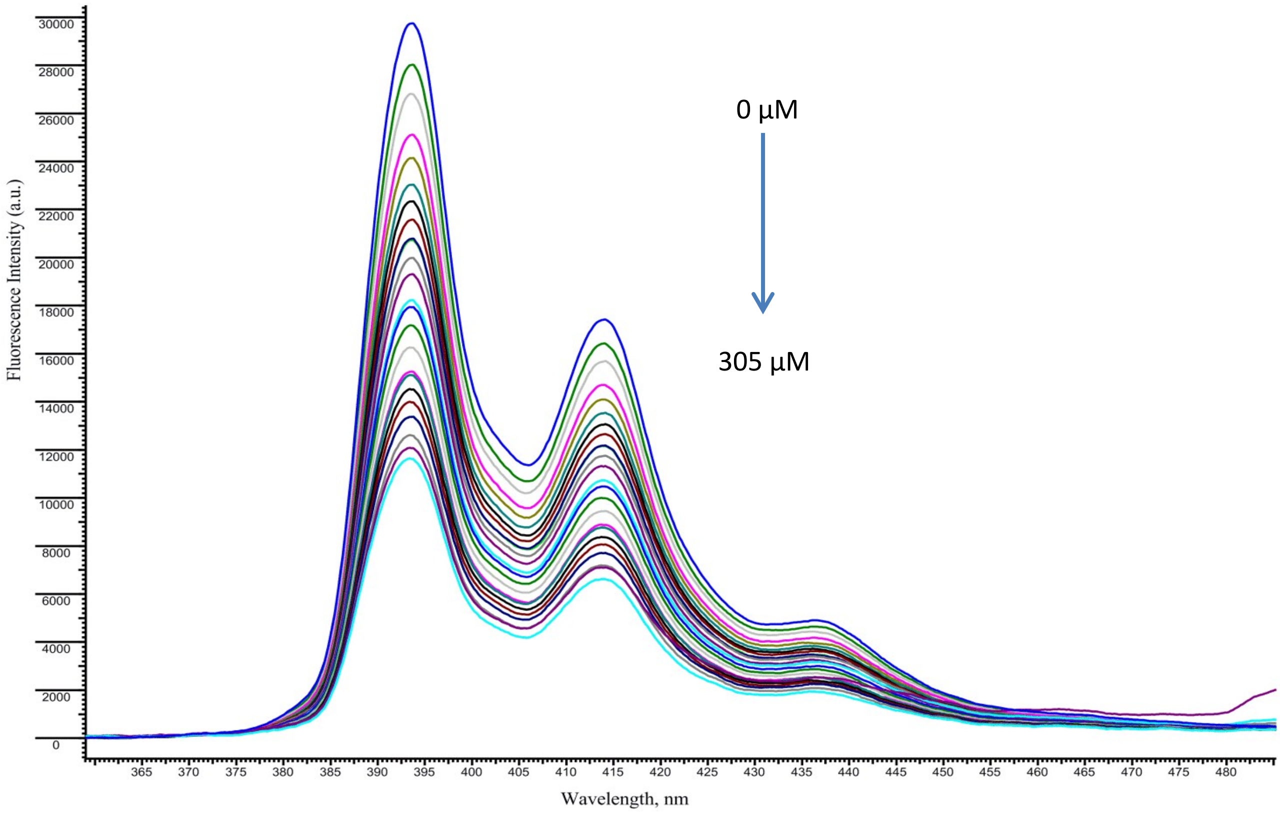

Fig.S30 Fluorescence quenching of the fluorophore **4a** with RDX in THF

 300 μM

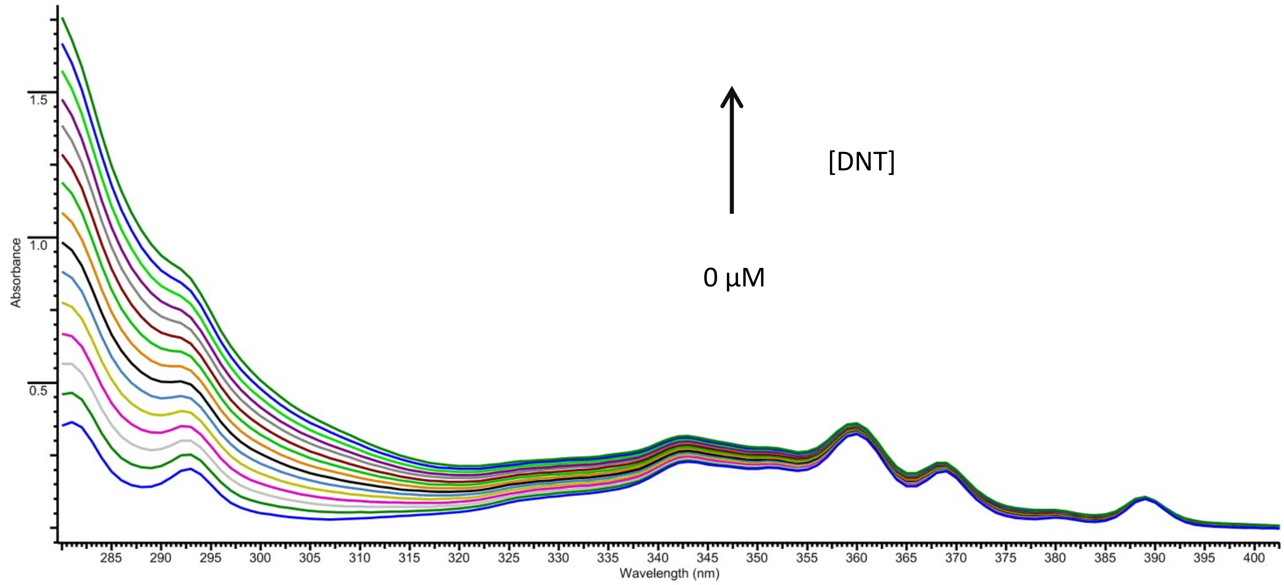

Fig.S31 Absorbance quenching of the fluorophore **4a** with 2, 4-dinitrotoluene in THF

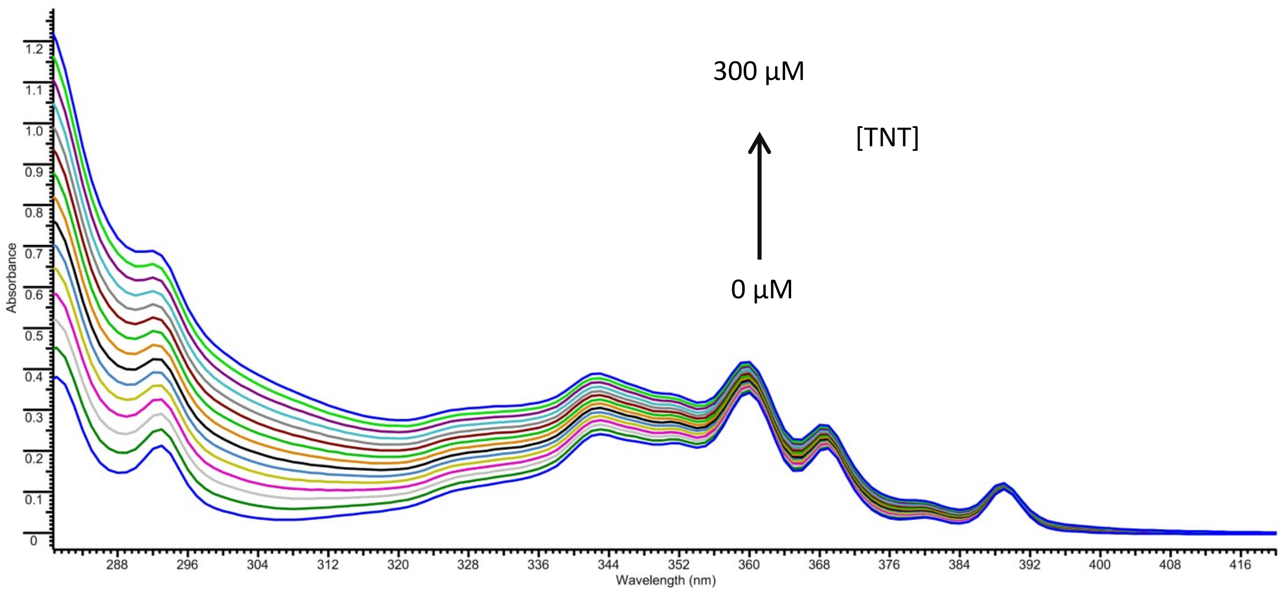

Fig.S32 Absorbance quenching of the fluorophore **4a** with 2,4,6-trinitrotoluene in THF

Estimation of the detection limit for sensor 4a

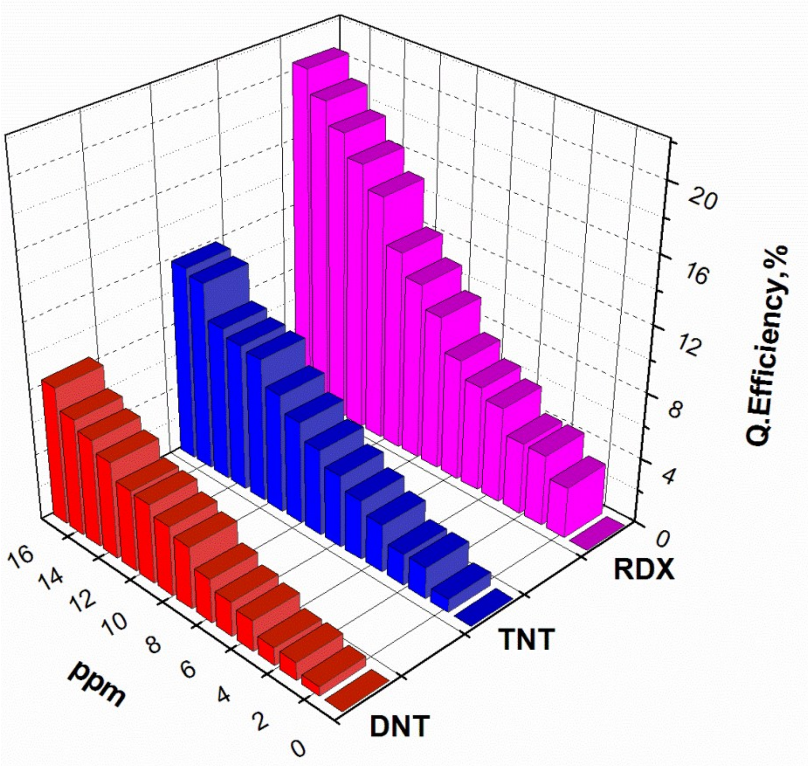

Fig.S33 Estimation of the detection limit for sensor **4a**

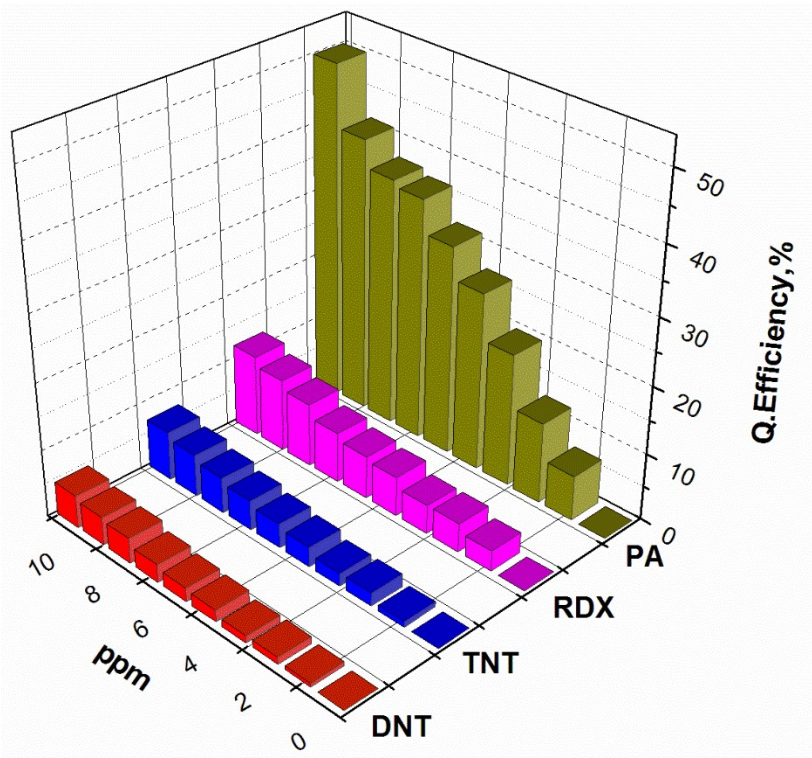

Fig.S34 Estimation of the detection limit for sensor **4a**

PLQY

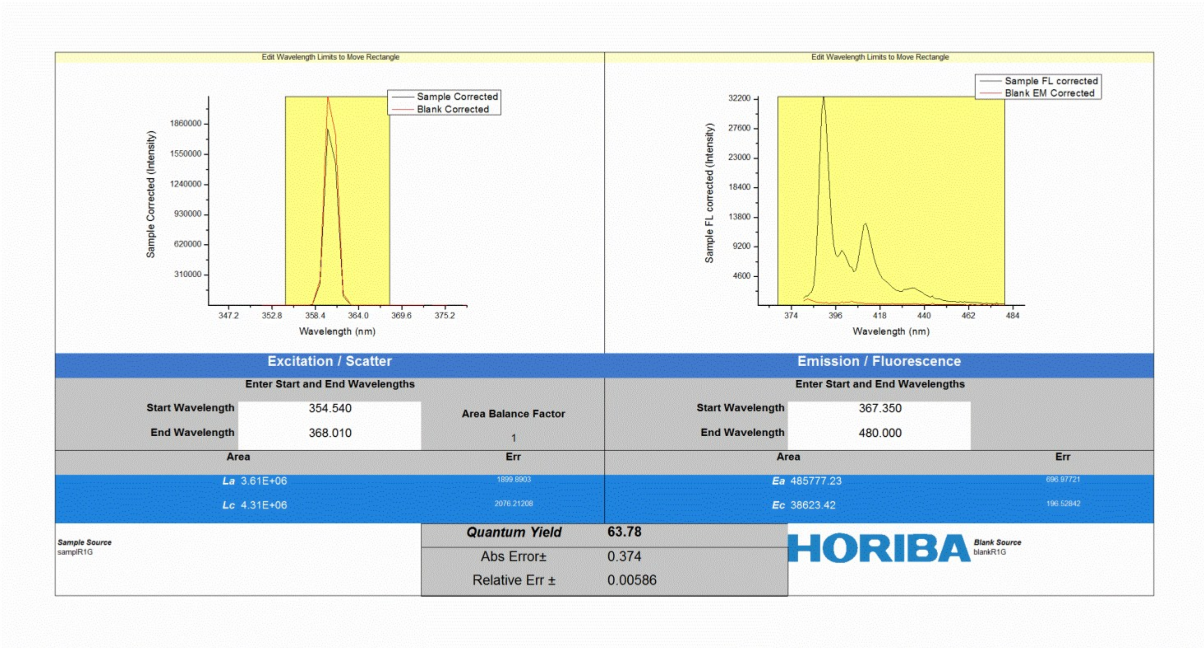

	Ksv (R) in THF
NB	806 (R=0.9883)
DNT	836 (R=0.9914)
TNT	1321 (R=0.9942)
TNP(PA)	8354 (R=0.9941)
RDX	1548 (R=0.9794)

Compound 4b

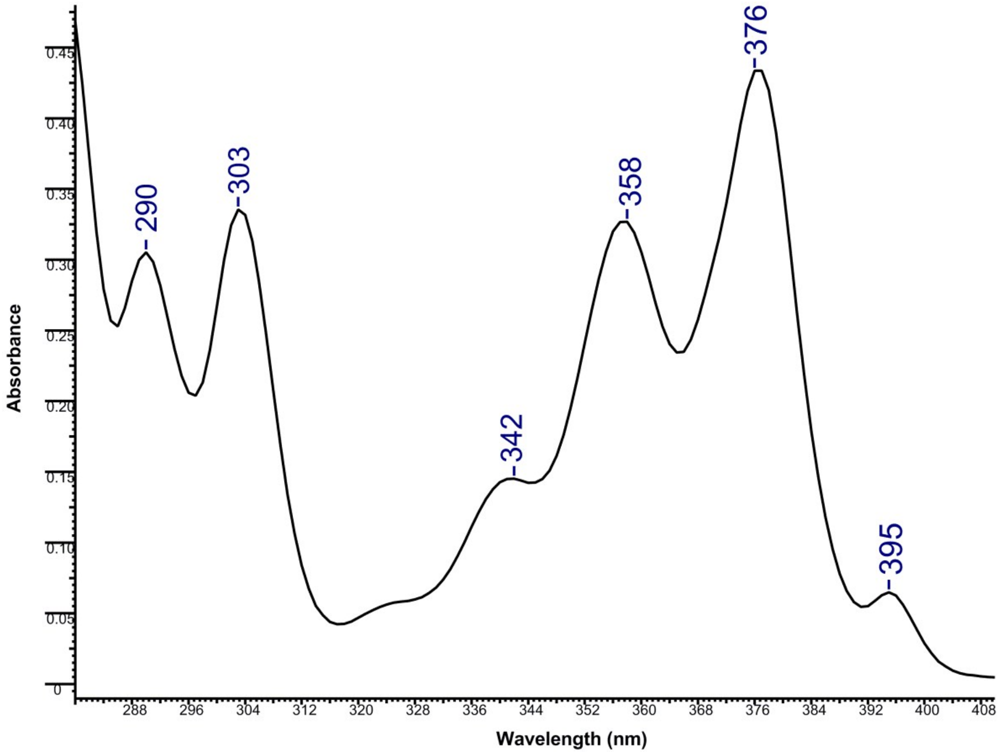

Fig.S35 Electronic absorption spectrum of compound **4b**

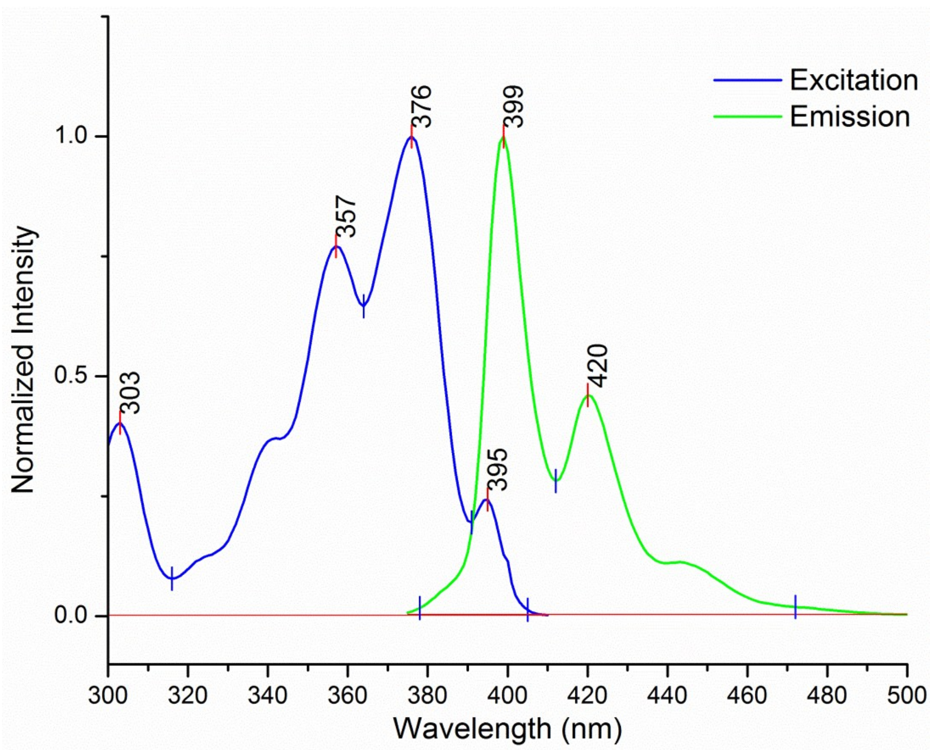

Fig.S36 Fluorescence excitation and emission spectrum of compound **4b**

Fluorescence quenching with 2, 4-dinitritoluene in THF

The fluorescence quenching of the fluorophore **4b** (1.0×10^{-5} M) with 2, 4-dinitrotoluene (2.0×10^{-3} M) was carried out in THF.

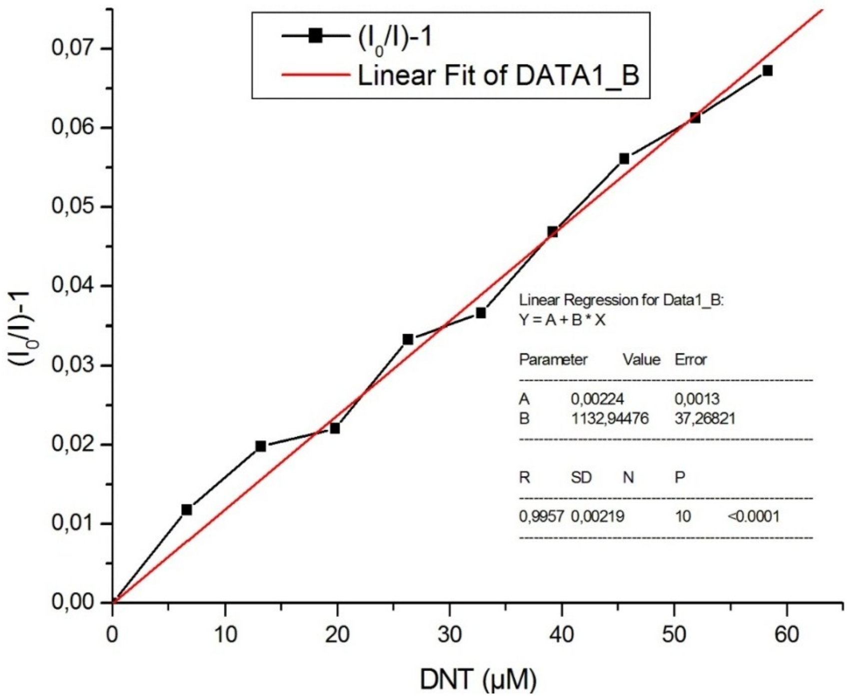

Fig.S37 Stern-Volmer plot

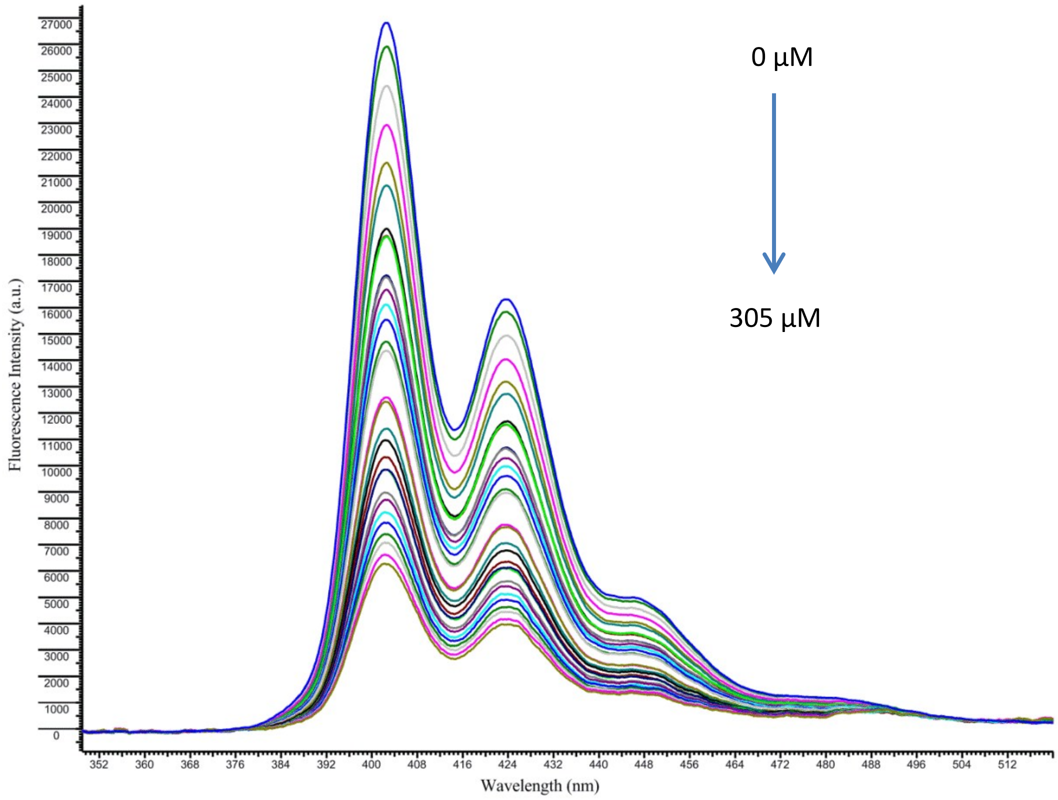

Fig.S38 Fluorescence quenching of the fluorophore **4b** with 2, 4-dinitrotoluene in THF

Fluorescence quenching with 2, 4-dinitritoluene in toluene

The fluorescence quenching of the fluorophore **4b** (1.0 $\times 10^{-5}$ M) with 2, 4-dinitrotoluene (2.0 $\times$ 10^{-3} M) was carried out in toluene.

DNT (µM)	$(I_0/I)-1$
0,00E+00	0,00000
6,64E+00	0,00965
1,32E+01	0,02085
1,98E+01	0,02085
2,63E+01	0,02929
3,28E+01	0,02988
3,92E+01	0,03866
4,56E+01	0,04032
5,19E+01	0,04230
5,83E+01	0,05161
6,45E+01	0,06889
7,07E+01	0,06906

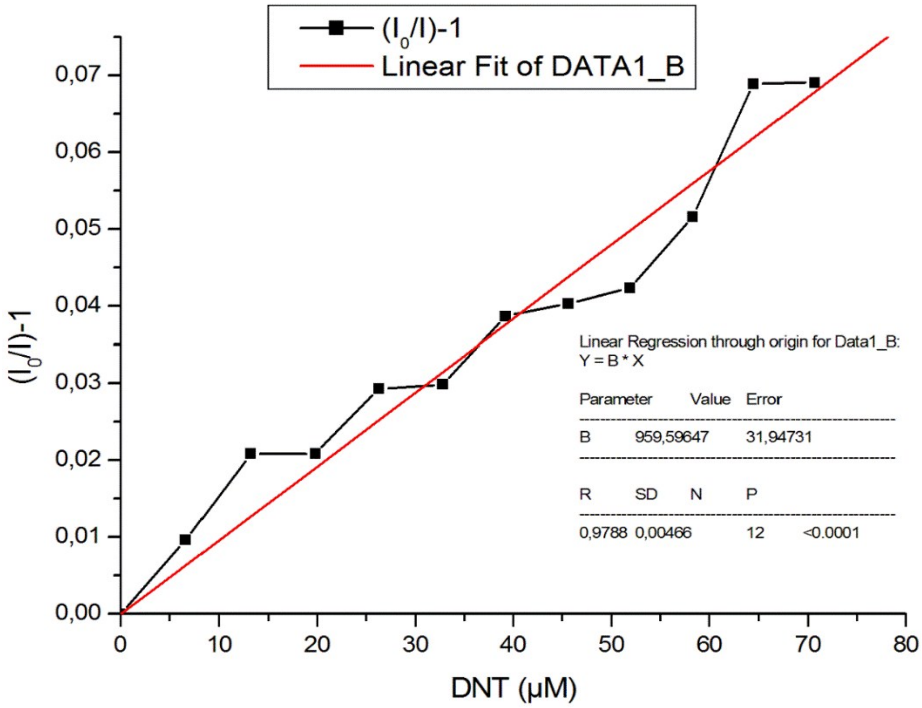

Fig.S39 Stern-Volmer plot

Fluorescence quenching with trinitrotoluene in THF

The fluorescence quenching of the fluorophore **4b** (1.0×10^{-5} M) with trinitrotoluene (2.0×10^{-3} M) was carried out in THF.

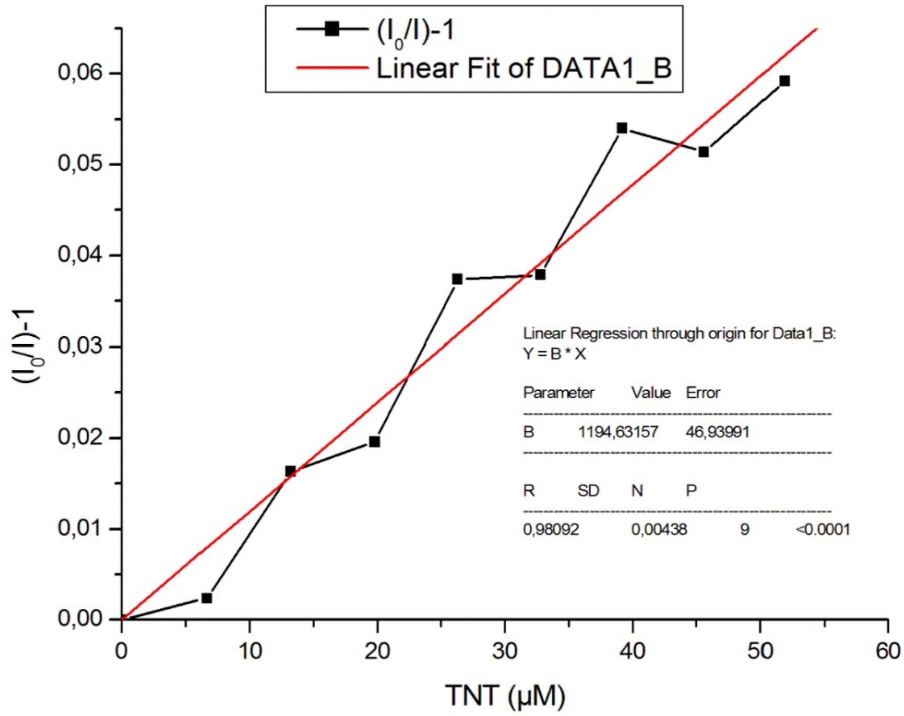

Fig.S40 Stern-Volmer plot

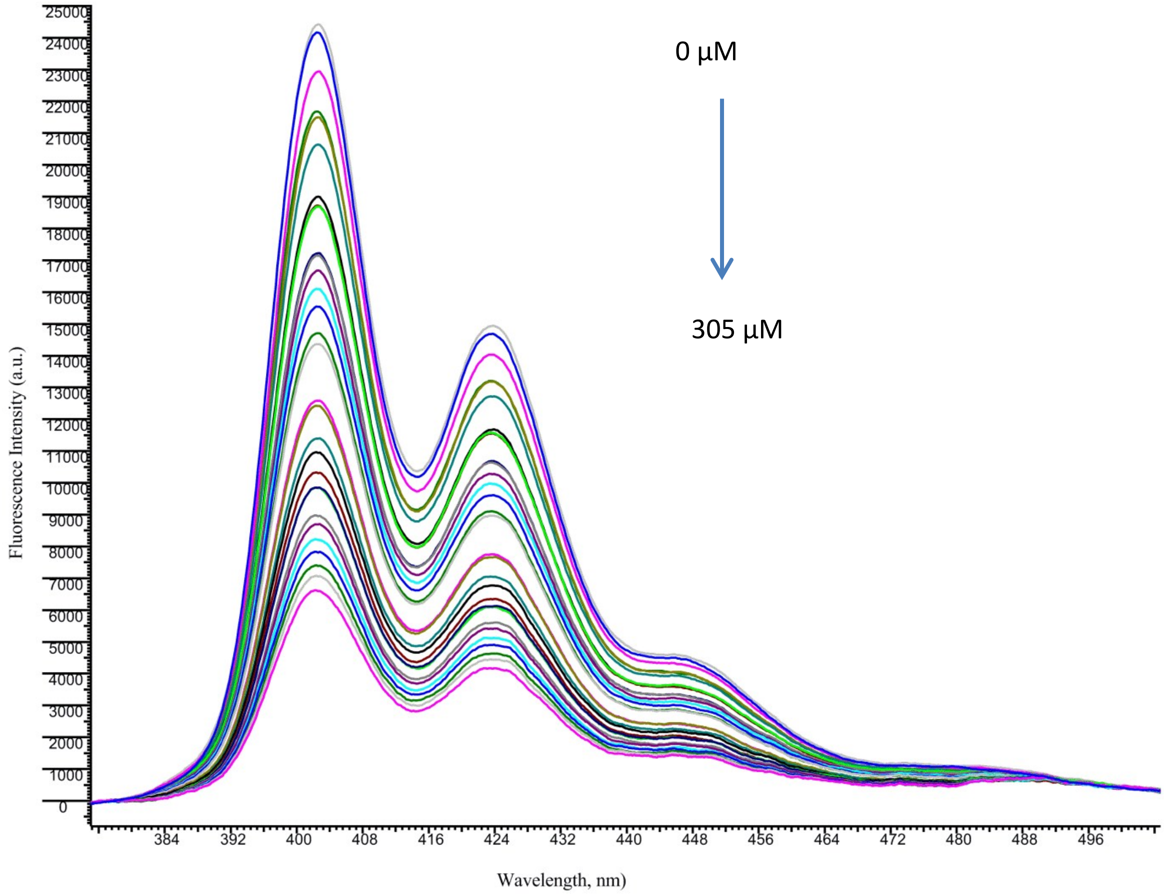

Fig.S41 Fluorescence quenching of the fluorophore **4b** with trinitrotoluene in THF

Fluorescence quenching with picric acid in THF

The fluorescence quenching of the fluorophore **4b** (1.0×10^{-5} M) with picric acid (2.0×10^{-3} M) was carried out in THF.

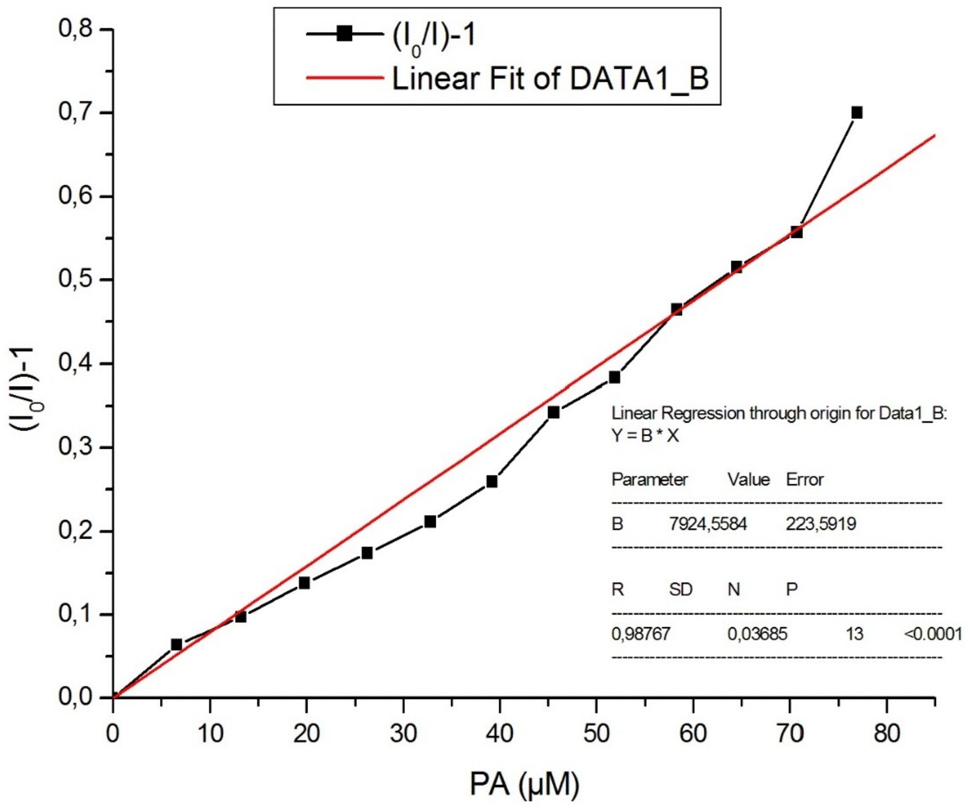

Fig.S42 Stern-Volmer plot

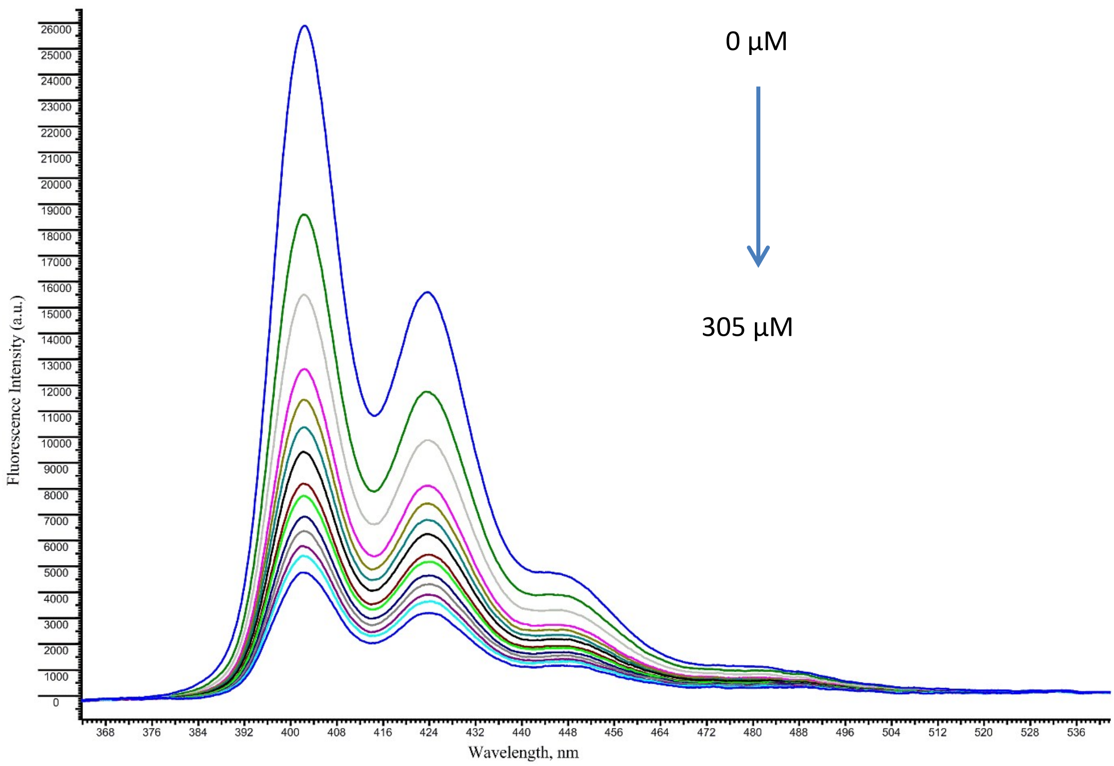

Fig.S43 Fluorescence quenching of the fluorophore **4b** with picric acid in THF

Fluorescence quenching with picric acid in toluene

The fluorescence quenching of the fluorophore **4b** (1.0×10^{-5} M) with picric acid (2.0×10^{-3} M) was carried out in toluene.

PA (µM)	$(I_0/I)-1$
0,00E+00	0,00000
6,64E+00	0,09709
1,32E+01	0,17726
1,98E+01	0,29447
2,63E+01	0,47234
3,28E+01	0,57155
3,92E+01	0,69578
4,56E+01	0,84285
5,19E+01	0,94581
5,83E+01	1,01377
6,45E+01	1,23852
7,07E+01	1,42511
7,69E+01	1,87606

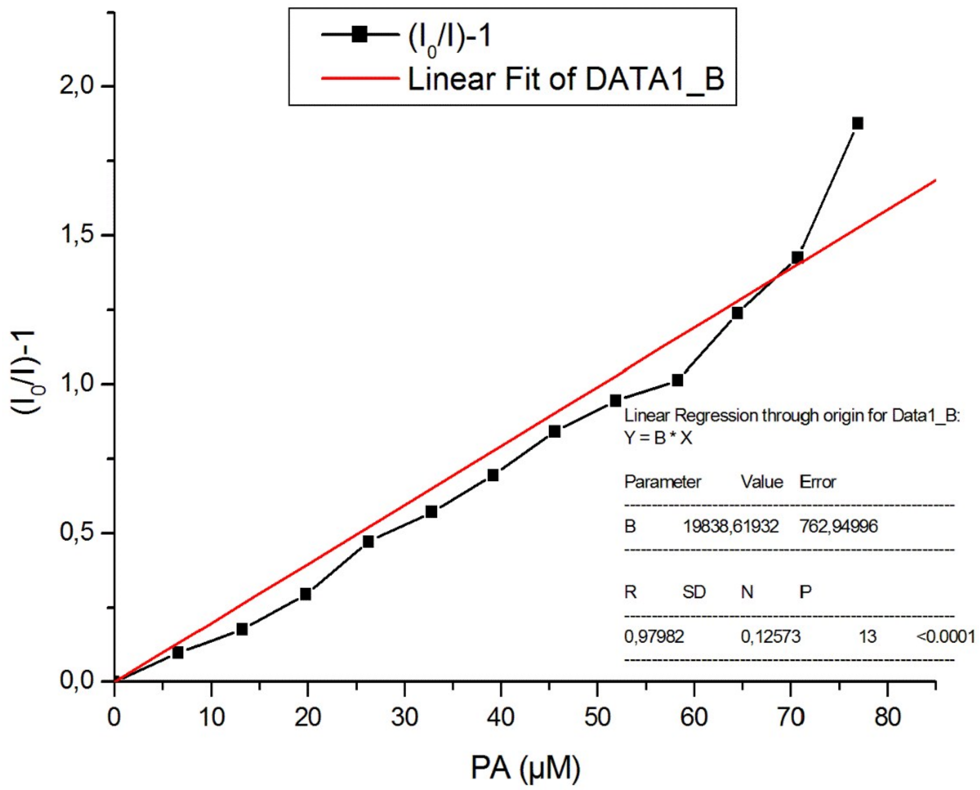

Fig.S44 Stern-Volmer plot

	Ksv (R) in THF	Ksv (R) in Toluene
DNT	1132 (R=0.9957)	959 (R=0.9788)
TNT	1194 (R=0.961)	-
PA	7924 (R=0.9877)	19638 (R=0.9798)

Estimation of the detection limit for sensor 4b

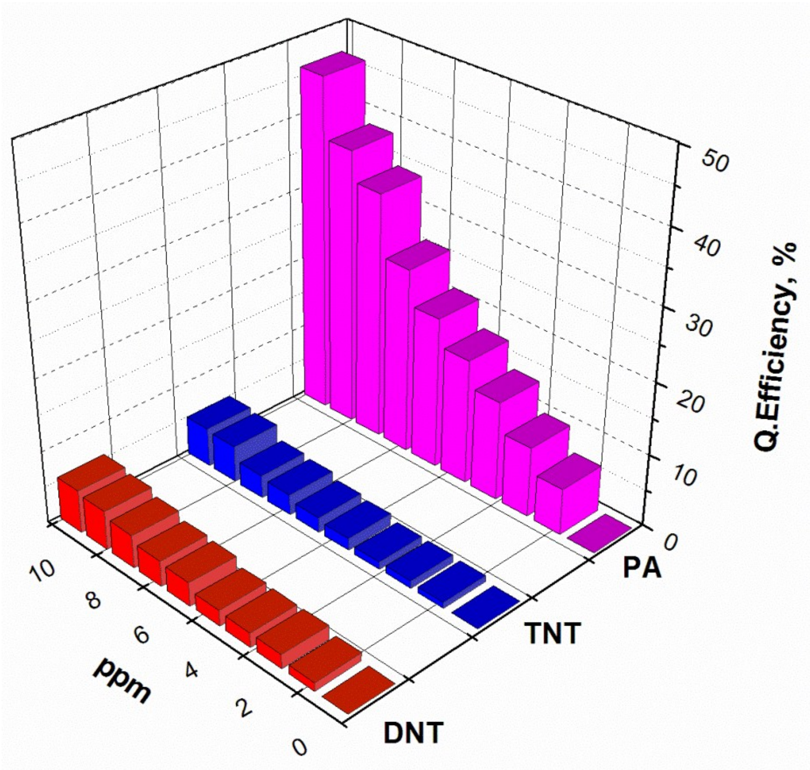

Fig.S45 Estimation of the detection limit for sensor **4b**

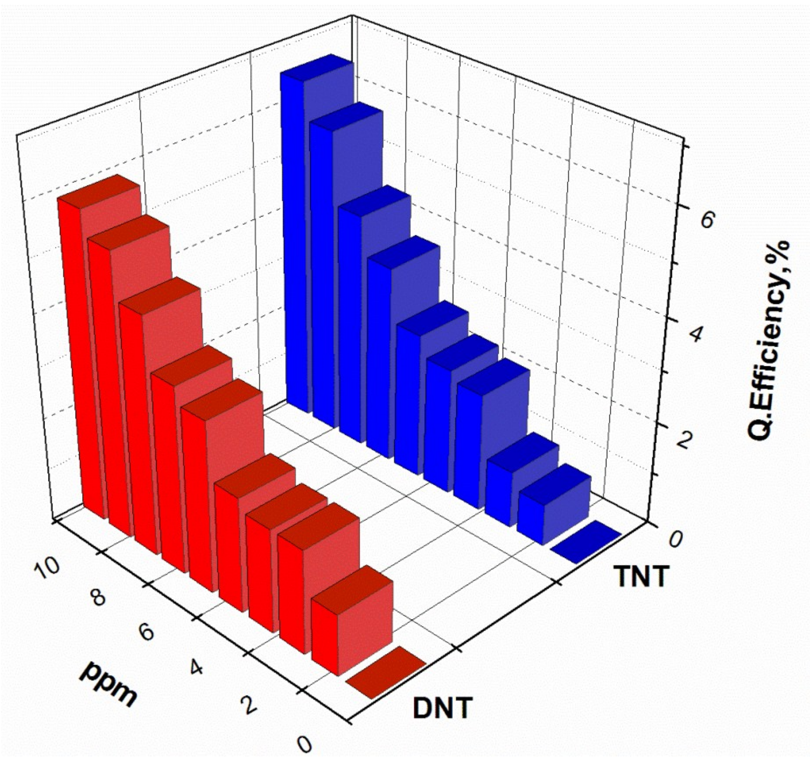

Fig.S46 Estimation of the detection limit for sensor **4b**

Electronic Supplementary Information

PLQY

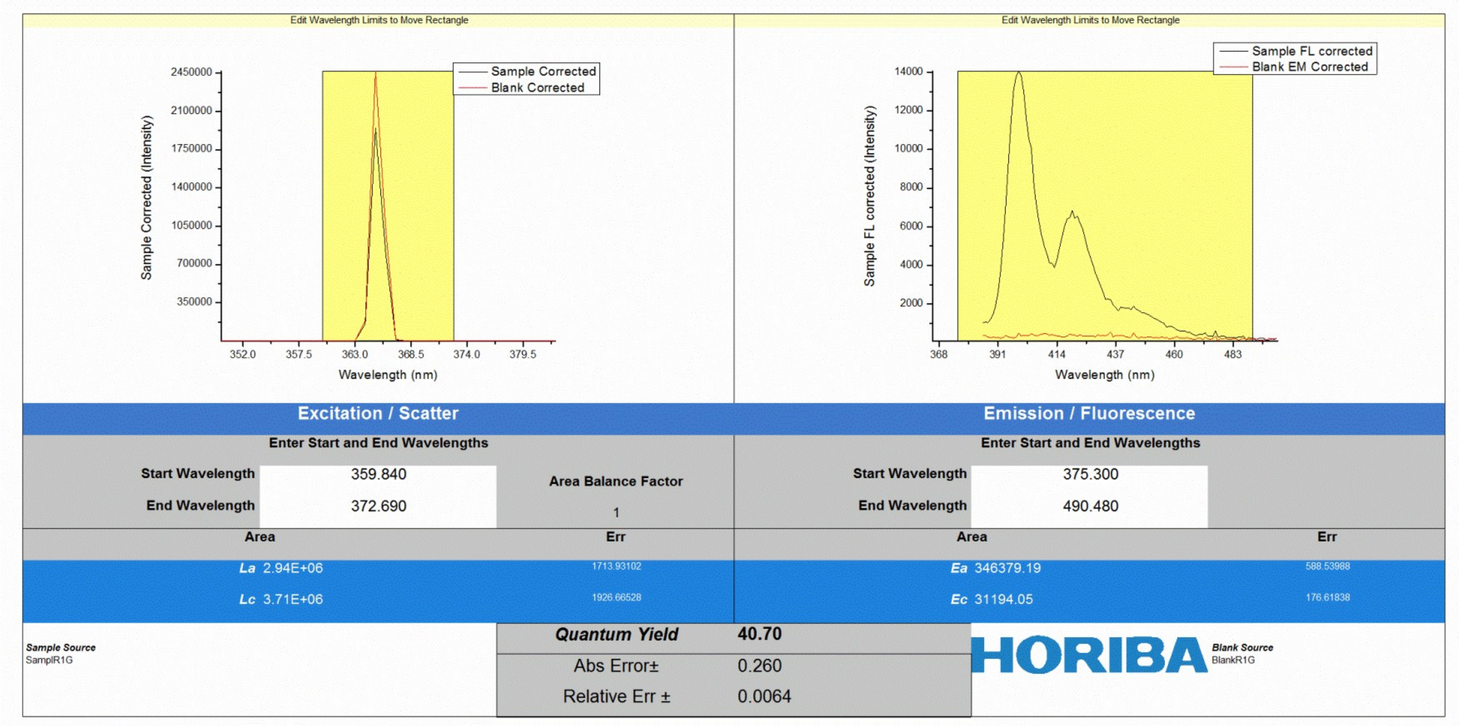

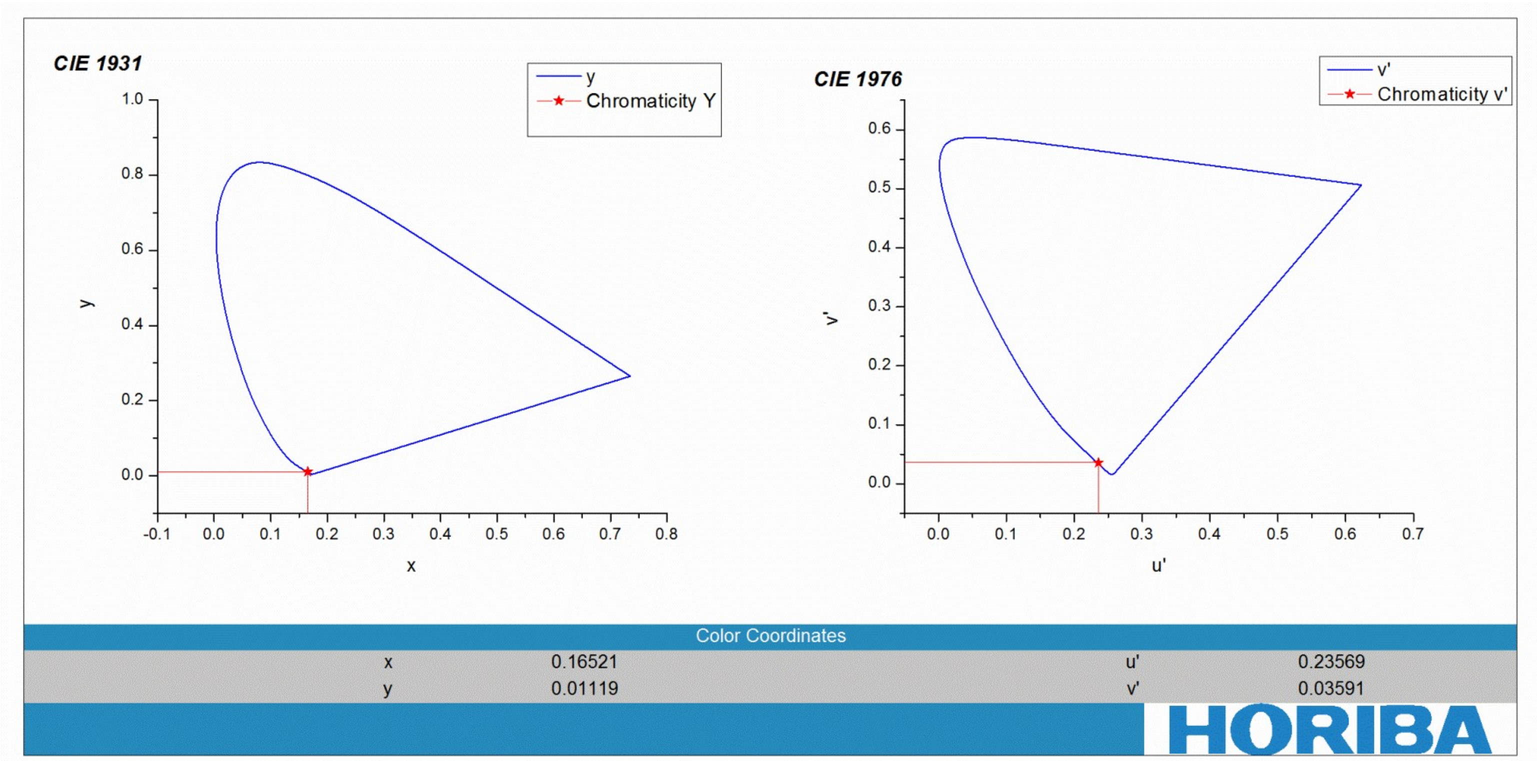

Compound 4c

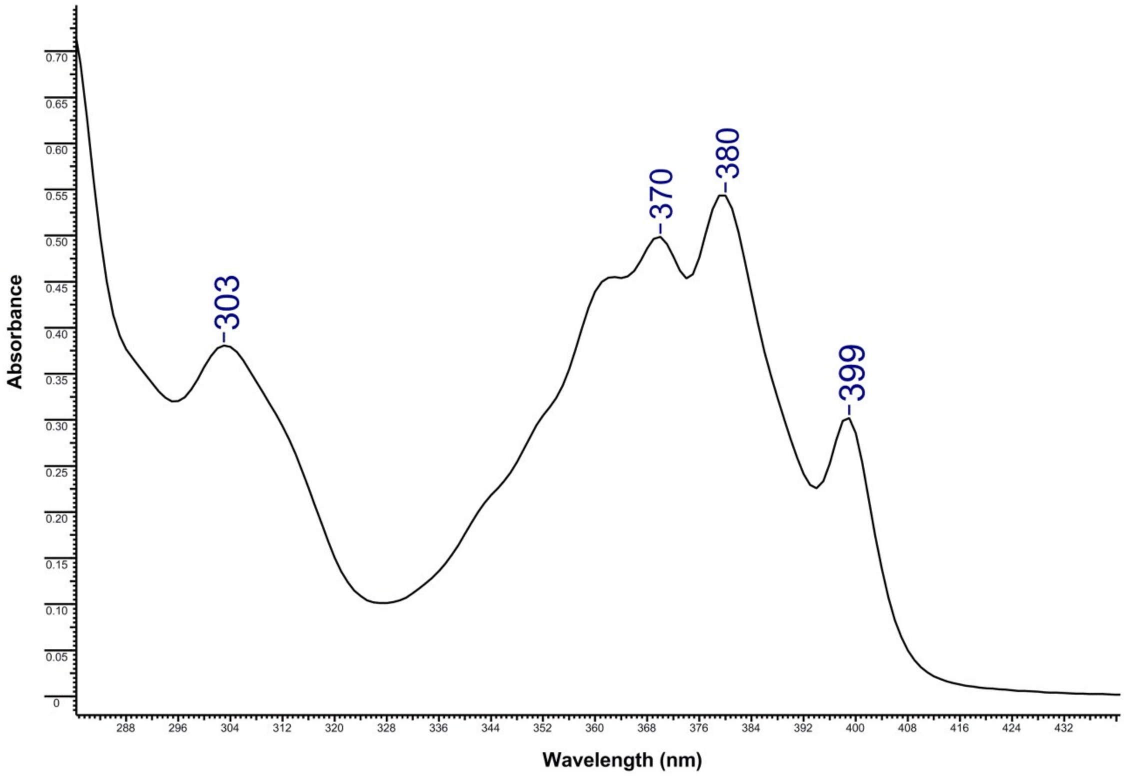

Fig.S47 Electronic absorption spectrum of compound **4c**

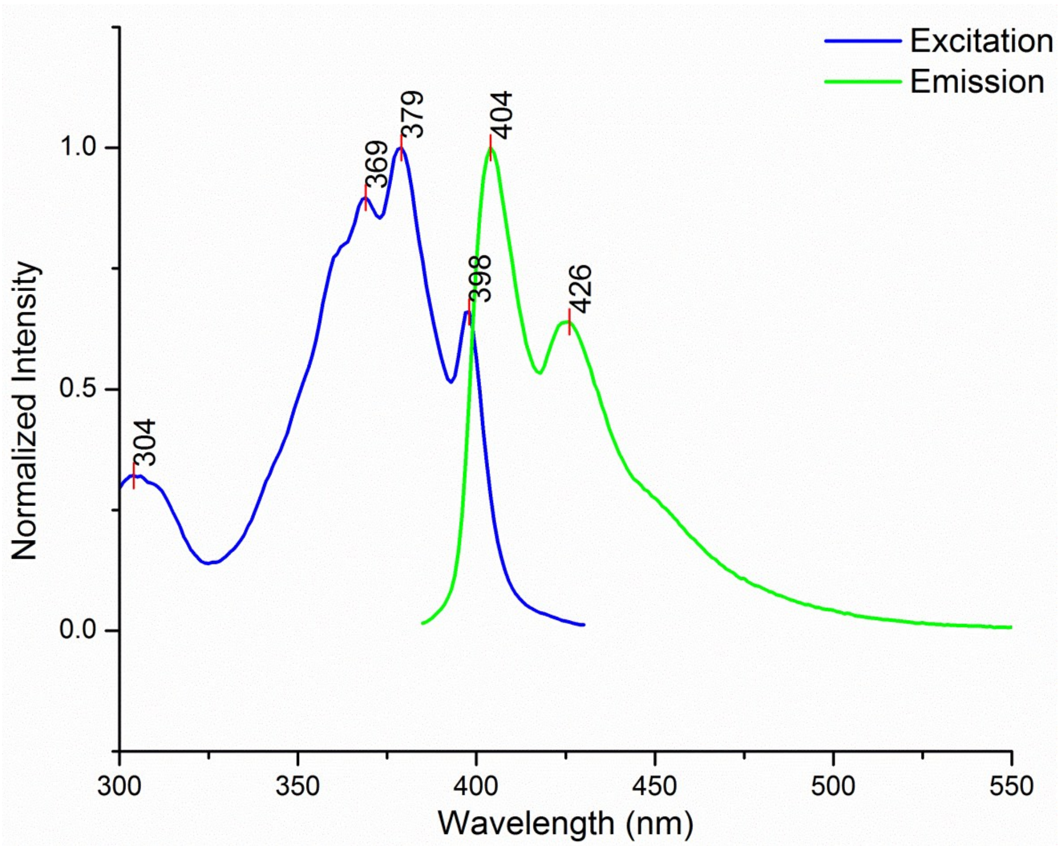

Fig.S48 Fluorescence excitation and emission spectrum of compound **4c**

Fluorescence quenching with 2,4-dinitritoluene in THF

The fluorescence quenching of the fluorophore **4c** (1.0×10^{-5} M) with 2, 4-dinitrotoluene (2.0×10^{-3} M) was carried out in THF.

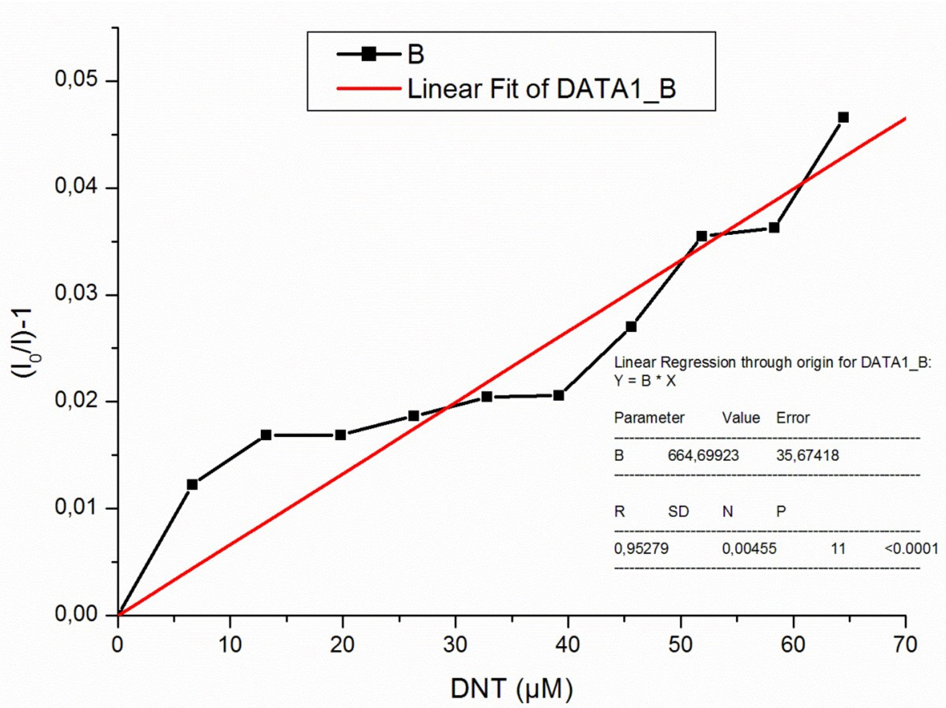

Fig.S49 Stern-Volmer plot

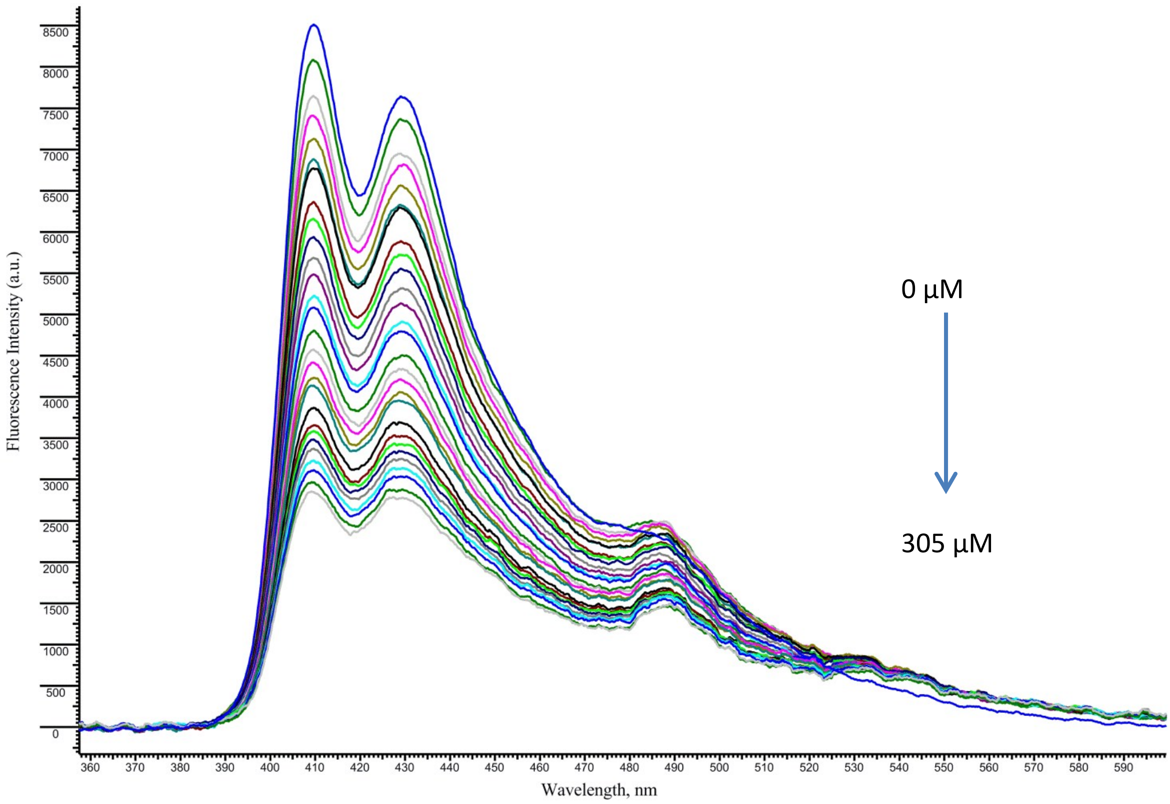

Fig.S50 Fluorescence quenching of the fluorophore **4c** with 2,4-DNT in THF

Fluorescence quenching with trinitrotoluene in THF

The fluorescence quenching of the fluorophore **4c** (1.0×10^{-5} M) with trinitrotoluene (2.0×10^{-3} M) was carried out in THF.

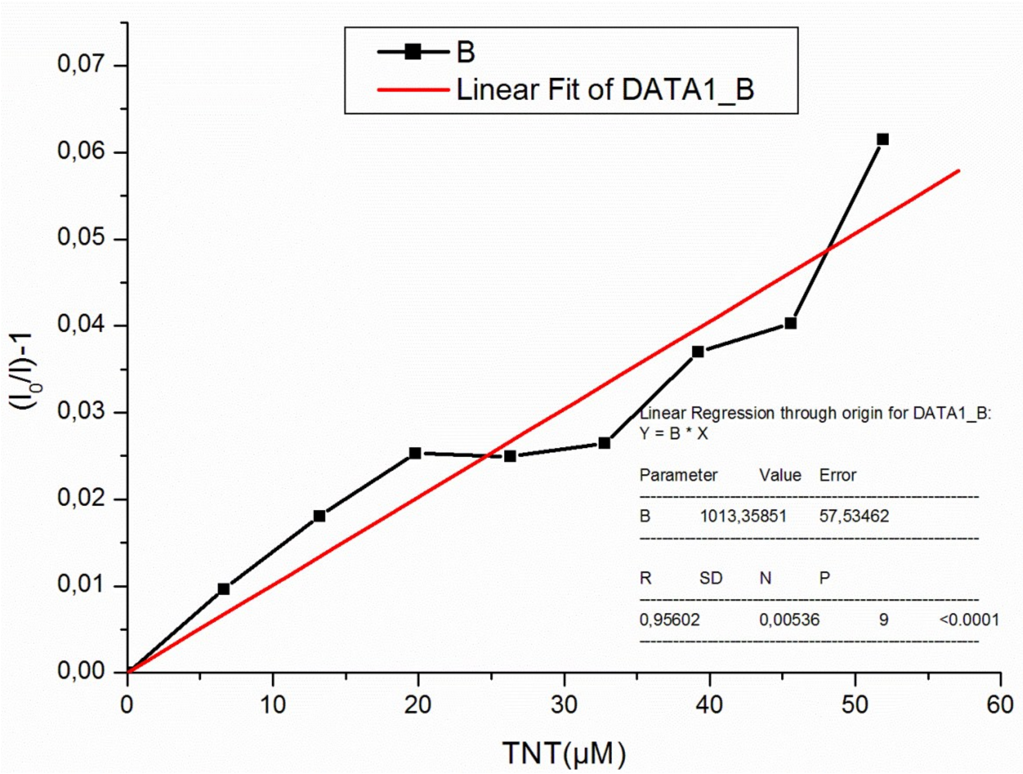

Fig.S51 Stern-Volmer plot

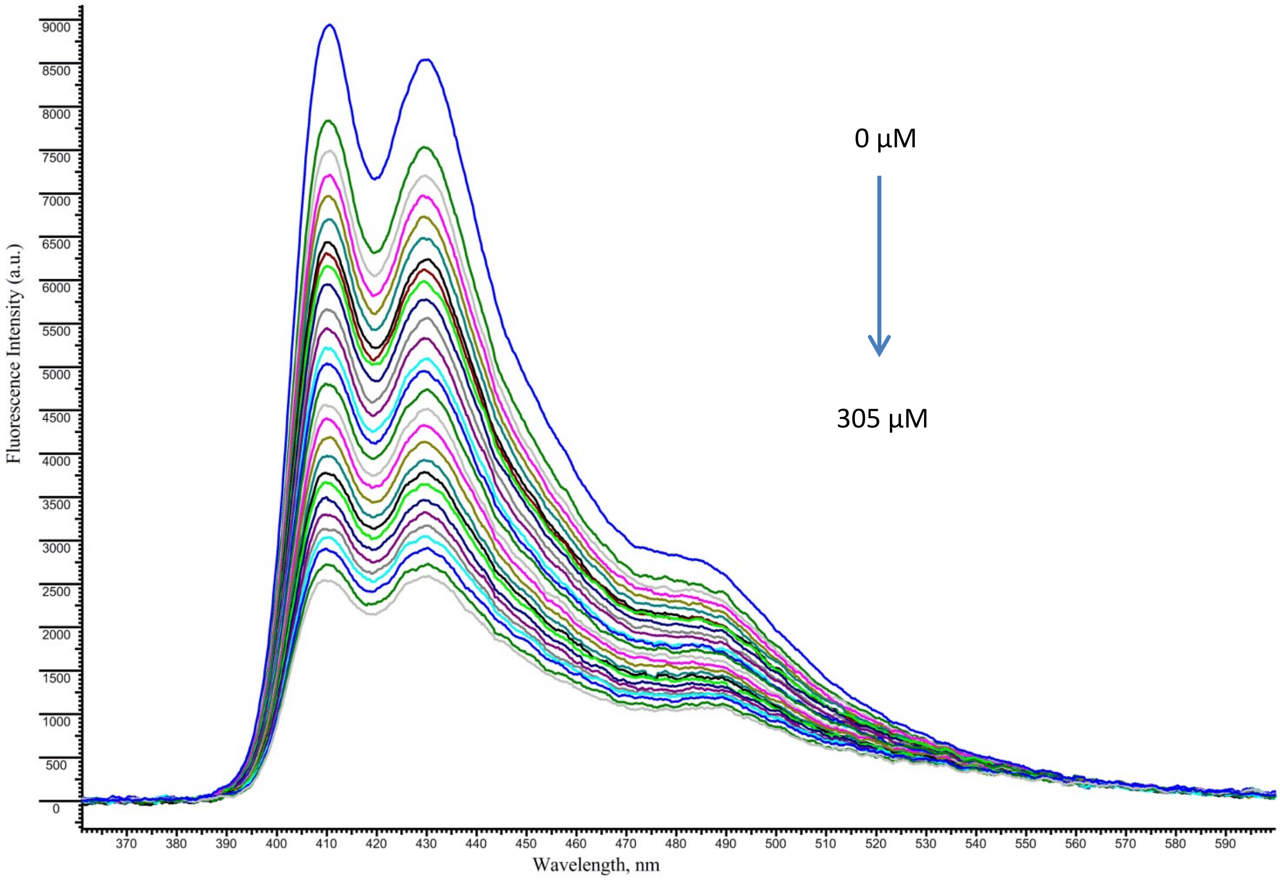

Fig.S52 Fluorescence quenching of the fluorophore **4c** with TNT in THF

Fluorescence quenching with picric acid in THF

The fluorescence quenching of the fluorophore **4c** (1.0×10^{-5} M) with picric acid (2.0×10^{-3} M) was carried out in THF.

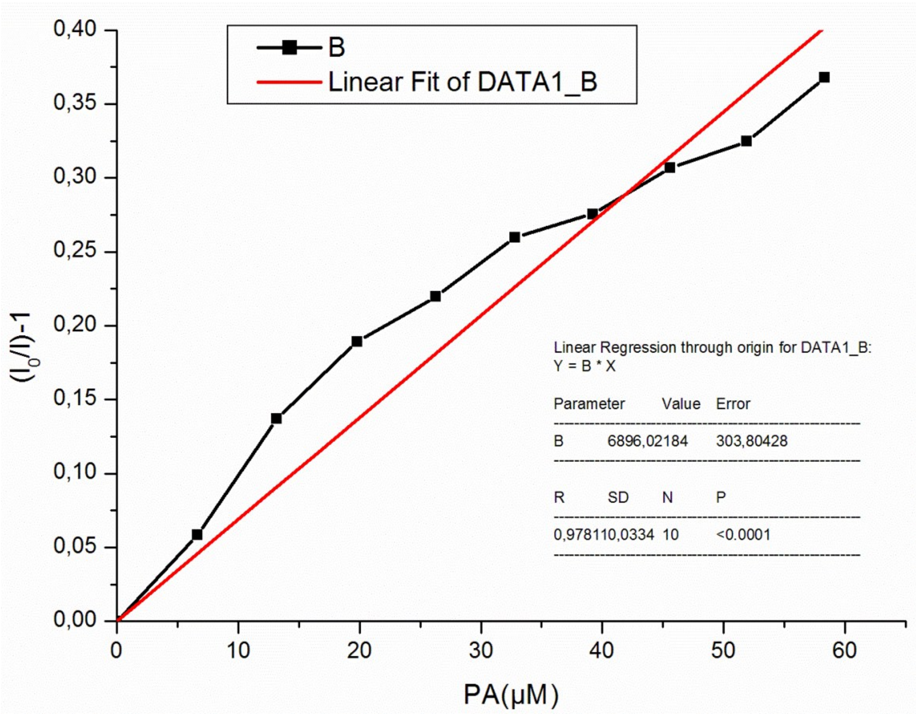

Fig.S53 Stern-Volmer plot

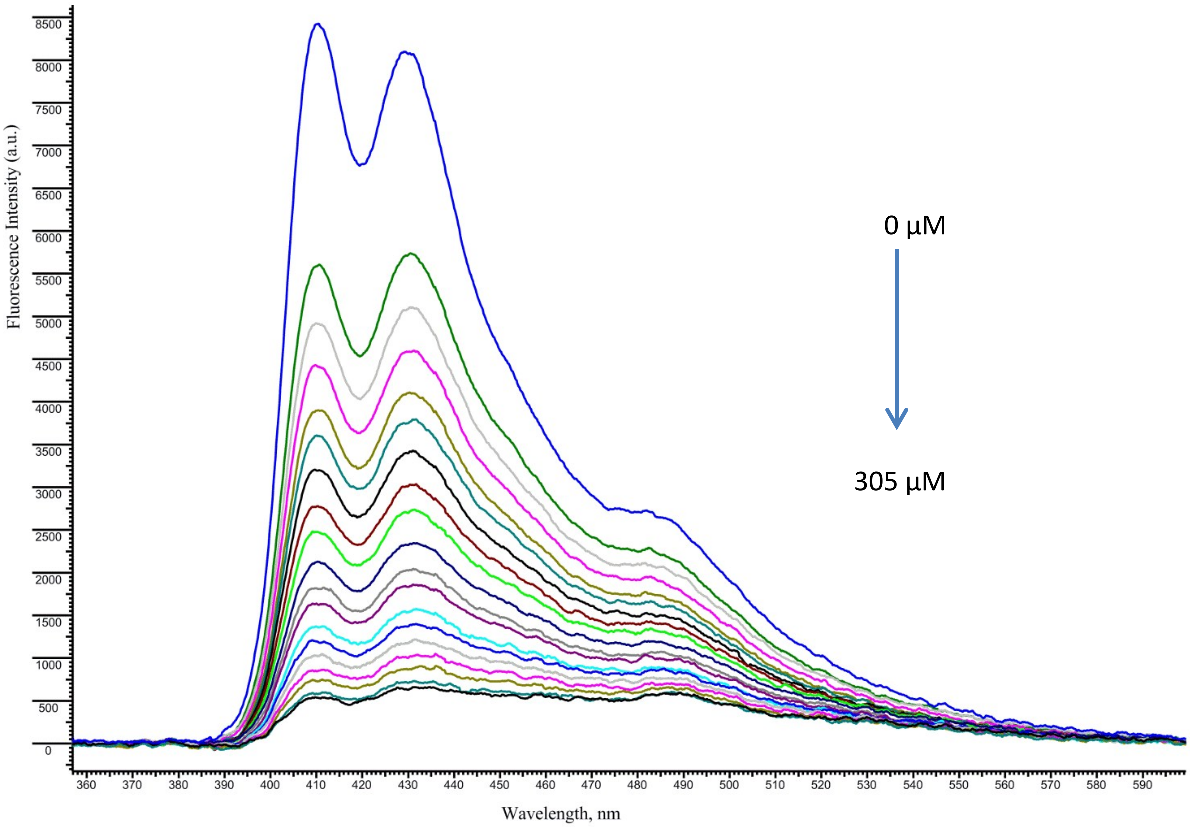

Fig.S54 Fluorescence quenching of the fluorophore **4c** with PA in THF

	Ksv (R) in THF
DNT	665 (R=0.9528)
TNT	1013 (R=0.9560)
PA	6896 (R=0.9781)

Estimation of the detection limit for sensor 4c

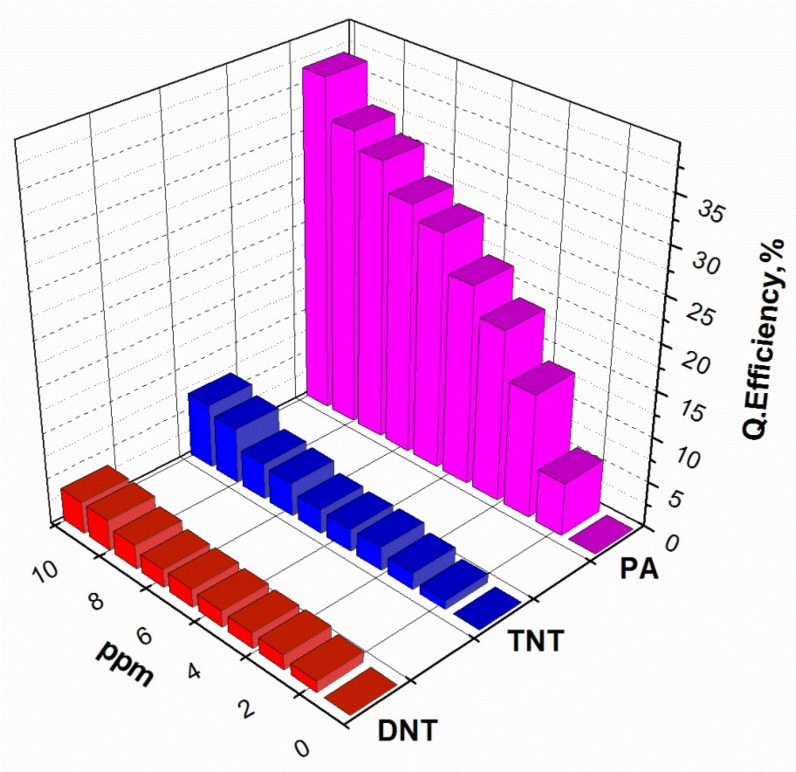

Fig.S55 Estimation of the detection limit for sensor **4c**

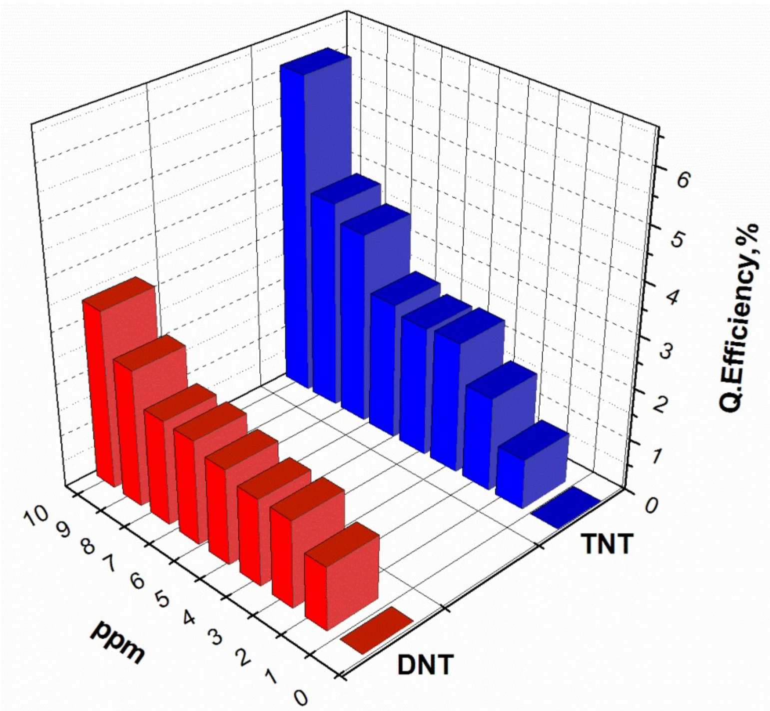

Fig.S56 Estimation of the detection limit for sensor **4c**

PLQY

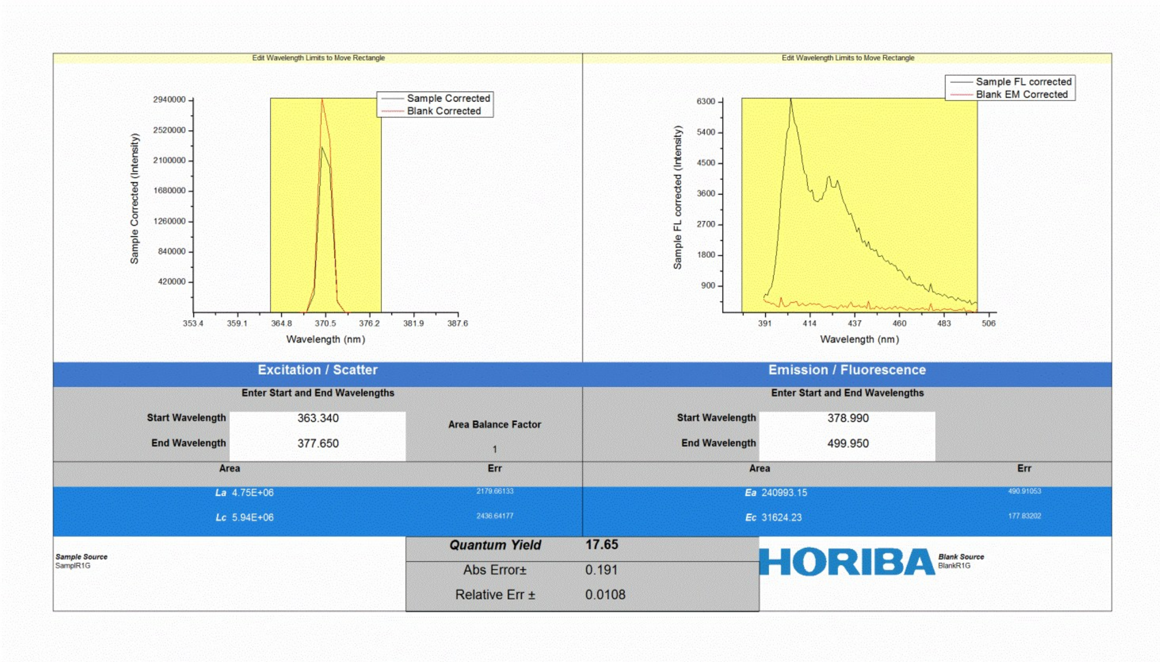
Edit Wavelength Limits to Move Rectangle
Sample Corrected
Blank Corrected
Sample Corrected (Intensity)
Wavelength (nm)
Edit Wavelength Limits to Move Rectangle
Sample FL corrected
Blank EM Corrected
Sample FL corrected (Intensity)
Wavelength (nm)
Excitation / Scatter
Enter Start and End Wavelengths
Start Wavelength 363.340
End Wavelength 377.650
Area Balance Factor 1
Area
Err
La 4.75E+06
Lc 5.94E+06
Emission / Fluorescence
Enter Start and End Wavelengths
Start Wavelength 378.990
End Wavelength 499.950
Area
Err
Ea 240993.15
Ec 31624.23
Sample Source SamplR1G
Quantum Yield 17.65
Abs Error± 0.191
Relative Err ± 0.0108
HORIBA
Blank Source BlankR1G

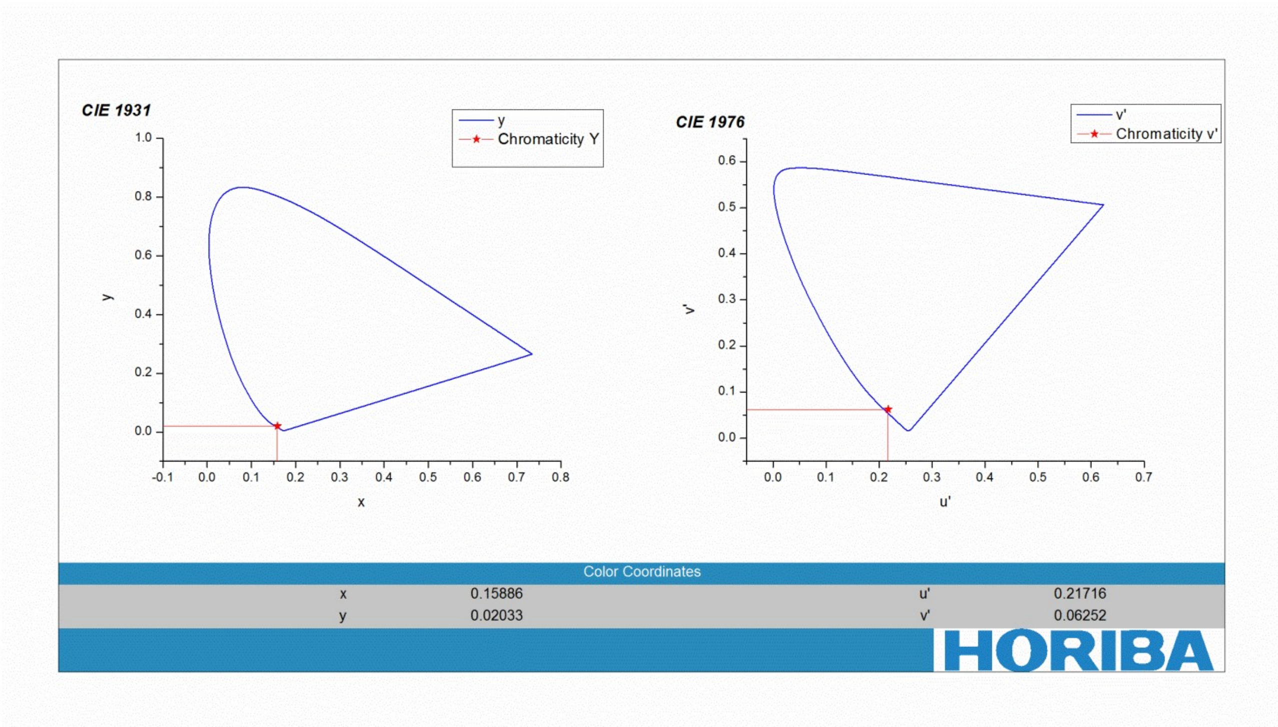
CIE 1931
y
Chromaticity Y
x
CIE 1976
v'
Chromaticity v'
u'
Color Coordinates
x 0.15886
y 0.02033
u' 0.21716
v' 0.06252
HORIBA

Estimation of the detection limit presented in terms of the fluorescence quenching efficiency (%) after addition of TNT for all sensors

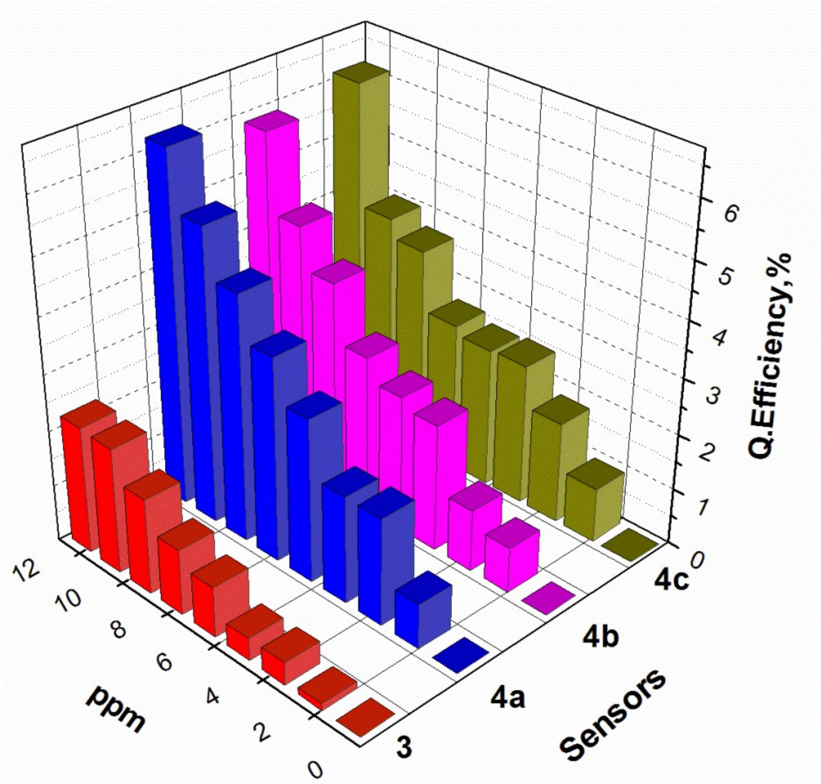

Fig.S57 Estimation of the detection limit presented in terms of the fluorescence quenching efficiency (%) after addition of TNT in THF with different concentrations

Fluorescence quenching with benzoquinone in THF

The fluorescence quenching of the fluorophore **4a** (1.0×10^{-6} M) with benzoquinone (2.0×10^{-2} M) was carried out in THF.

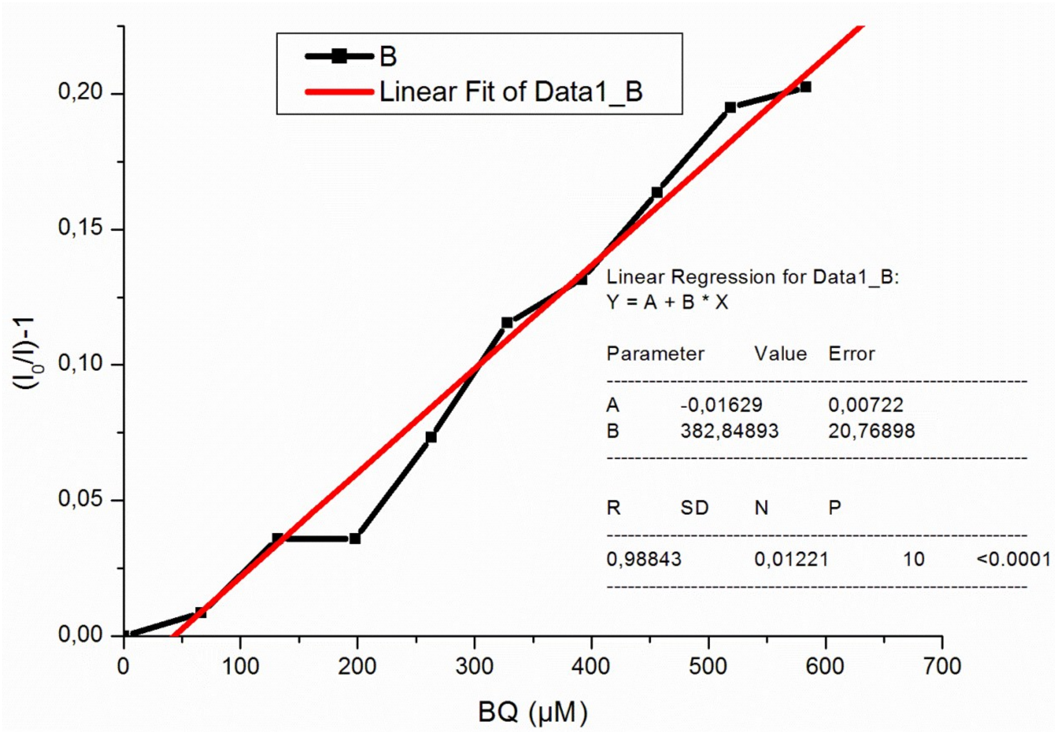

Fig.58 Stern-Volmer plot

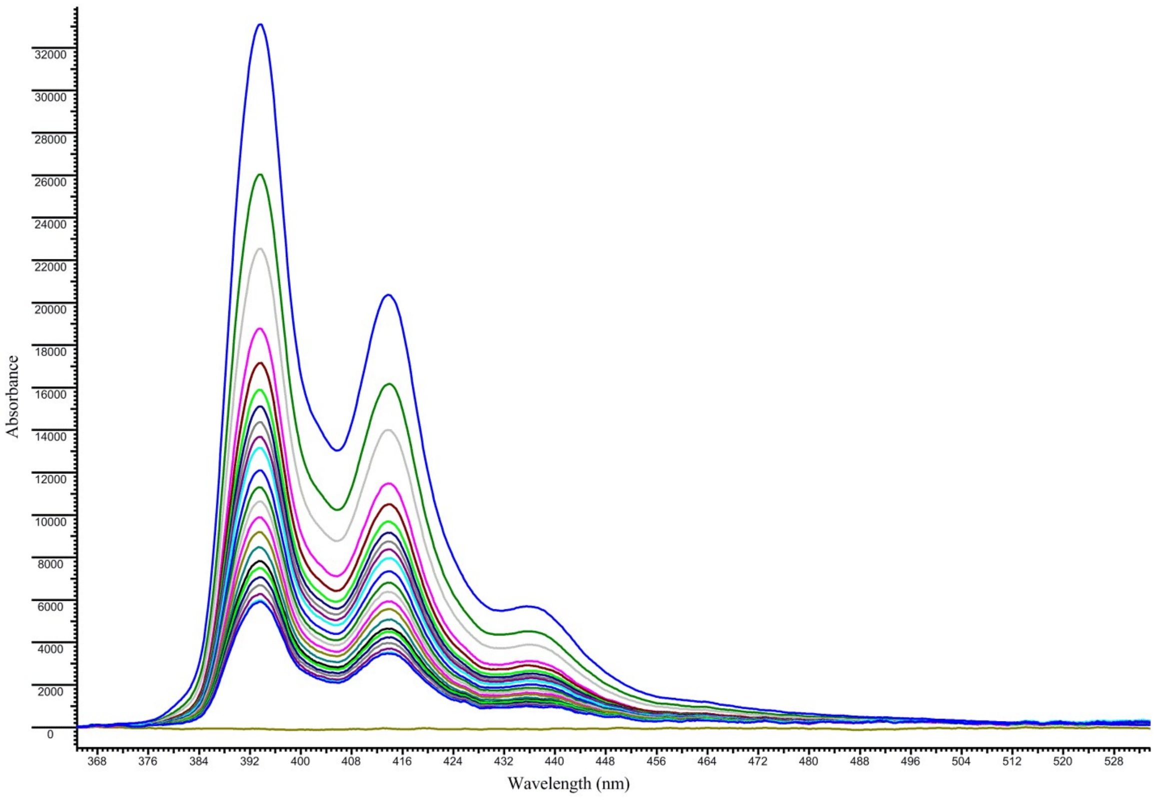

Fig.59 Fluorescence quenching of the fluorophore **4a** with benzoquinone in THF

The detection of lifetime of 4a fluorophore at different mole ratios of TNT and RDX

Table S1 Fluorescence lifetime data of pure **4a** fluorophore at different mole ratios of TNT

Mole ratio vs TNT	**4a fluorophore (ns)** **τ**
0,0	4,780
1:0,2	4,629
1:0,4	4,521
1:0,6	4,606
1:0,8	4,631
1:1,0	4,804
1:1,2	4,794

	0 eq	0.2 eq	0.4 eq	0.6 eq	0.8 eq	1.0 eq	1.2 eq
A	7,7861E-01	6,7935E-01	7,1202E-01	6,6055E-01	6,6179E-01	7,0080E-01	6,6318E-01
B1	-1,0671E-01	-1,0358E-01	-1,1102E-01	-1,0412E-01	-1,1007E-01	-1,0086E-01	-1,0393E-01
B2	9,8272E-02	9,6092E-02	9,9563E-02	9,7781E-02	1,0121E-01	9,2815E-02	9,7432E-02
B3	3,9659E-03	3,2914E-03	3,6824E-03	3,3812E-03	3,5095E-03	3,5837E-03	3,4578E-03
T1	3,6578E-10	3,4803E-10	3,4328E-10	3,5607E-10	3,5237E-10	3,3519E-10	3,4863E-10
T2	1,3749E-09	1,3514E-09	1,3393E-09	1,3443E-09	1,3428E-09	1,3965E-09	1,3801E-09
T3	4,7803E-09	4,6295E-09	4,5212E-09	4,6065E-09	4,6307E-09	4,8045E-09	4,7937E-09

$$F(x) = A + B1 * \exp\left(-\frac{x}{T1}\right) + B2 * exp\left(-\frac{x}{T2}\right) + B3 * exp\left(-\frac{x}{T3}\right)$$

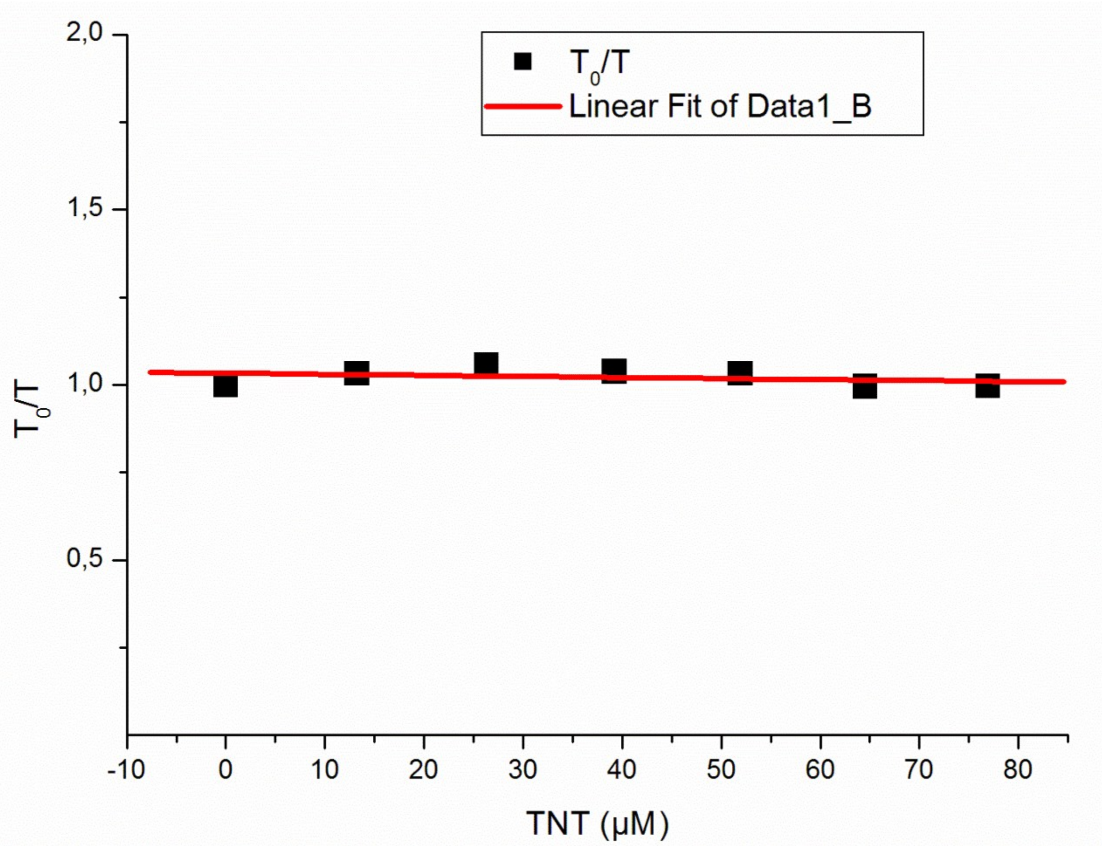

Fig.S60 T_0/T at 410 nm (λ_{ex}=375 nm) of **4a** as a function of the concentration of the quencher (TNT)

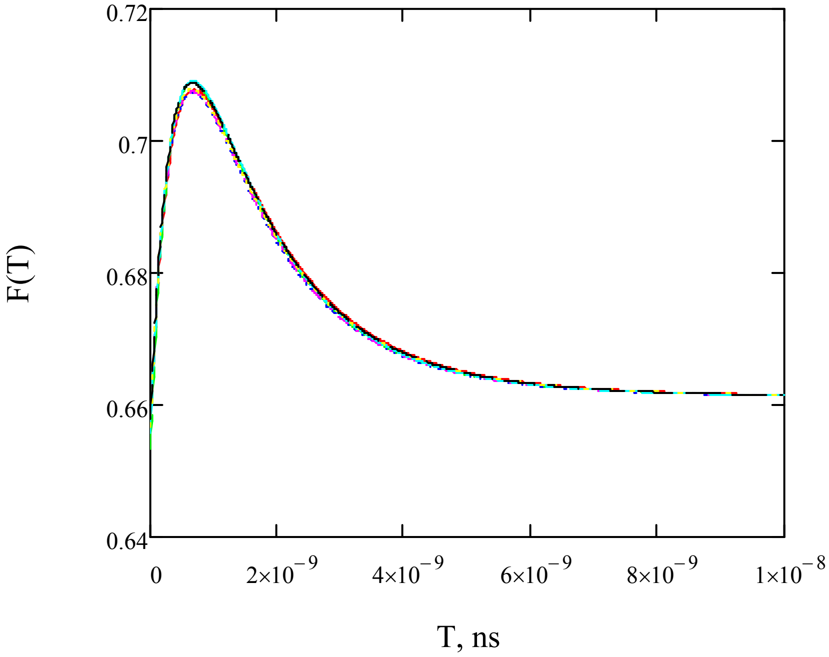

Fig.S61 F(T) of **4a** as a function of the concentration of the lifetime (T)

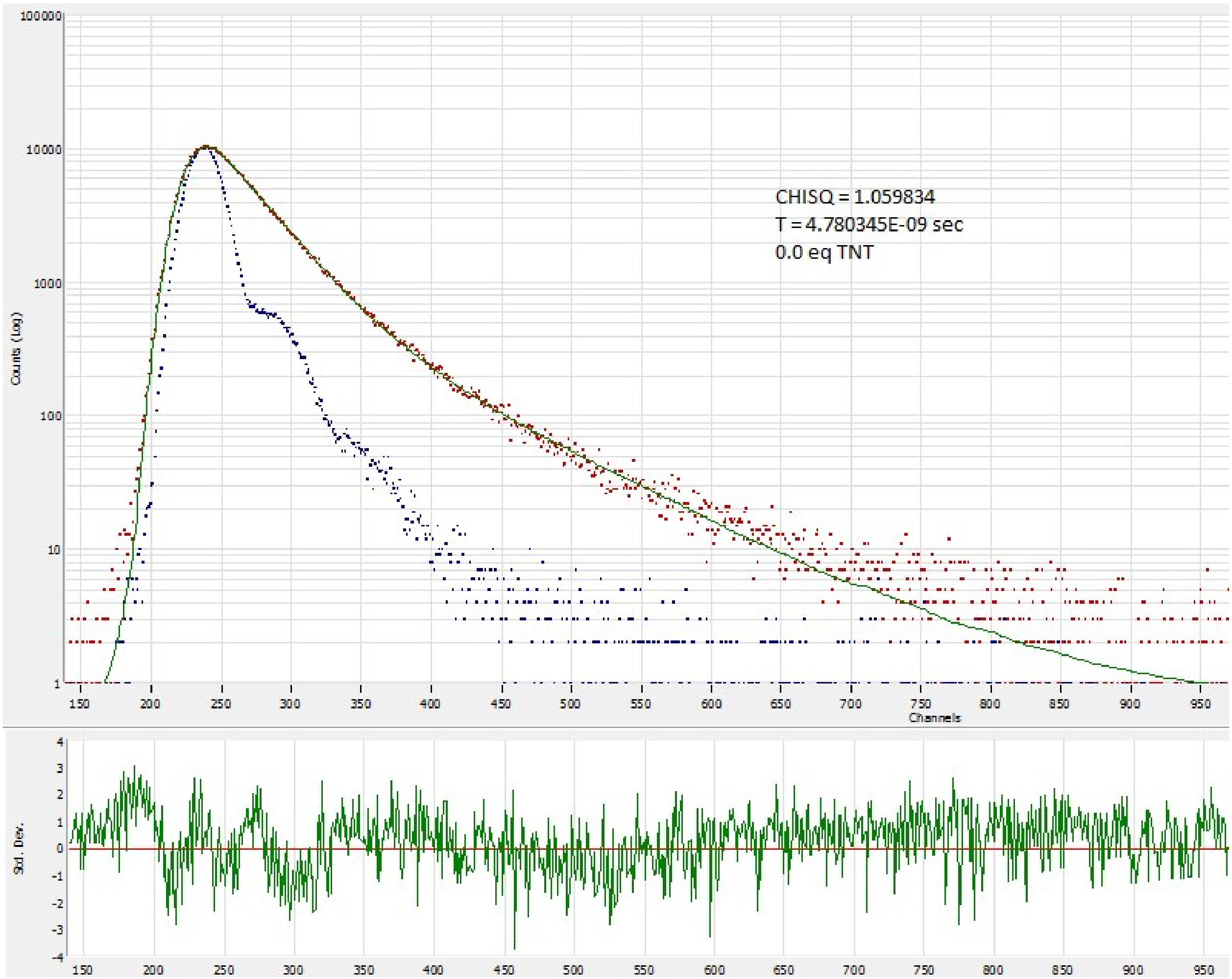

Fig. S62 Time-resolved fluorescence emission of **4a** adduct with TNT

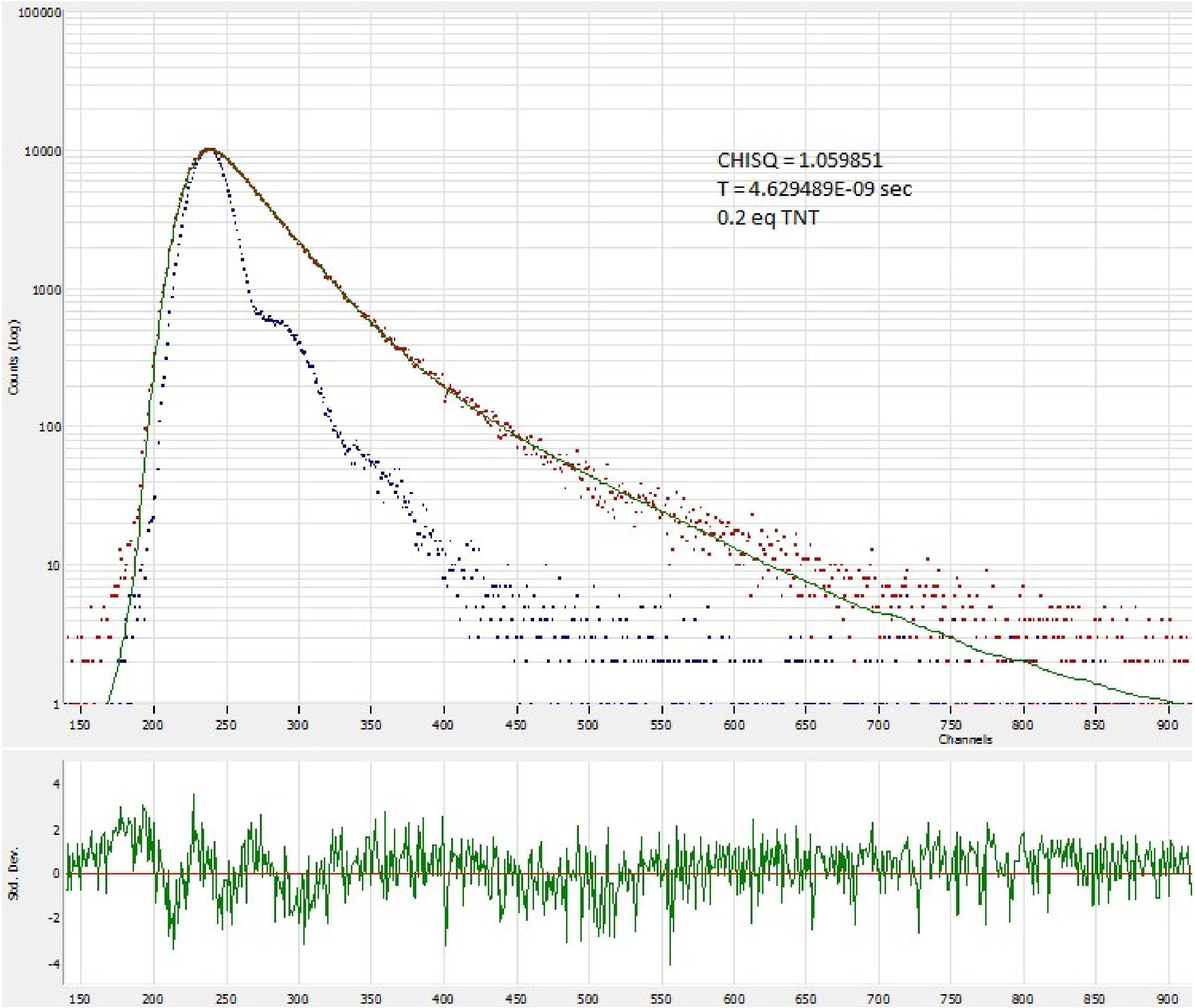

Fig.S63 Time-resolved fluorescence emission of **4a** adduct with TNT

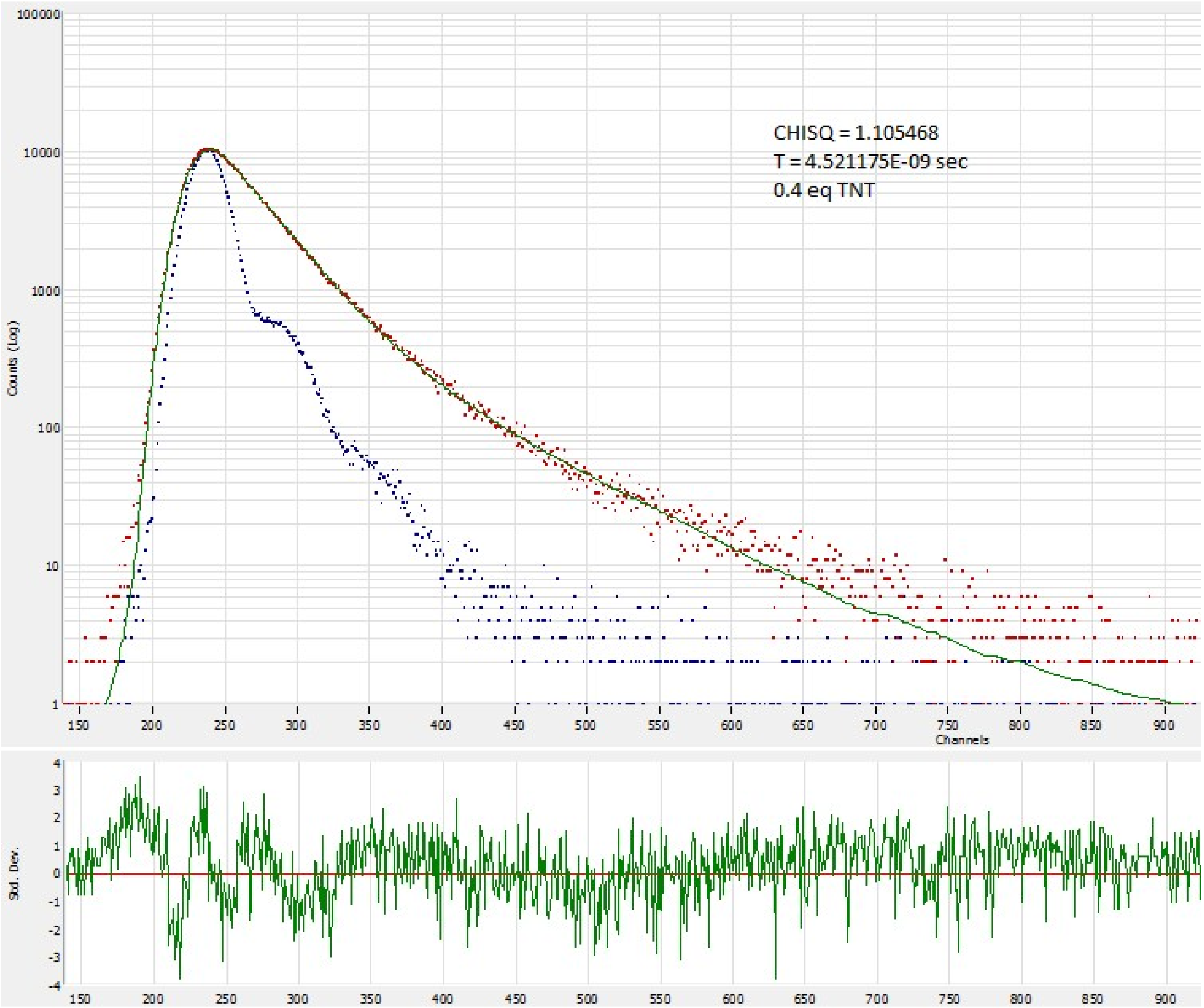

Fig.S64 Time-resolved fluorescence emission of **4a** adduct with TNT

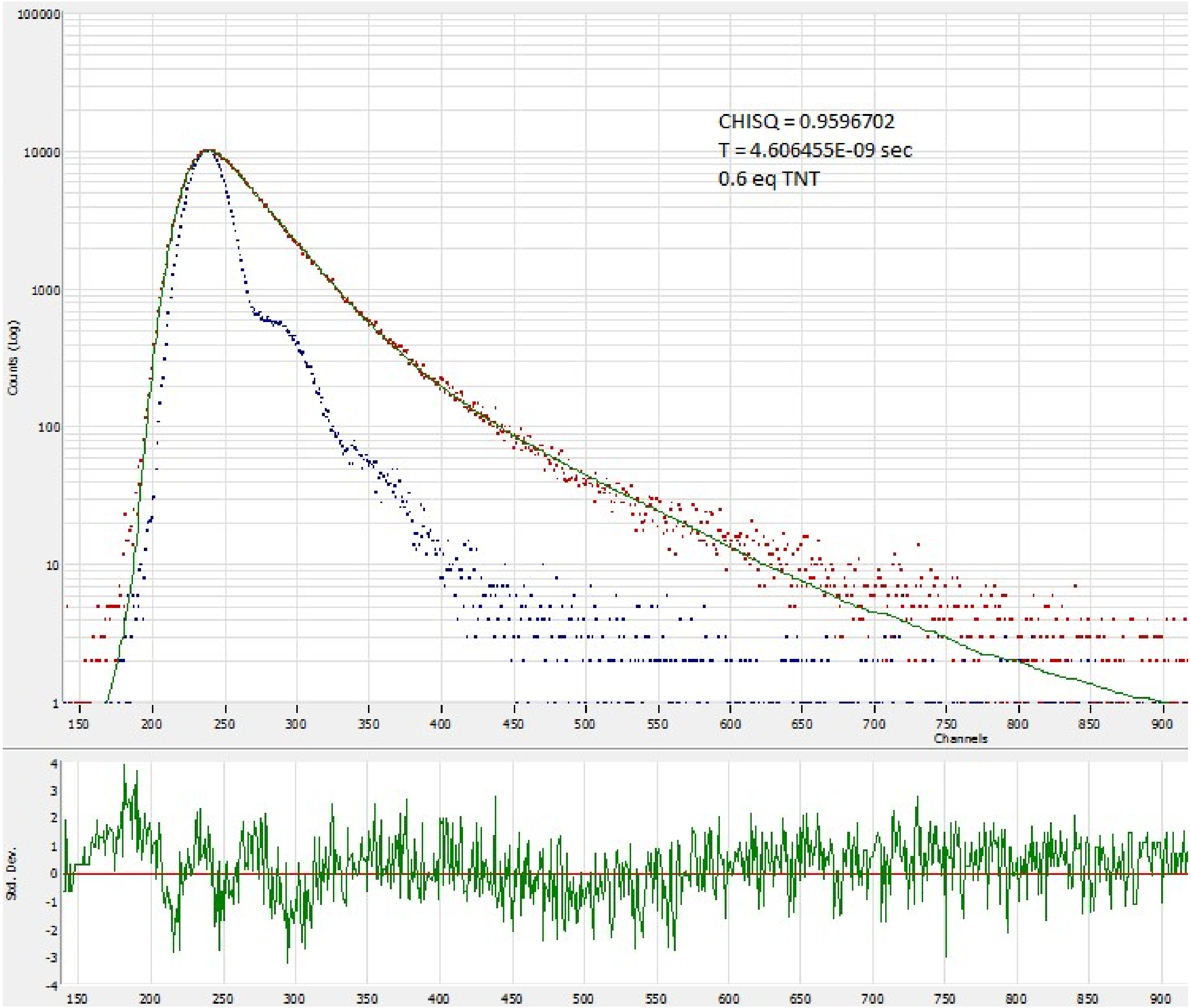

Fig.S65 Time-resolved fluorescence emission of **4a** adduct with TNT

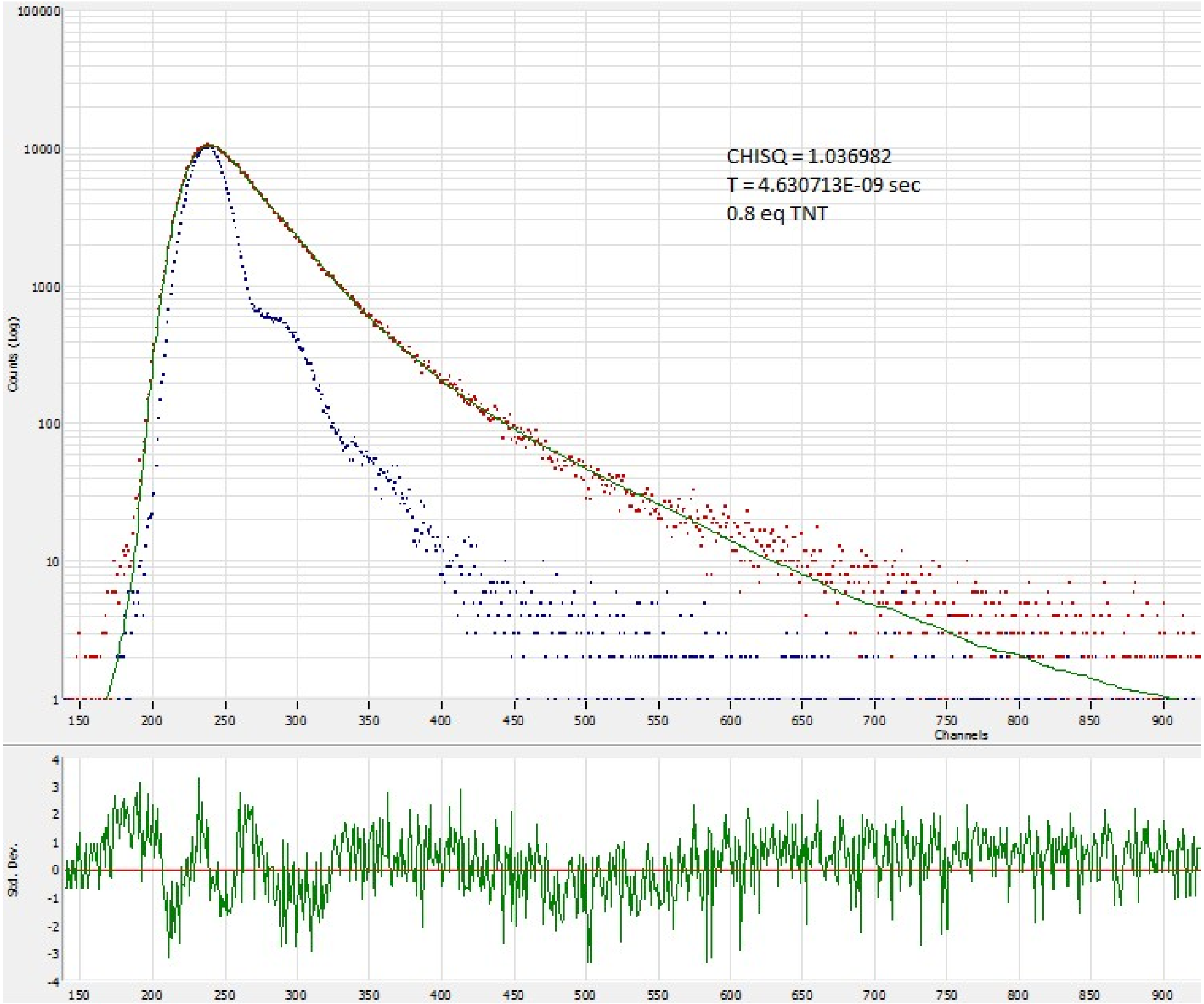

Fig.S66 Time-resolved fluorescence emission of **4a** adduct with TNT

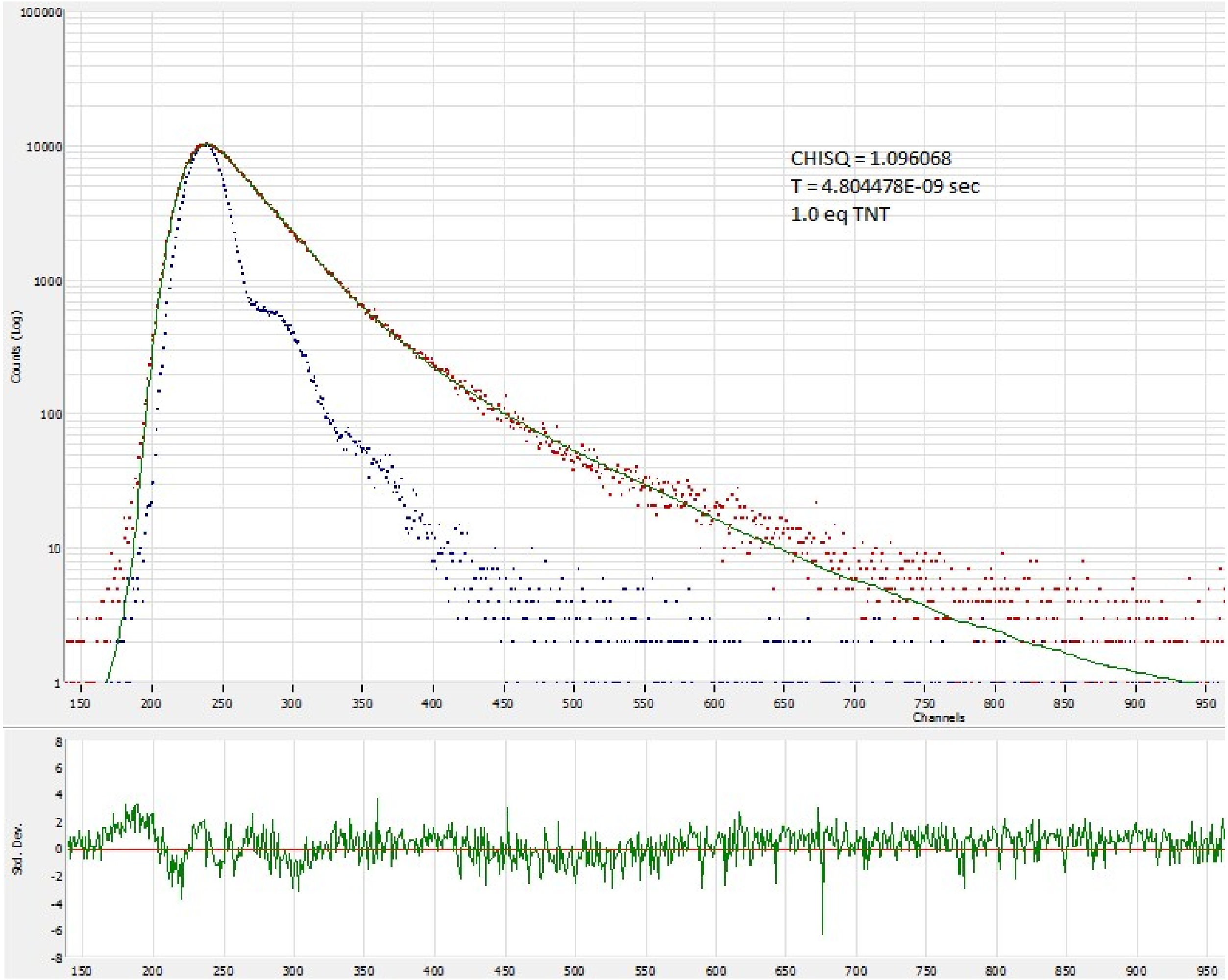

Fig.S67 Time-resolved fluorescence emission of **4a** adduct with TNT

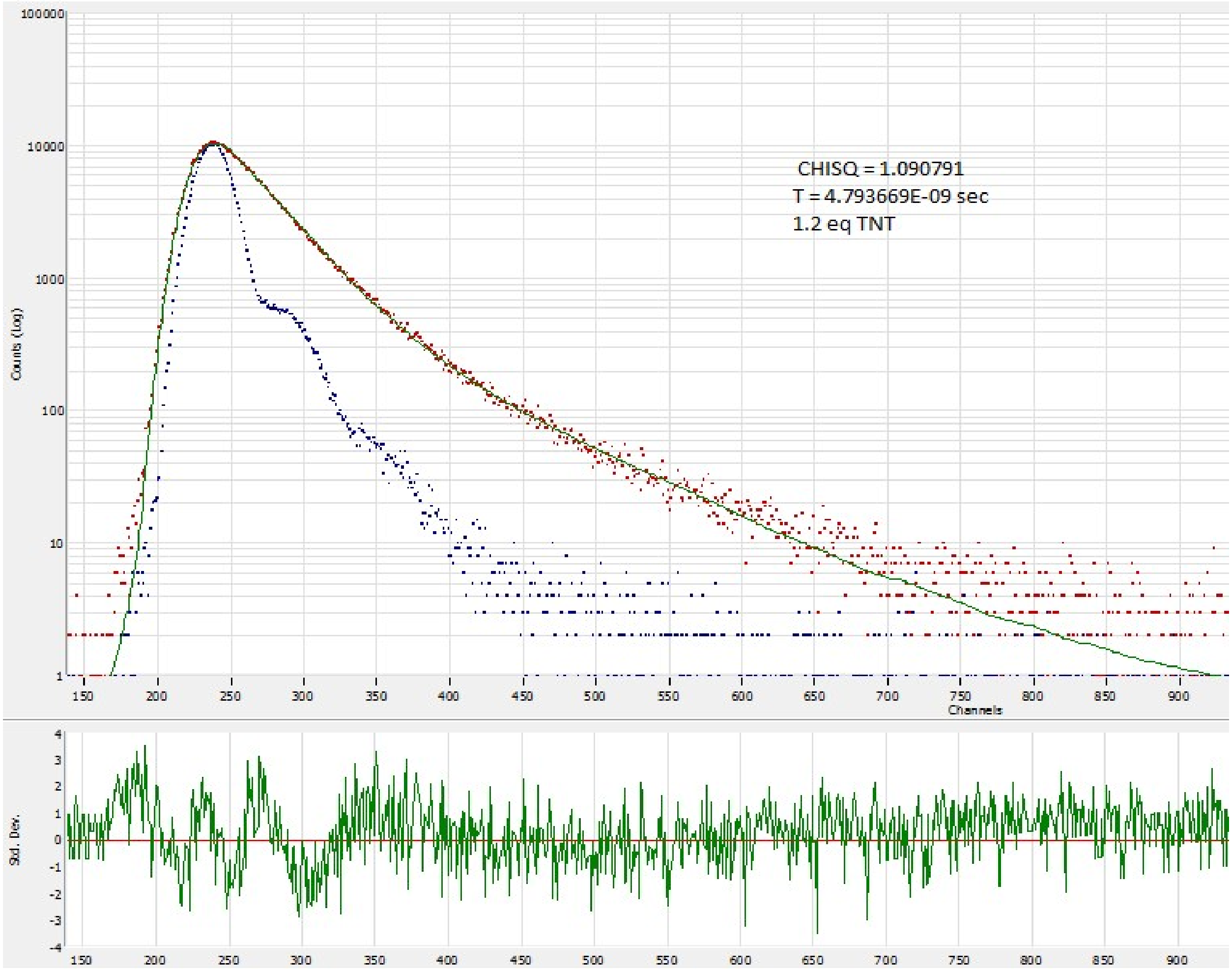

Fig. S68 Time-resolved fluorescence emission of **4a** adduct with TNT

Table S2 Fluorescence lifetime data of pure **4a** fluorophore at different mole ratios of RDX

Mole ratio vs RDX	**4a fluorophore (ns) τ**
0,0	4,780
1:0,2	4,848
1:0,4	5,030
1:0,6	4,853
1:0,8	4,873
1:1,0	5,096
1:1,2	5,055

	0 eq	0.2 eq	0.4 eq	0.6 eq	0.8 eq	1.0 eq	1.2 eq
A	7,1327E-01	7,5777E-01	7,2002E-01	7,0253E-01	6,6691E-01	7,5615E-01	7,4626E-01
B1	-9,6570E-02	-9,7154E-02	-8,9702E-02	-1,0262E-01	-9,7272E-02	-9,4523E-02	-9,4775E-02
B2	8,8529E-02	8,9827E-02	8,2111E-02	9,0933E-02	8,6985E-02	8,5049E-02	8,3076E-02
B3	3,2474E-03	3,7888E-03	3,3031E-03	3,3421E-03	3,2048E-03	3,5147E-03	3,5206E-03
T1	2,9035E-10	2,9863E-10	2,6329E-10	2,8621E-10	2,6715E-10	2,5702E-10	2,7255E-10
T2	1,3568E-09	1,3839E-09	1,4260E-09	1,3688E-09	1,3886E-09	1,4338E-09	1,4317E-09
T3	4,7803E-09	4,8476E-09	5,0301E-09	4,8532E-09	4,8727E-09	5,0957E-09	5,0551E-09

$$F(x) = A + B1 * \exp\left(-\frac{x}{T1}\right) + B2 * exp\left(-\frac{x}{T2}\right) + B3 * exp\left(-\frac{x}{T3}\right)$$

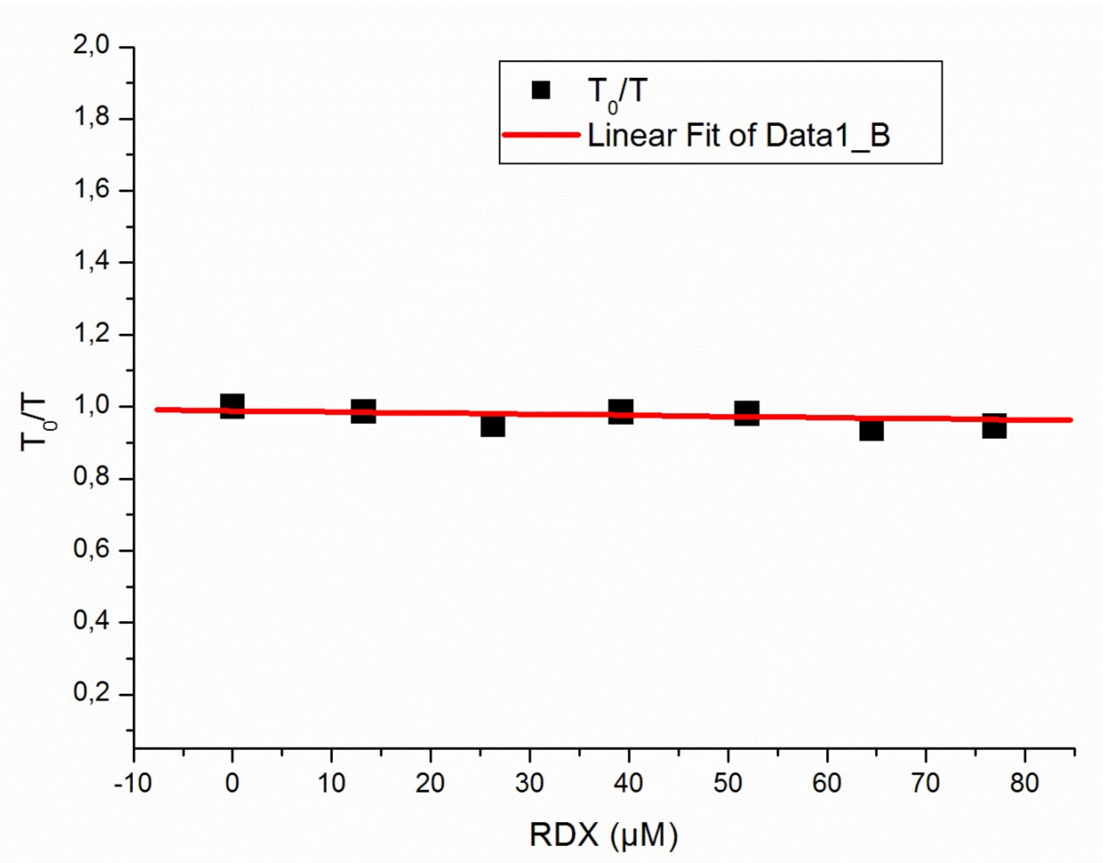

Fig.S69 T_0/T at 410 nm (λ_{ex}=375 nm) of **4a** as a function of the concentration of the quencher (RDX)

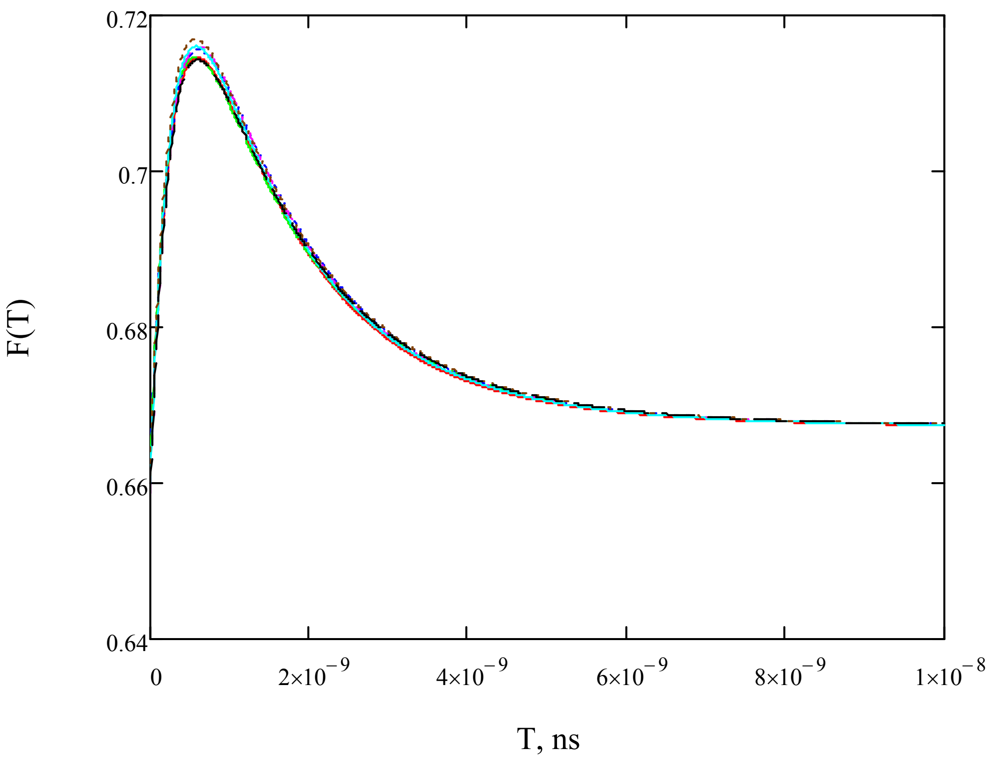

Fig.S70 F(T) of **4a** as a function of the concentration of the lifetime (T)

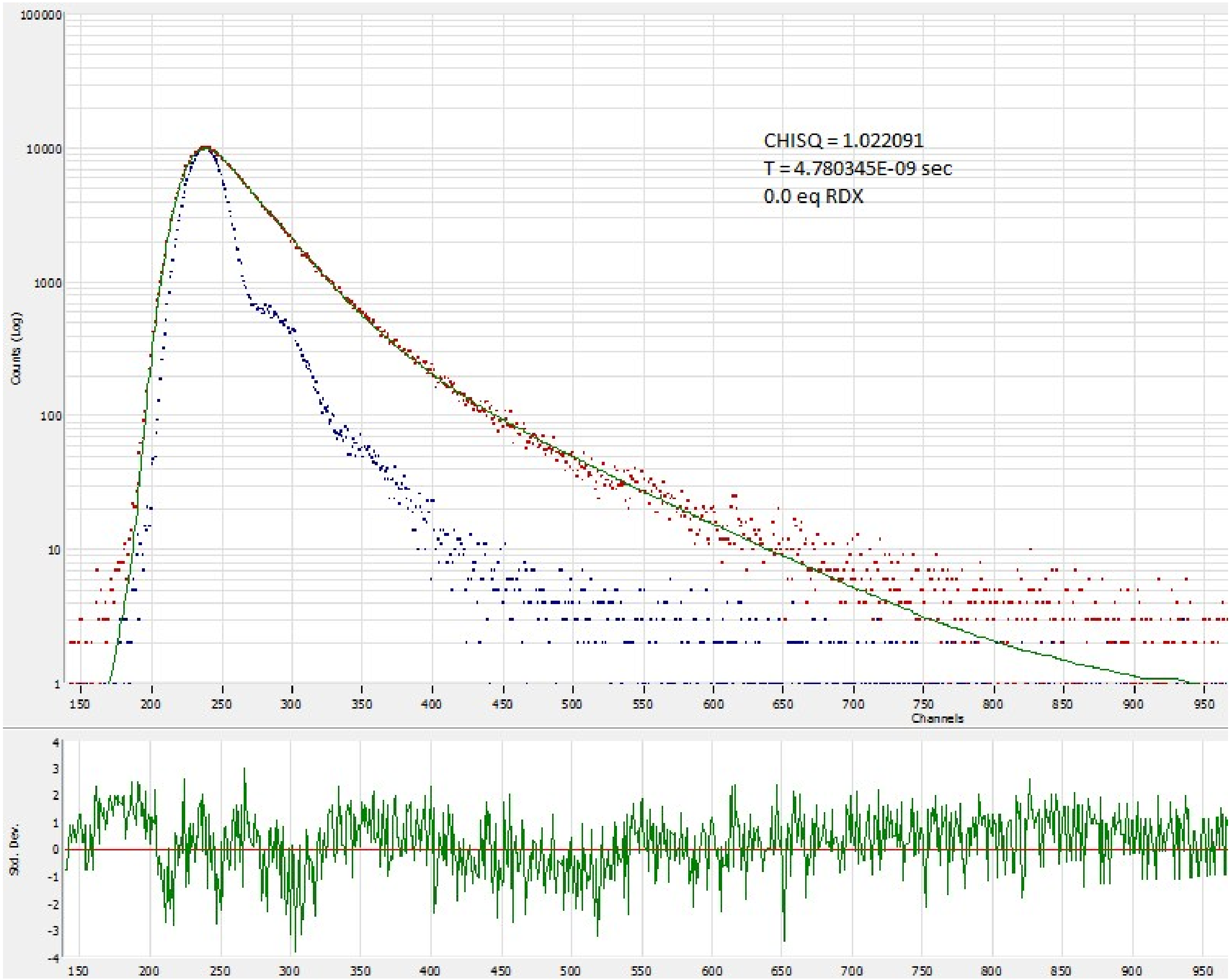

Fig.S71 Time-resolved fluorescence emission of **4a** adduct with RDX

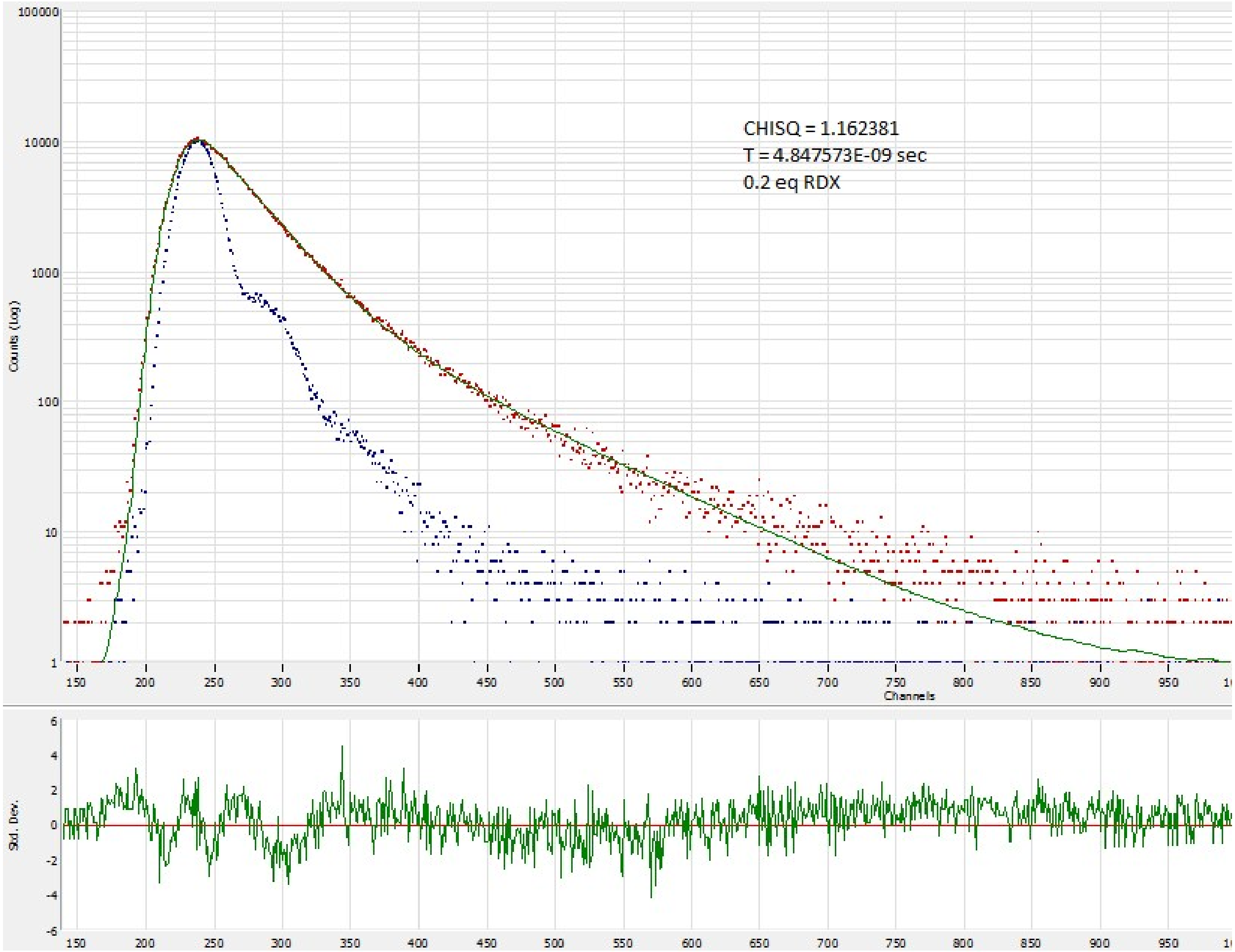

Fig.S72 Time-resolved fluorescence emission of **4a** adduct with RDX

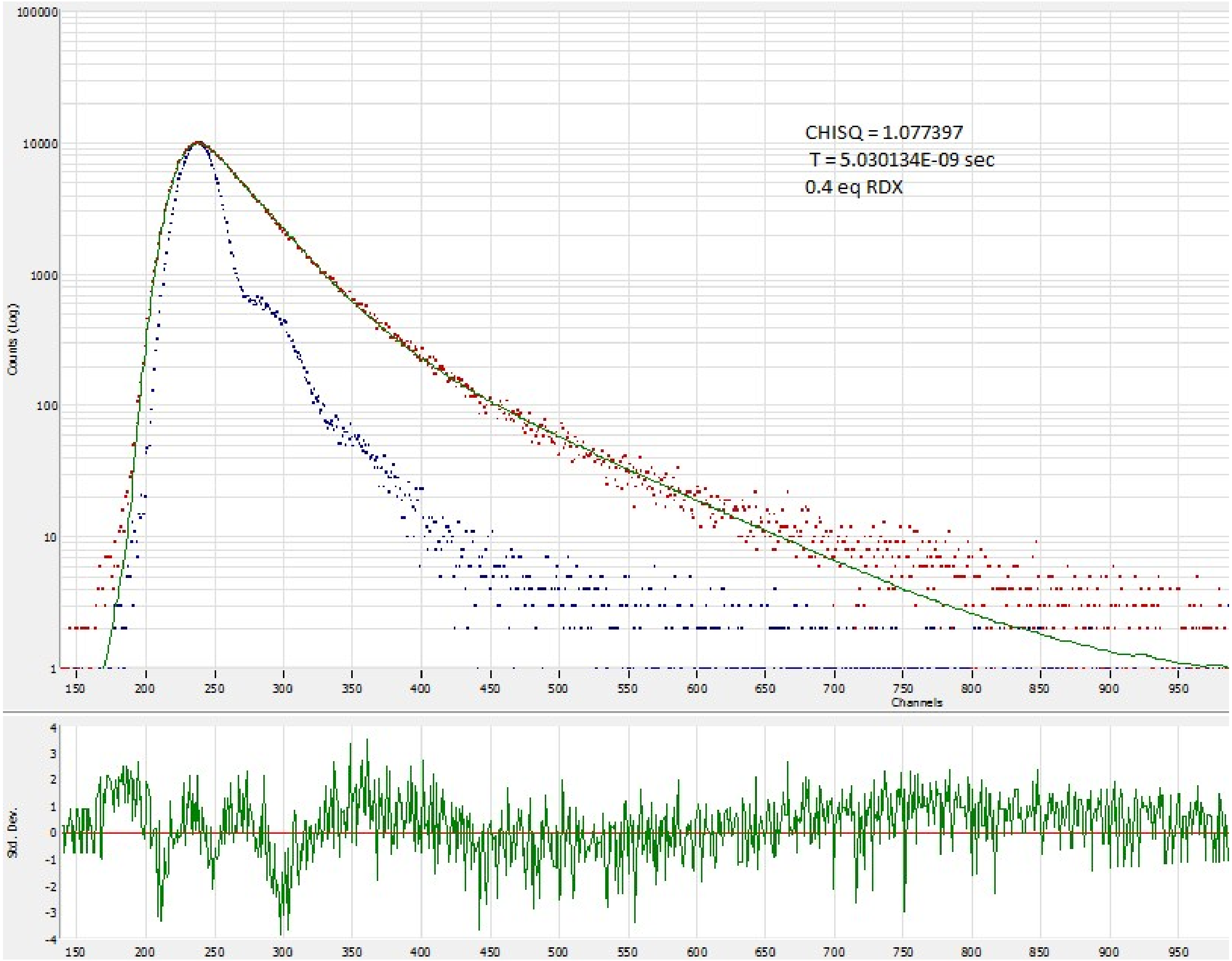

Fig.S73 Time-resolved fluorescence emission of **4a** adduct with RDX

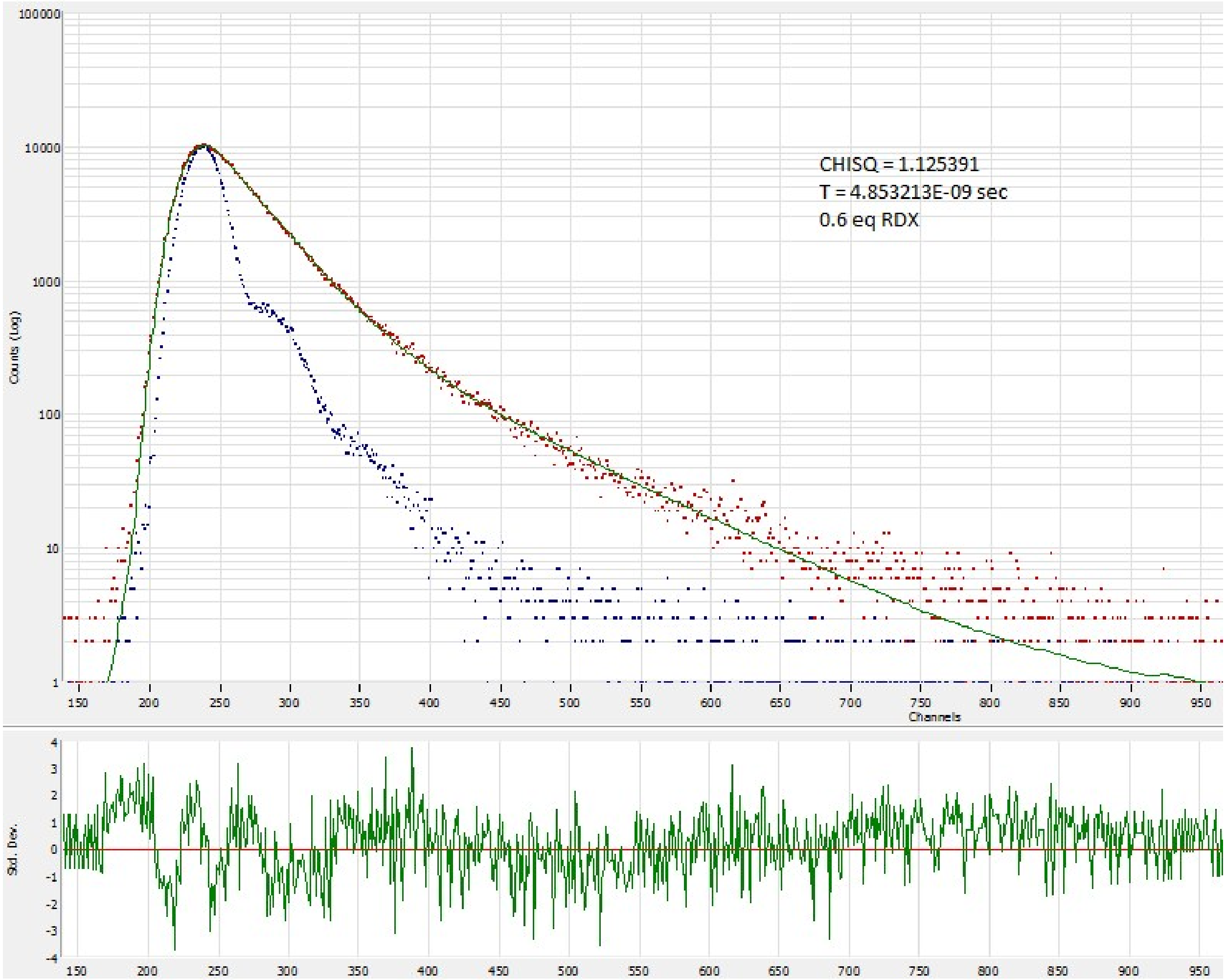

Fig.S74 Time-resolved fluorescence emission of **4a** adduct with RDX

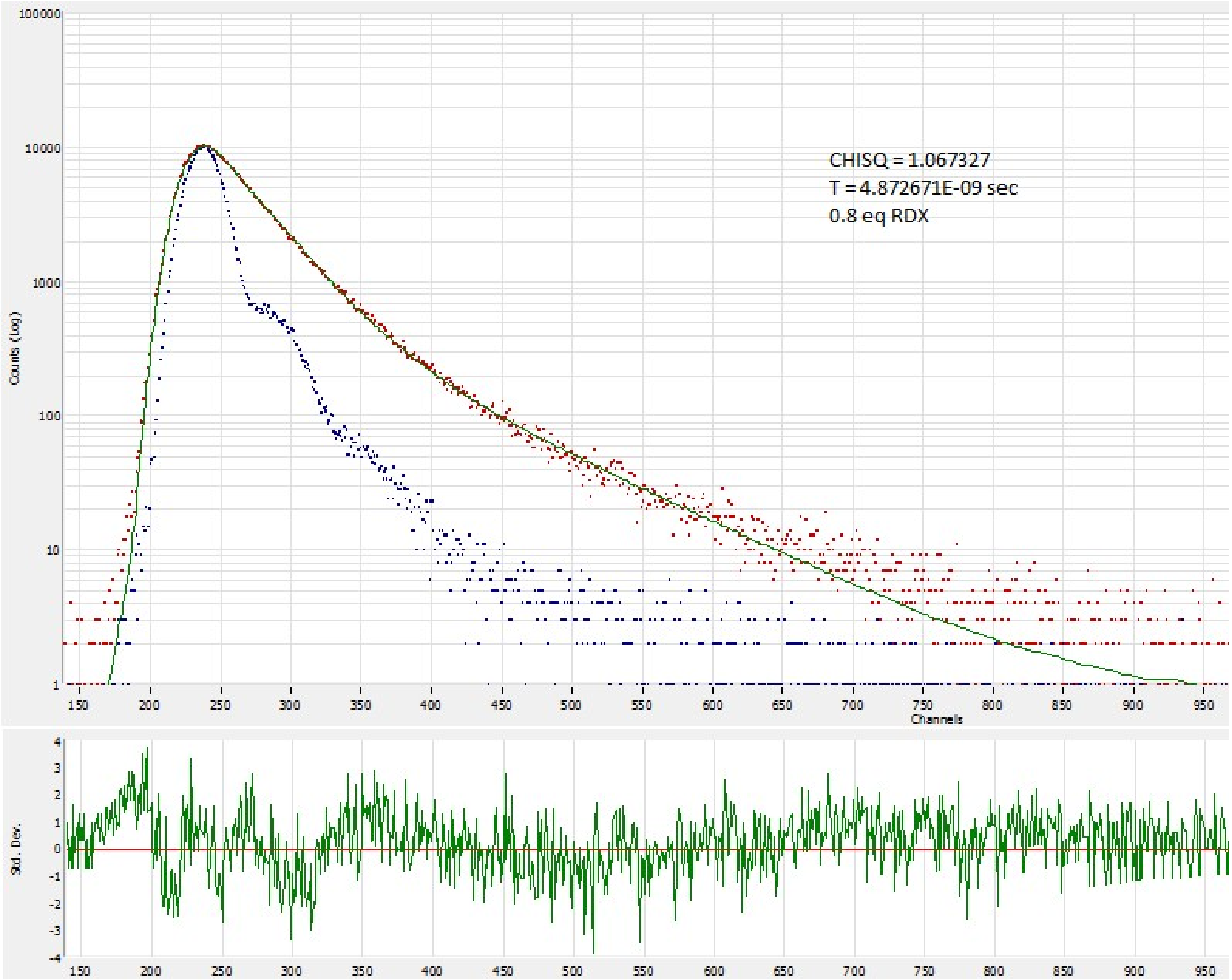

Fig.S75 Time-resolved fluorescence emission of **4a** adduct with RDX

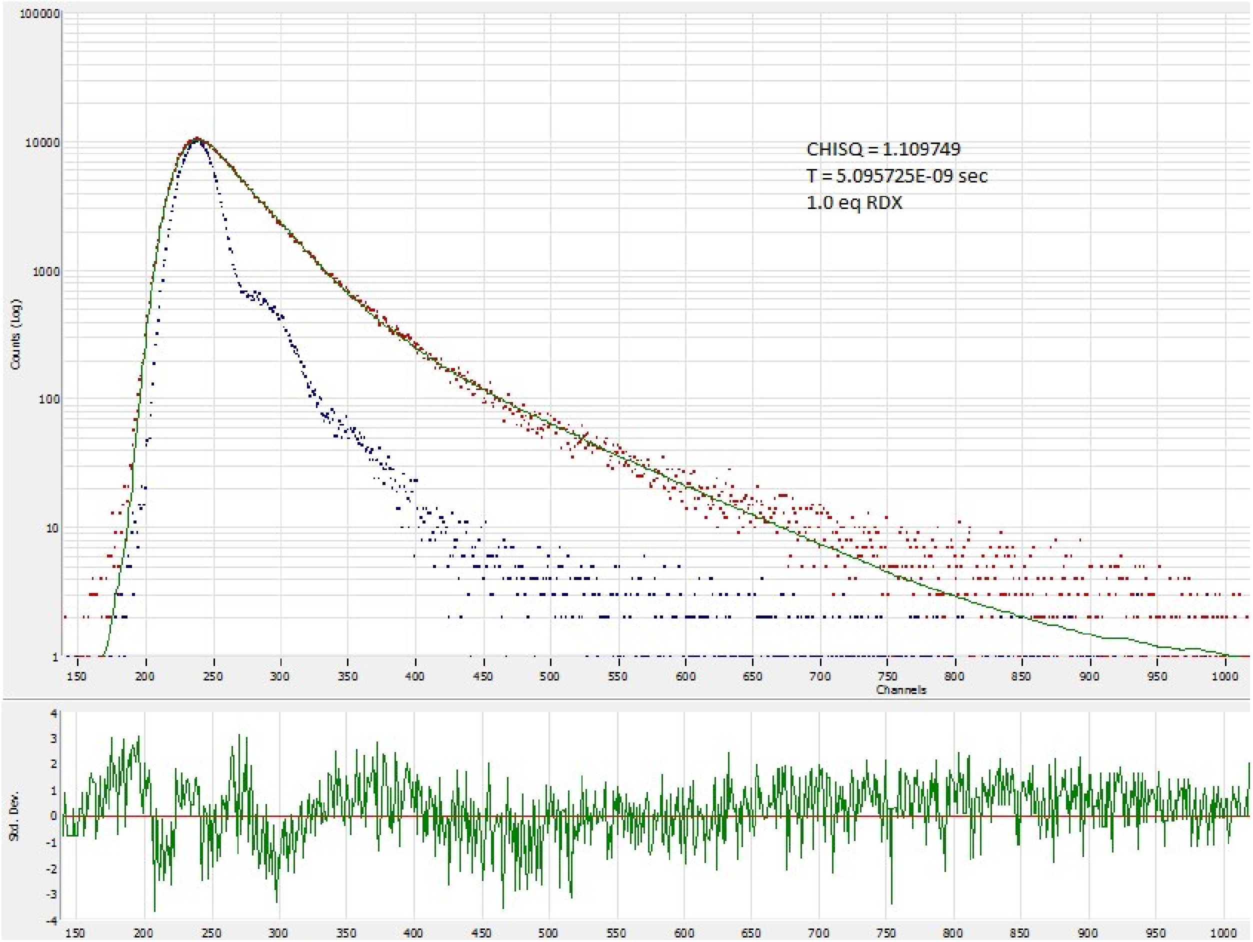

Fig.S76 Time-resolved fluorescence emission of **4a** adduct with RDX

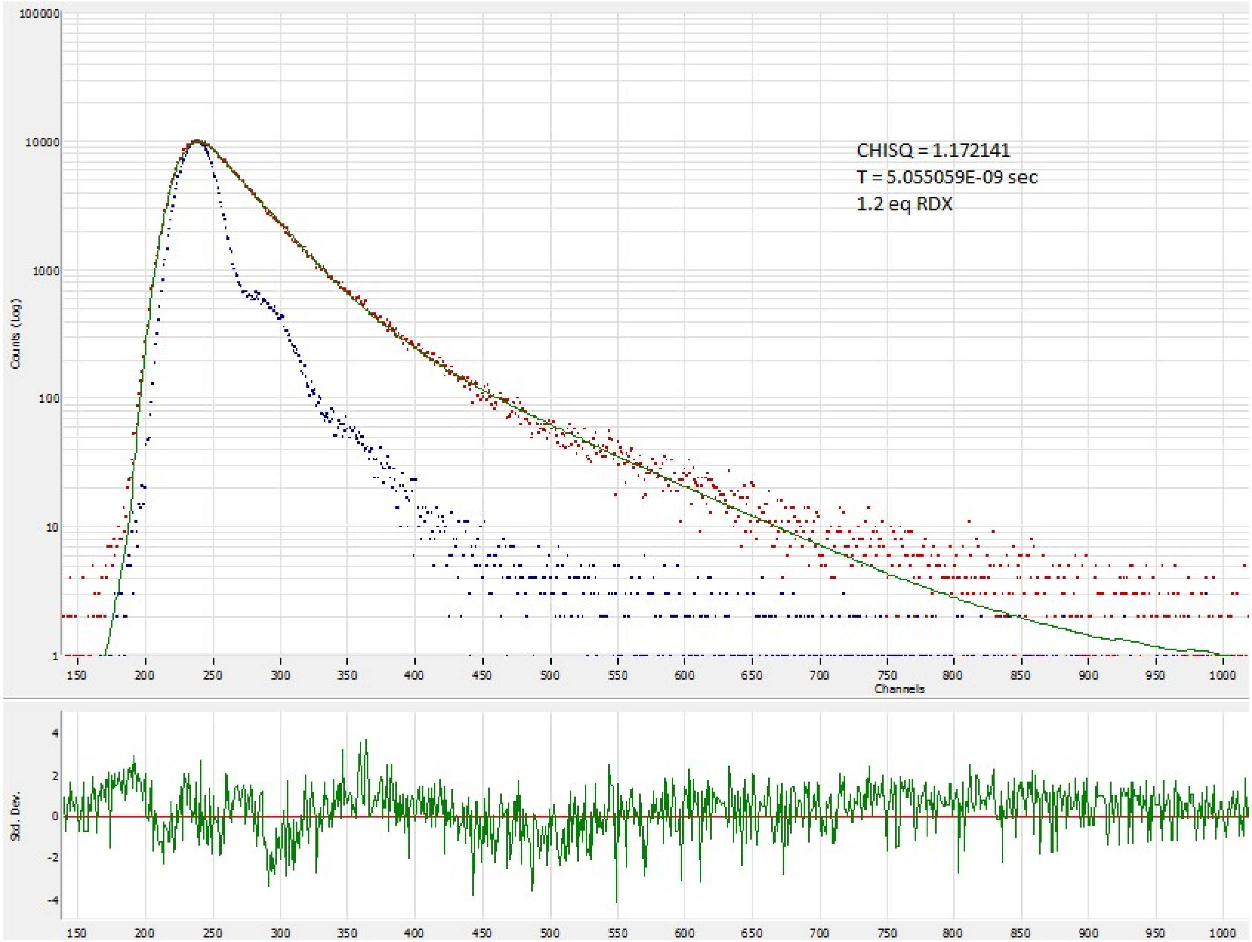

Fig.S77 Time-resolved fluorescence emission of **4a** adduct with RDX

Fluorescence quenching in polymer matrices

The THF solutions of sensors **3,4a-c** in polyurethane (*c.a.* 5 % w/w) were solution-casted in wells of aluminium chips to form sensor films. After evaporation of the solvent these chips were exposed to vapours of components of nitro-explosives (TNT, 2,4-DNT and RDX) at equilibrium.
The blank samples were prepared by placing the scotch-tape film over the wells to prevent the penetration of the vapors of nitro-explosives.

^{1}H & ^{13}C NMR Spectra of fluorophores 2,3,4a,4b,4c

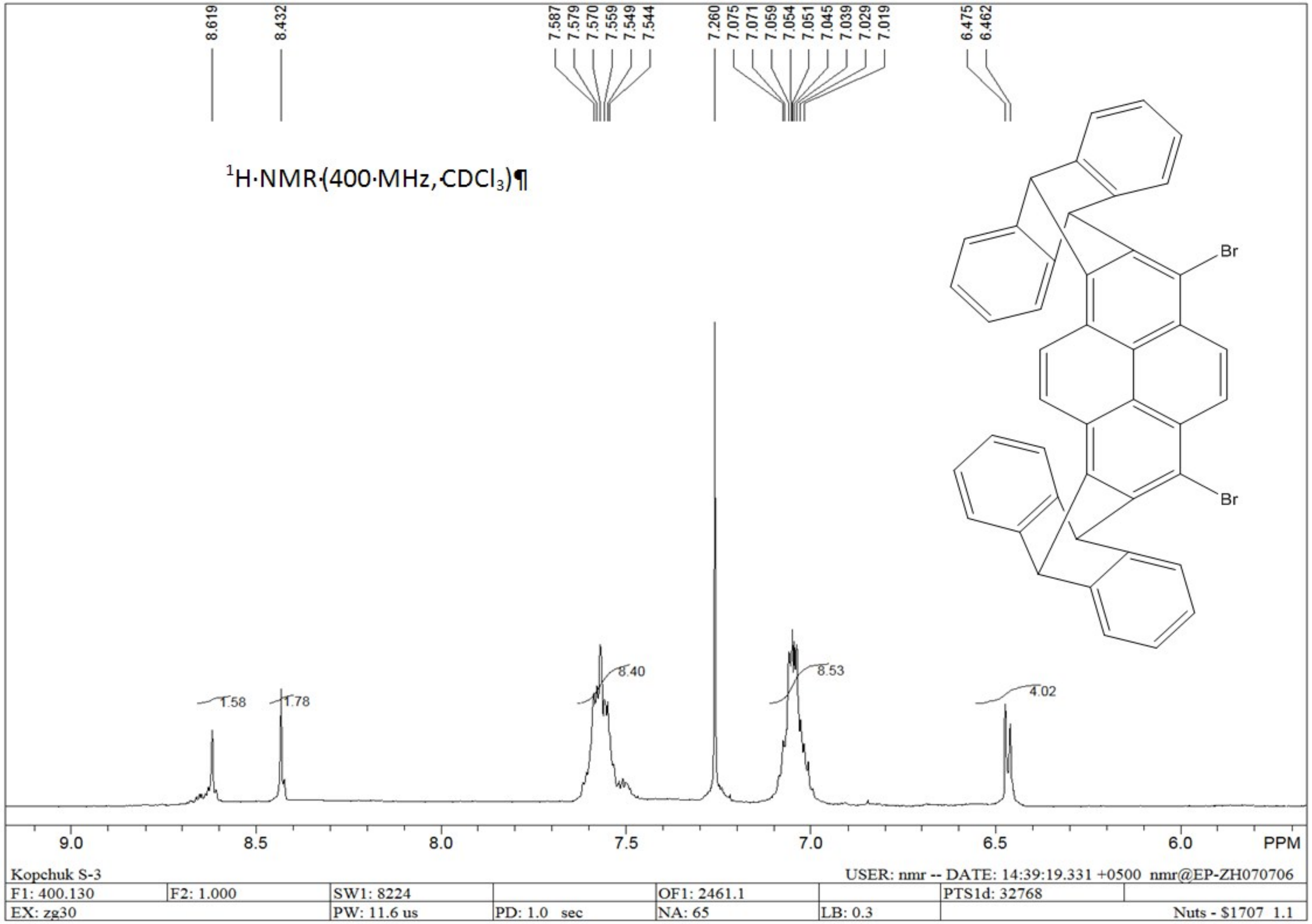

Fig. S78 ^{1}H NMR (400 MHz) of iptycene **2**

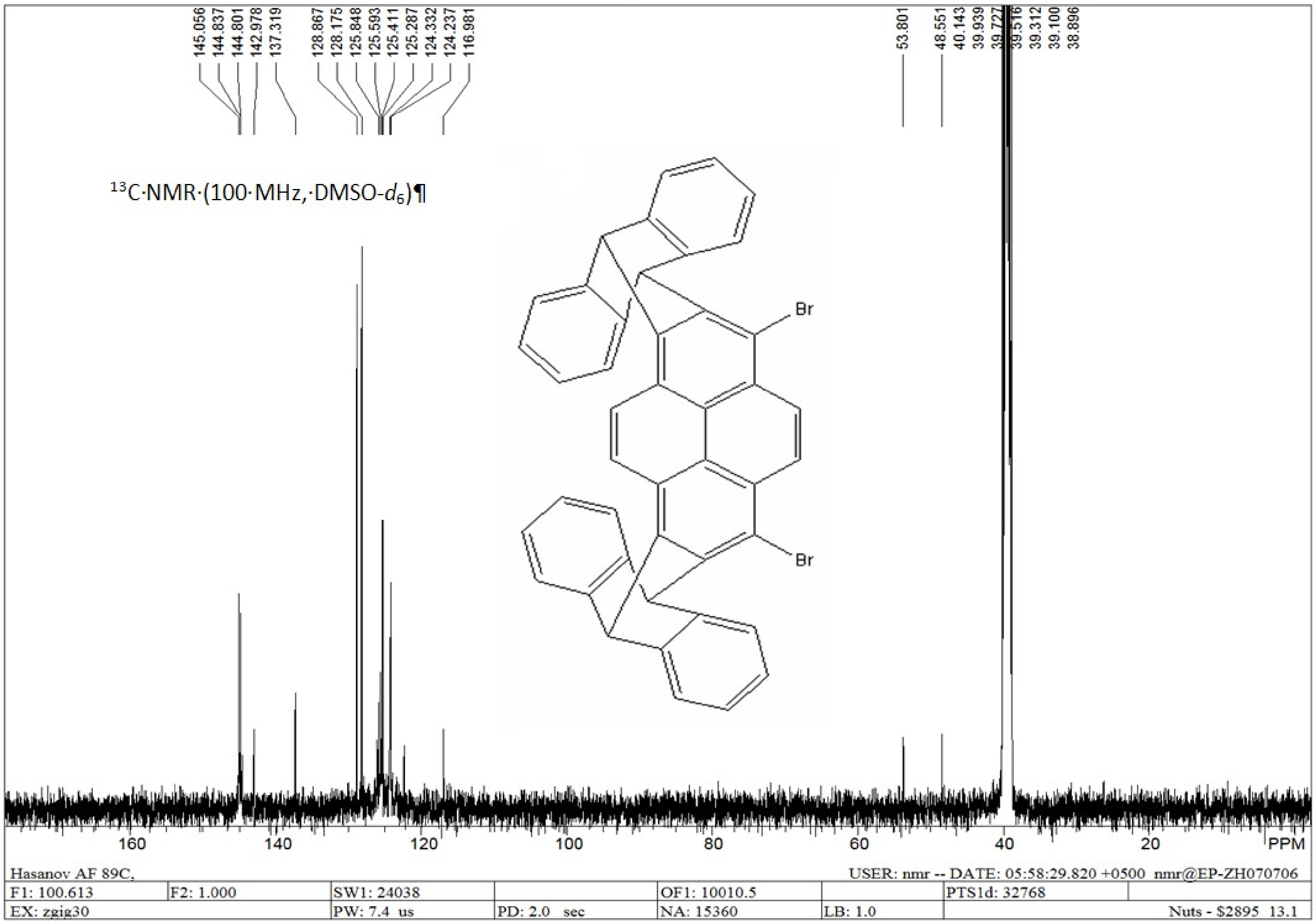

Fig. S79 ^{13}C NMR (100 MHz) of iptycene **2**

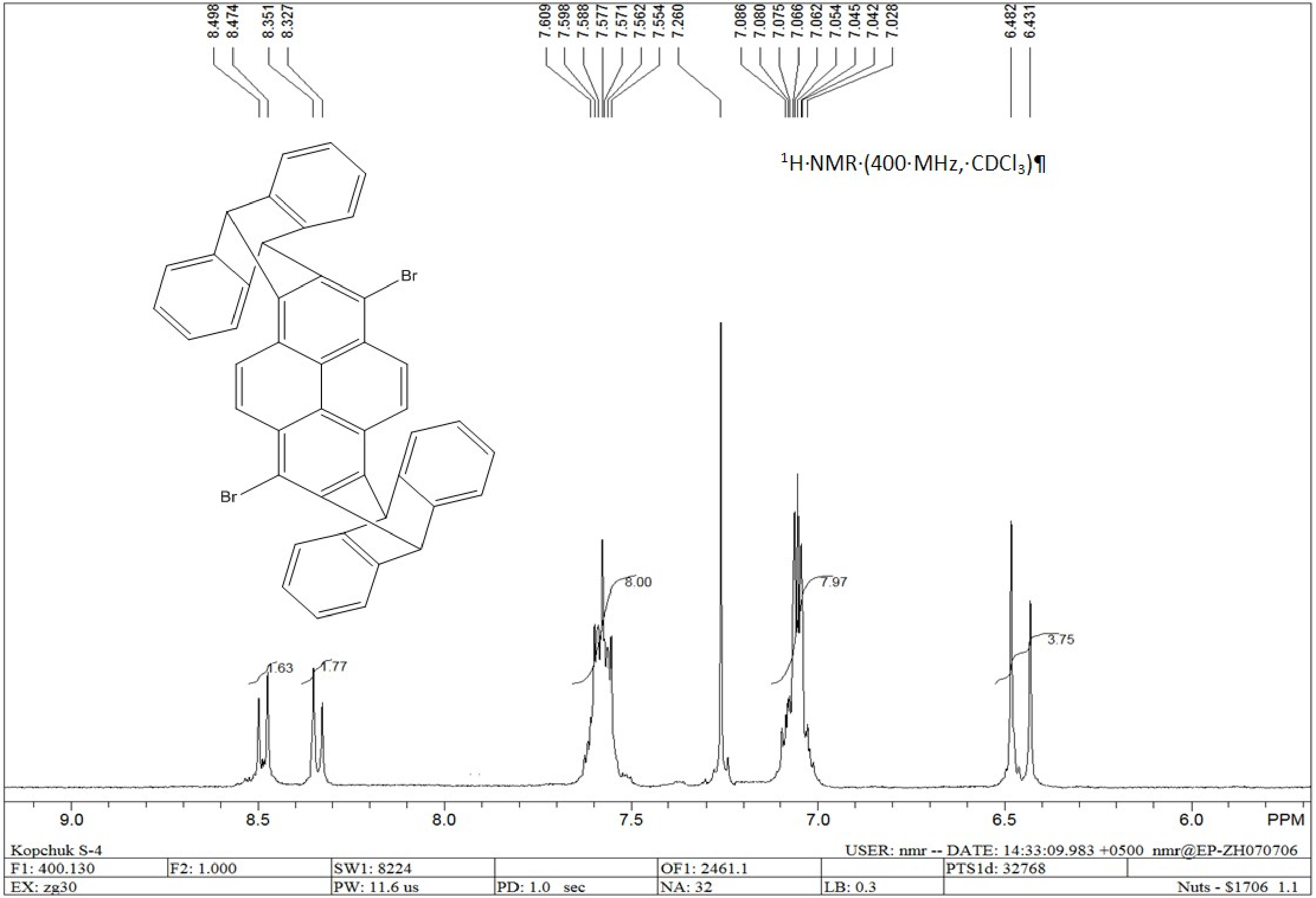

Fig. S80 ^{1}H NMR (400 MHz) of iptycene **3**

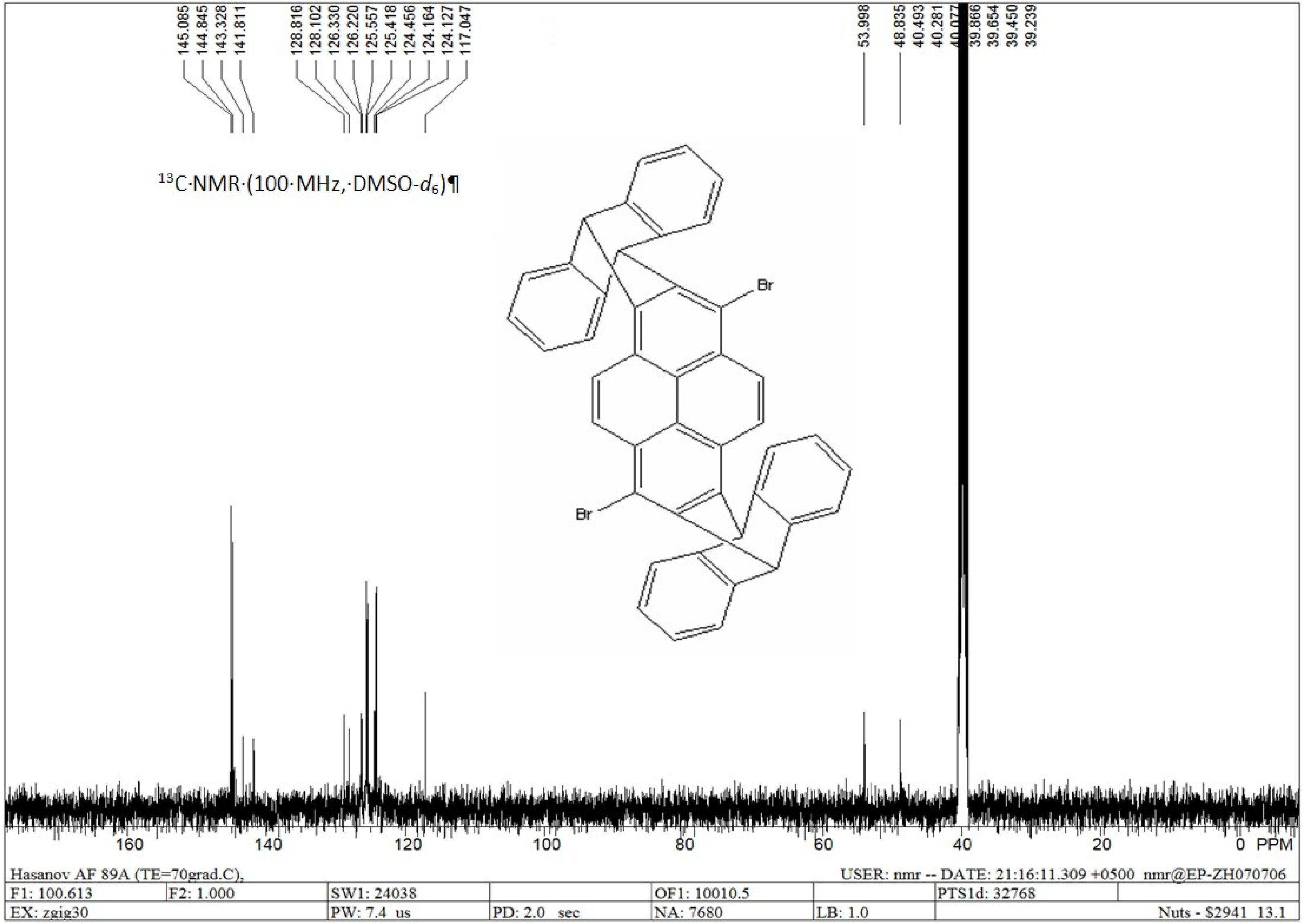

Fig. S81 ^{13}C NMR (100 MHz) spectrum of fluorophore **3**

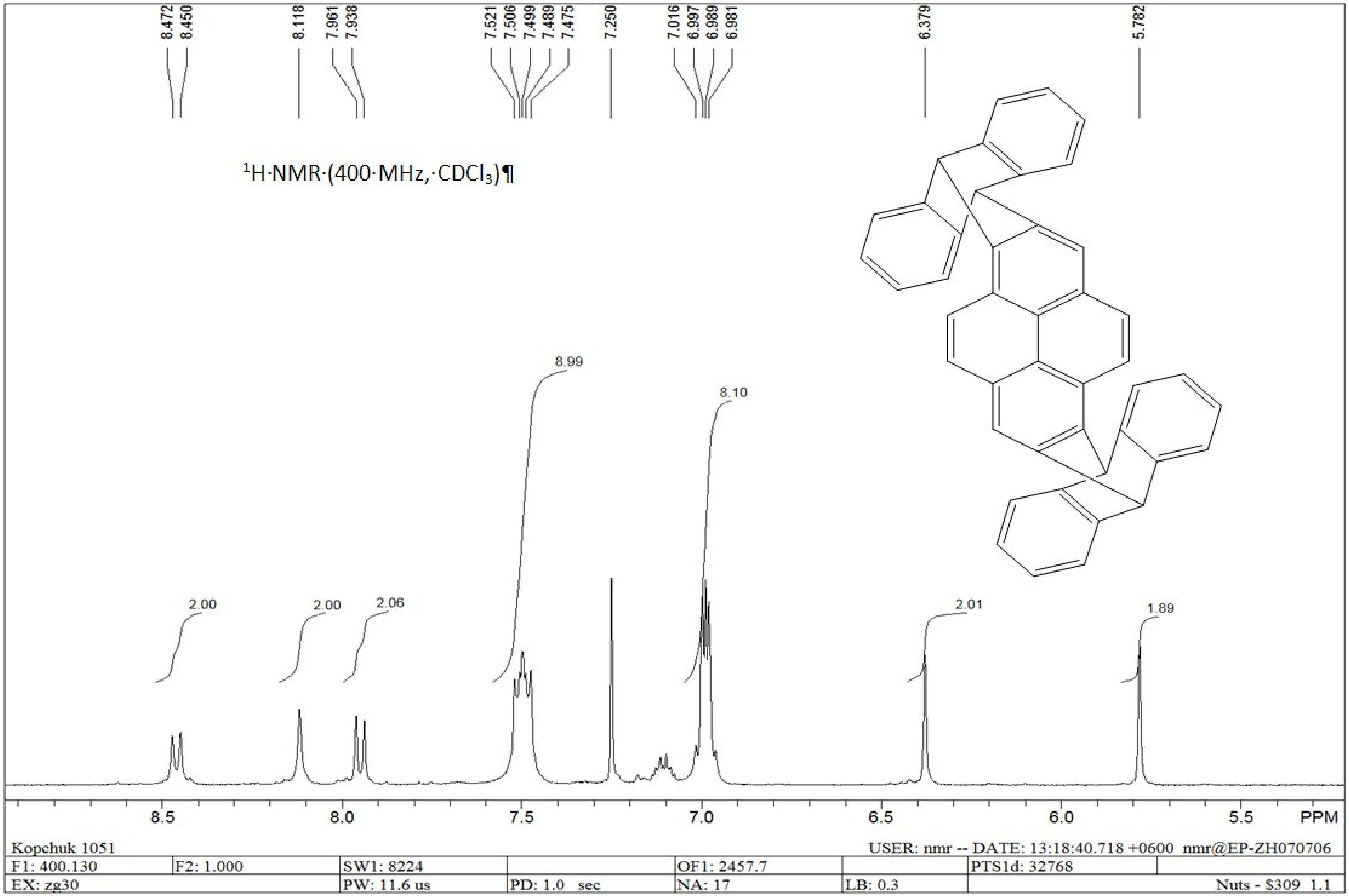

Fig. S82 ^{1}H NMR (400 MHz) of iptycene **4a**

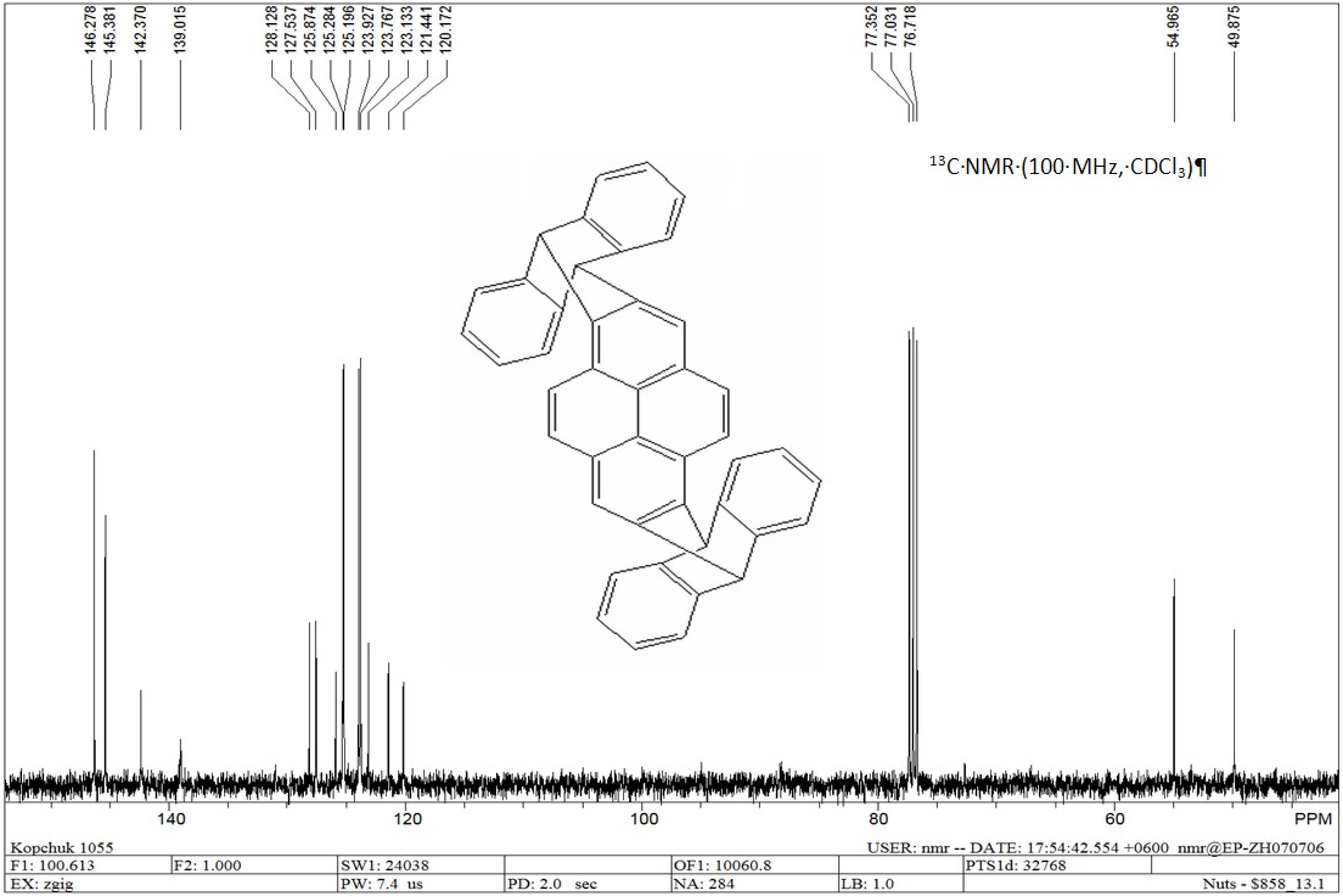

Fig. S83 ^{13}C NMR (100 MHz) iptycene **4a**

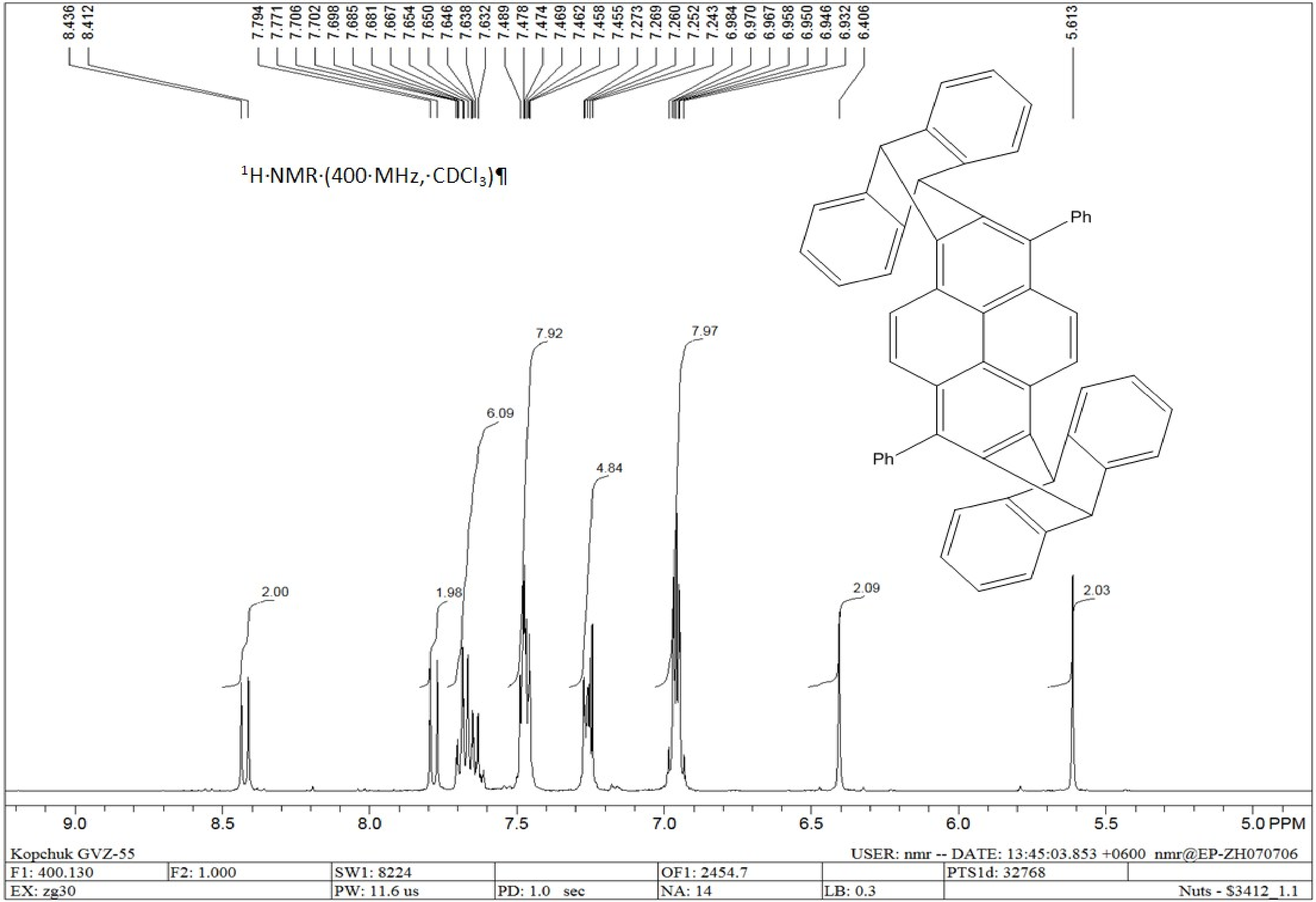

Fig. S84 ^{1}H NMR (400 MHz) iptycene **4b**

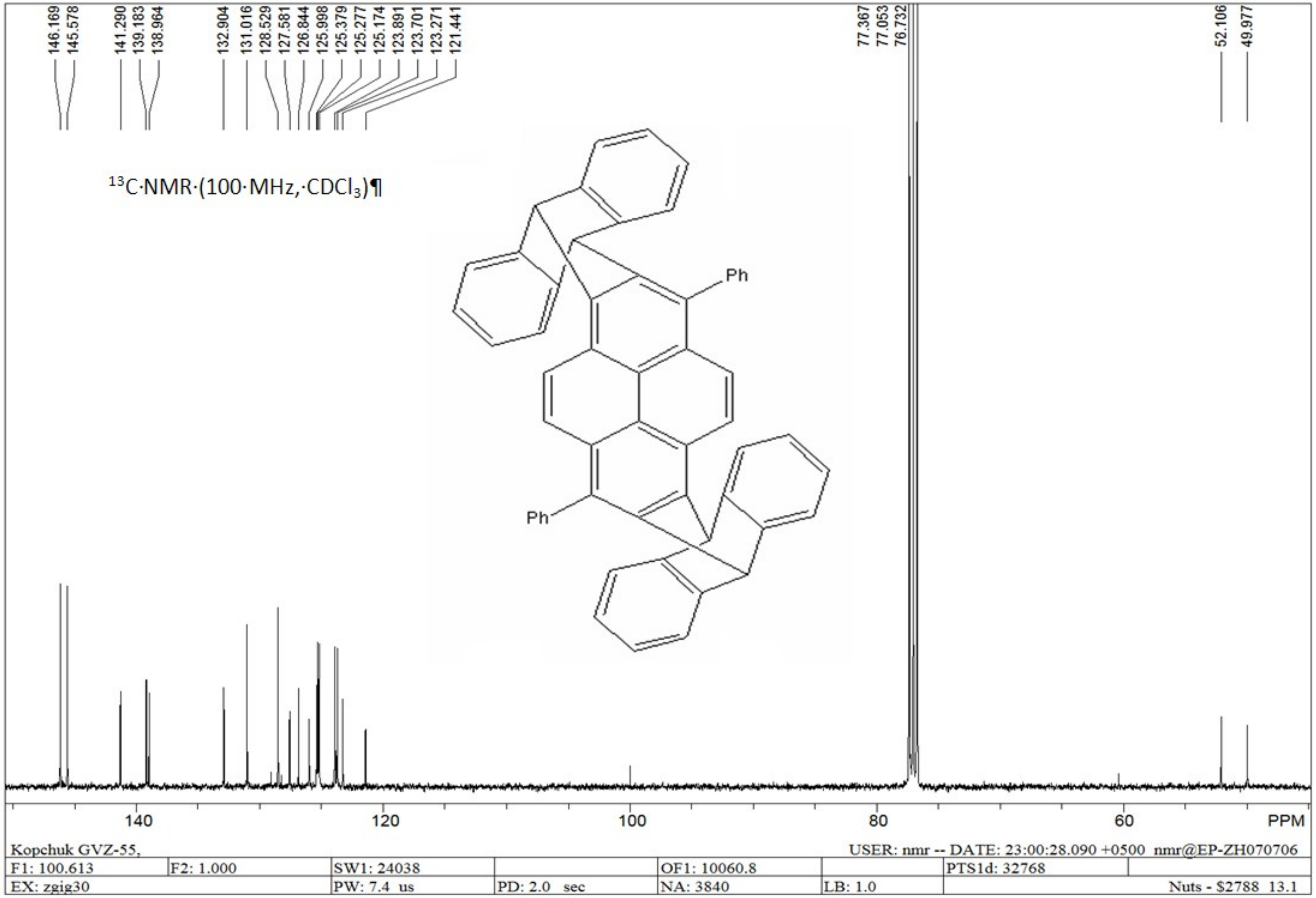

Fig. S85 ^{13}C NMR (100 MHz) of iptycene **4b**

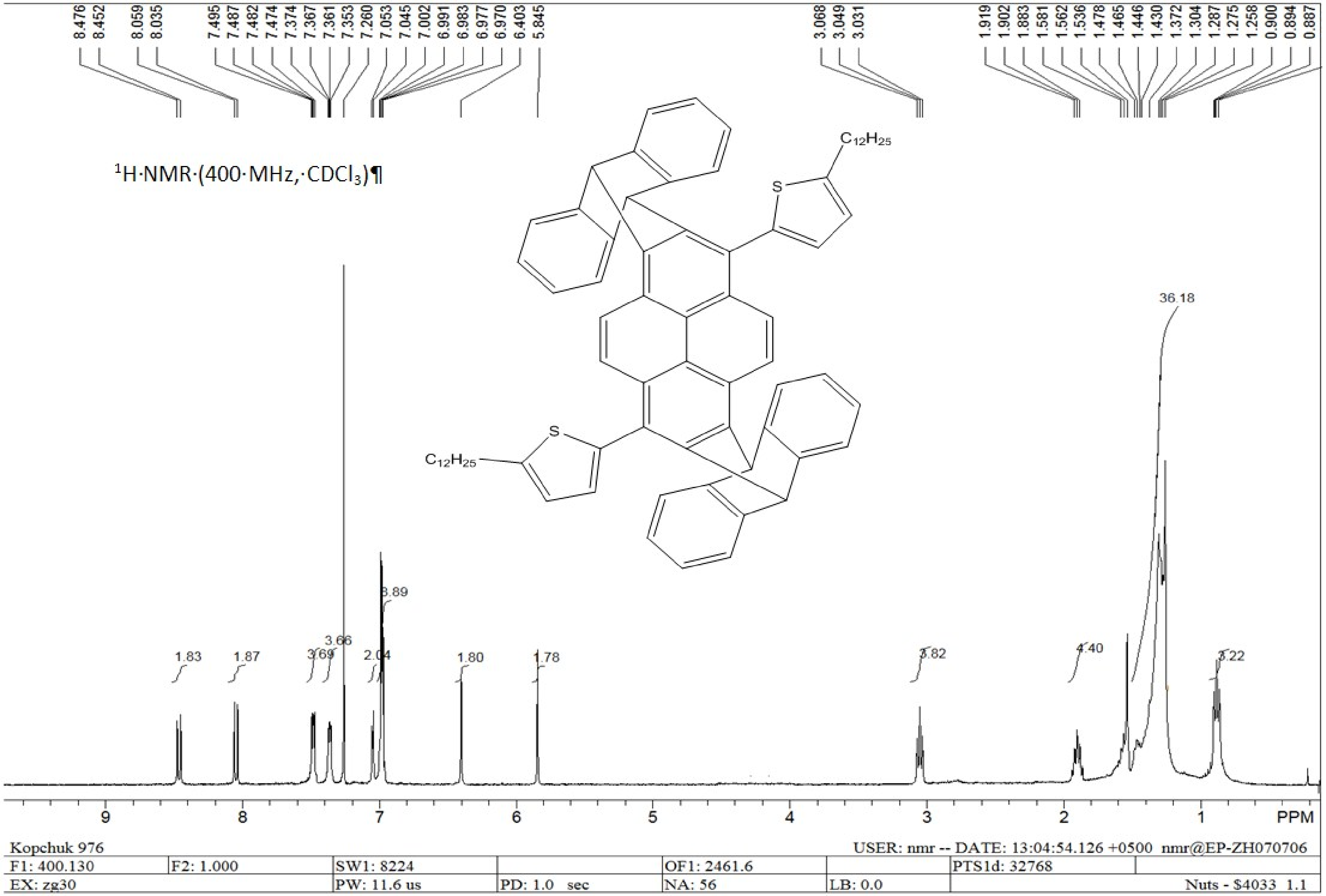

Fig. S86 ^{1}H NMR (400 MHz) of iptycene **4c**

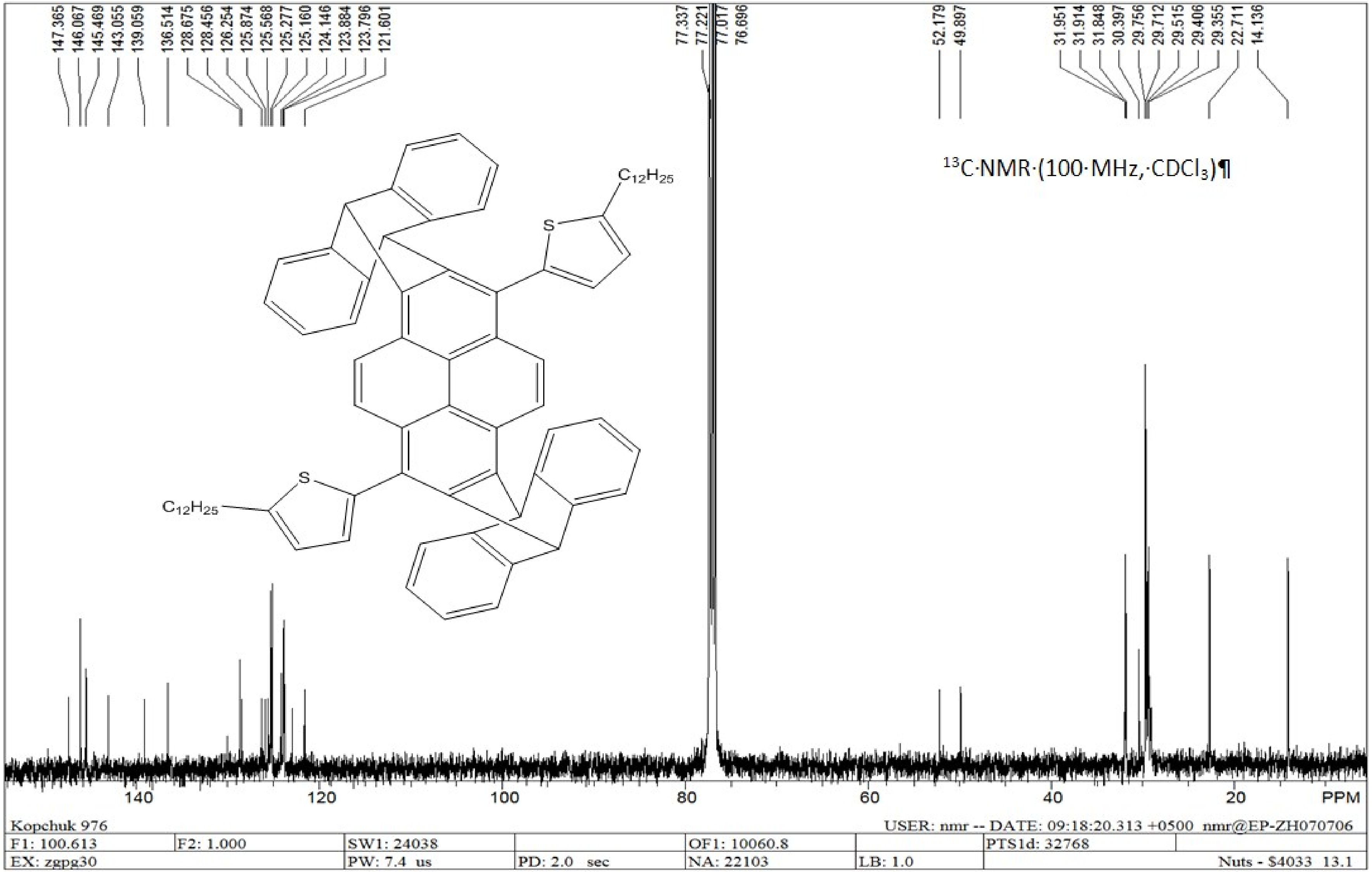

Fig. S87 ^{13}C NMR (100 MHz) iptycene **4c**

X-ray data for the complex "iptycene 3·nitrobenzene"

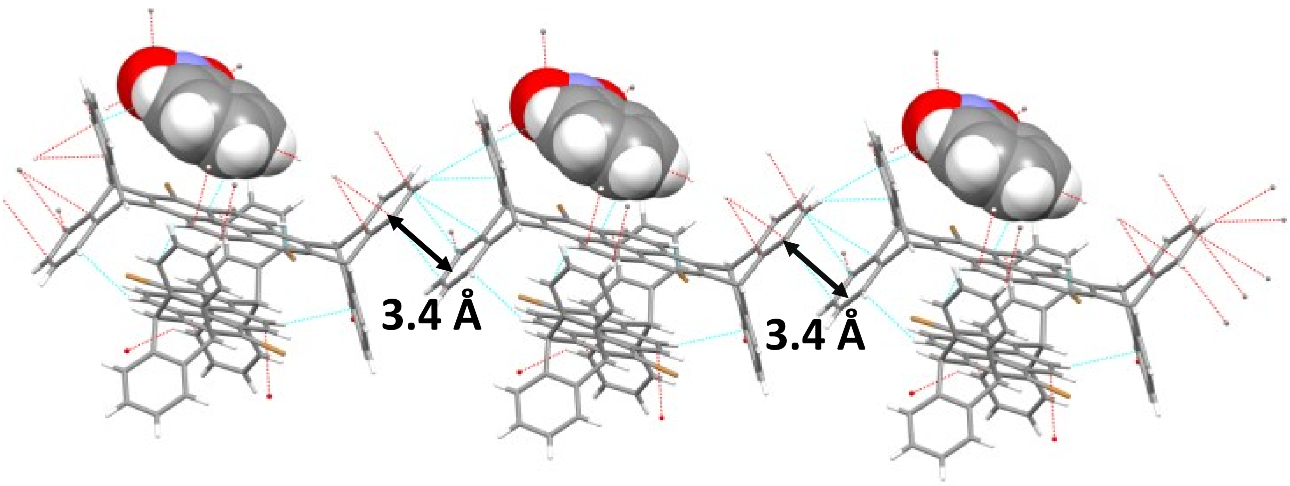

Fig. S88. The crystal packing of compound **3** crystallized from toluene-nitrobenzene solution. The interlunar distances between phenylene moieties are indicated.

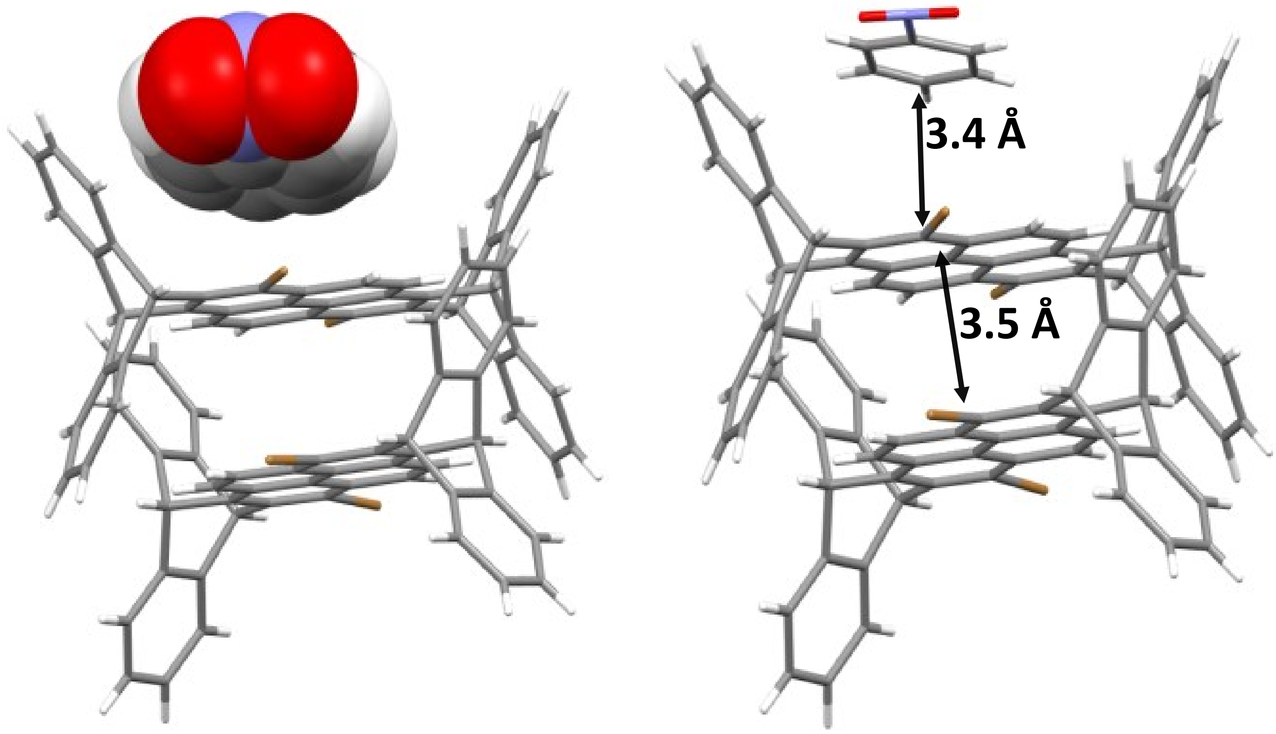

Fig. S89. Molecular structure of "iptycene **3** nitrobenzene" complex. The interplanar distances between the pyrene moiety and nitrobenzene molecule are indicated.

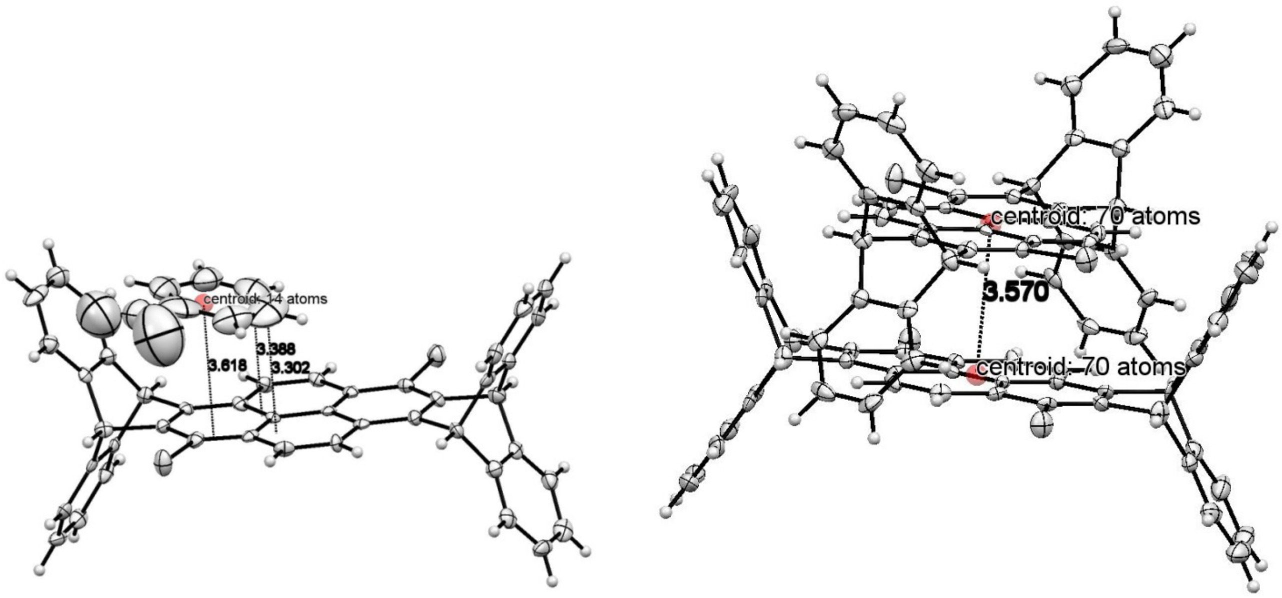

Fig. S90. Molecular structure of "iptycene **3** nitrobenzene" complex. The interplanar distances between the pyrene moiety and nitrobenzene molecule are indicated.

The XRD analysis of complex «**3***$PhNO_2$» was performed on a Xcalibur 3 diffractometer on standard procedure (MoK-irradiation, graphite monochromator, ω-scans, step 1°). The crystal was kept at 150(2) K during data collection. Using SHELXTL2 [1], the structure was solved with the ShelXS [1] structure solution program using Direct Methods and refined with the ShelXL [1] refinement package using Least Squares minimization in anisotropic approximation for non-hydrogen atoms. H-atoms were added in the calculated positions and were included in the refinement in the "rider" model.

Crystal Data. Crystal size 0.167x0.086x0.023 mm^{-1}, system is triclinic, space group P-1, a= 13.0874(6) Å, b= 15.5471(12) Å, c= 22.686(2) Å, α= 70.666(7)°, β = 88.978(8)°, γ= 67.069(6) °, V = 3978.5(5) Å^3, Z = 1, μ(MoKα)= 2.085 mm^{-1}. On the angles 2.61 < Θ < 26.37° 33893 reflections measured, 15642 unique (R_{int} = 0.0535) and 7584 with I>2σ(I) which were used in all calculations. The final R_1= 0.1166, wR_2= 0.1024 (all data) and R_1= 0.0479, wR_2= 0.0963 (I>2σ(I)). Goodness-of-fit on F^2 1.019, largest diff. peak/hole / ēÅ^{-3} 0.984/-0.589.

Table S3. Crystal data and structure refinement for 3•$C_6H_5NO_2$

C_{221} H_{140} Br_8 N_4 O_8 Chemical_formula_weight	3618.65
Symmetry_cell_setting	Triclinic
Symmetry_space_group_name_H-M	P-1
Symmetry_equiv_pos_as_xyz	'x, y, z' '-x, -y, -z'
Cell_length_a	13.0874(6)
Cell_length_b	15.5471(12)
Cell_length_c	22.686(2)
Cell_angle_alpha	70.666(7)
Cell_angle_beta	88.978(8)
Cell_angle_gamma	67.069(6)
Cell_volume	3978.5(5)
Cell_formula_units_Z	1
Cell_measurement_temperature	150(2)
Cell_measurement_reflns_used	7965
Cell_measurement_theta_min	2.6021
Cell_measurement_theta_max	33.4955
Exptl_crystal_description	prism
Exptl_crystal_colour	colorless
Exptl_crystal_size_max	0.1672

Exptl_crystal_size_mid	0.0858
Exptl_crystal_size_min	0.0226
Exptl_crystal_density_diffrn	1.510
Exptl_crystal_F_000	1838
Exptl_absorpt_coefficient_mu	2.085
Exptl_absorpt_correction_T_min	0.579
Exptl_absorpt_correction_T_max	0.851

CrysAlis RED, Oxford Diffraction Ltd., Version 1.171.29.9 (release 23-03-2006 CrysAlis171 .NET) (compiled Mar 23 2006,23:39:28)

Analytical numeric absorption correction using a multifaceted crystal model based on expressions derived by R.C. Clark & J.S. Reid.[1]

X-ray data for the complex "iptycene 3·mesitylene"

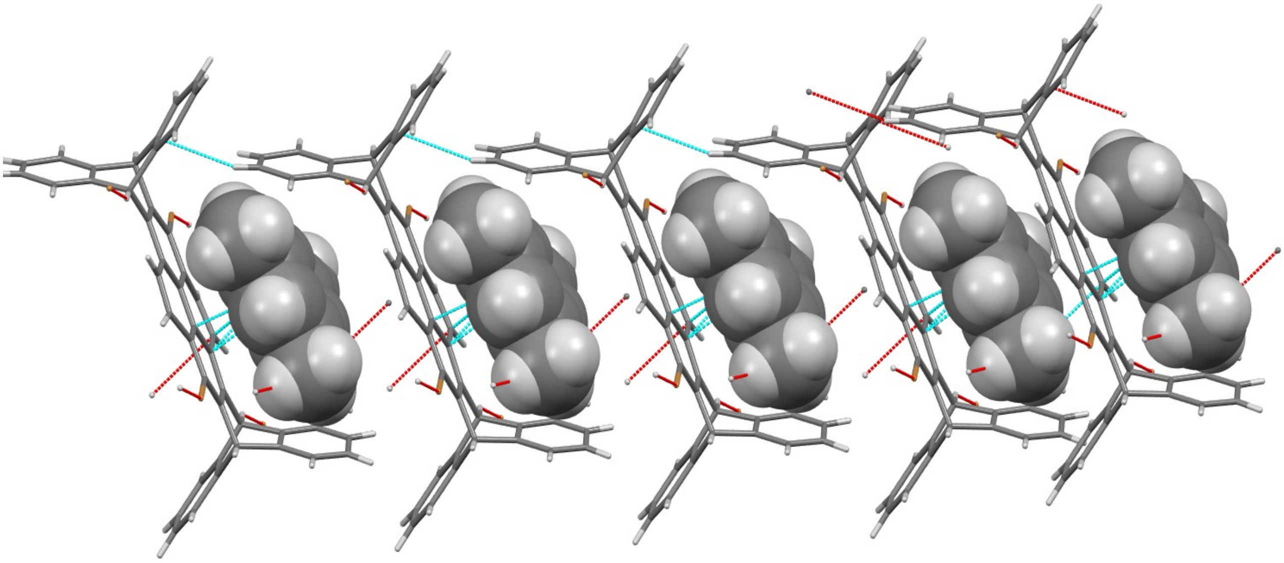

Fig. S91. The crystal packing of compound **3** crystallized from mesitylene solution.

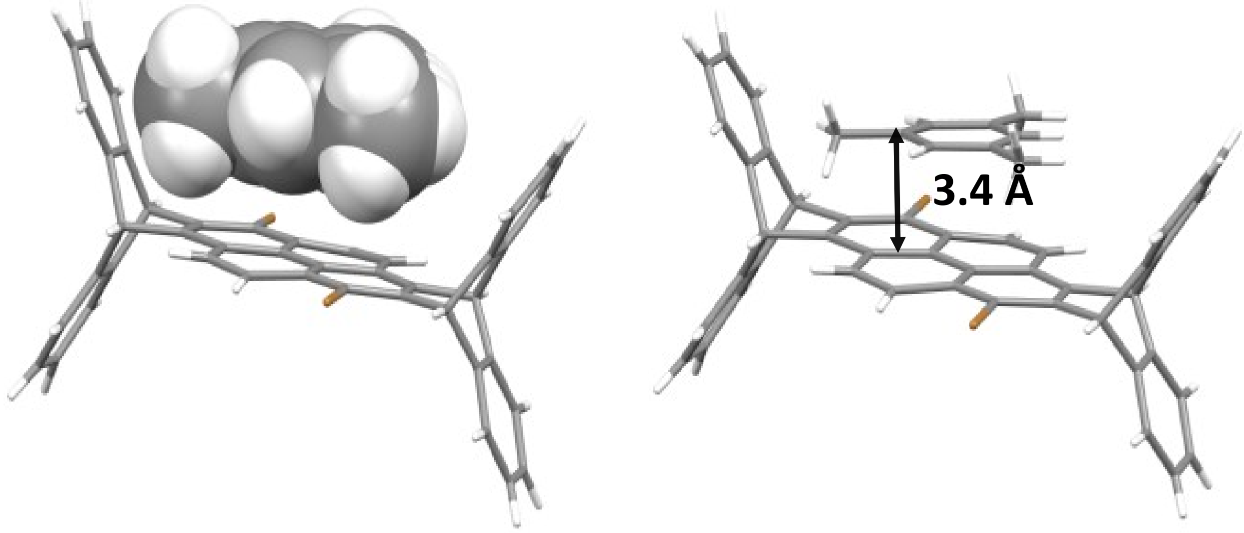

Fig. S92. Molecular structure of "iptycene **3** mesitylene" complex. The interplanar distance between the pyrene moiety and mesitylene molecule is indicated.

Experimental.

Single crystals of $C_{53}H_{36}Br_2$ were crystallized from 2,4,6-threemethylbenzene. The XRD experiment was accomplished on an "Xcalibur 3" diffractometer on standard procedure (MoK irradiation, graphite monochromator, ω-scans with 1° step). The crystal was kept at 295(2) K during data collection. Empirical absorption correction was applied. Using Olex2,[2] the structure was solved with the olex2.solve[3] structure solution program using Charge Flipping and refined with the ShelXL[4] refinement package using Least Squares minimization in anisotropic approximation for non-hydrogen atoms. The H-atoms were added in the calculated positions and were included in the refinement in the "rider" model. Results of the XRD analysis are presented below.

Crystal Data. $C_{53}H_{36}Br_2$, *M* =832.64, triclinic, *a* = 8.3886(7) Å, *b* = 9.0069(8) Å, *c* = 14.5283(13) Å, *α* = 76.634(8)°, *β* = 89.729(7)°, *γ* = 64.661(8)°, *V* = 959.66(14) Å^3, *T* = 295(2), space group P1 (no. 1), *Z* = 1, μ(Mo Kα) = 2.150 mm^{-1}, 7107 reflections measured, 5001 unique (R_{int} = 0.0306) which were used in all calculations. The final wR_2 was 0.1536 (all data) and R_1 was 0.0509 (I>2σ(I)).

Table S4. Crystal data and structure refinement.

Empirical formula	$C_{53}H_{36}Br_2$
Formula weight	832.64
Temperature/K	295(2)
Crystal system	triclinic
Space group	P1
a/Å	8.3886(7)
b/Å	9.0069(8)
c/Å	14.5283(13)
α/°	76.634(8)
β/°	89.729(7)
γ/°	64.661(8)
Volume/Å^3	959.66(14)
Z	1
ρ_{calc}mg/mm^3	1.441
m/mm^{-1}	2.150
F(000)	424.0
Crystal size/mm^3	0.25 × 0.2 × 0.15
2Θ range for data collection	5.18 to 52.74°
Index ranges	-9 ≤ h ≤ 10, -11 ≤ k ≤ 11, -18 ≤ l ≤ 13
Reflections collected	7107
Independent reflections	5001[R(int) = 0.0306]
Data/restraints/parameters	5001/330/497
Goodness-of-fit on F^2	1.006
Final R indexes [I>2σ (I)]	R_1 = 0.0509, wR_2 = 0.1305
Final R indexes [all data]	R_1 = 0.0751, wR_2 = 0.1536
Largest diff. peak/hole / e Å^{-3}	0.55/-0.46

Table S5. Fractional Atomic Coordinates (×10[4]) and Equivalent Isotropic Displacement Parameters (Å[2]×10[3]). U_{eq} is defined as 1/3 of of the trace of the orthogonalised U_{IJ} tensor.

Atom	*x*	*y*	*z*	U(eq)
Br1	5456.3(8)	7454.0(8)	9322.8(6)	55.9(4)
Br2	7444.1(8)	1496.9(7)	4494.5(6)	54.0(4)
C1	6528(15)	6655(17)	2972(9)	32(3)
C2	6382(15)	7915(15)	3425(10)	35(3)
C3	5095(16)	9568(17)	3011(10)	38(3)
C4	3954(18)	9834(19)	2225(11)	48(4)
C5	4038(18)	8590(20)	1776(12)	56(4)
C6	5324(18)	6961(19)	2160(12)	50(4)
C7	7943(17)	4846(18)	3551(11)	47(4)
C8	9628(17)	5175(19)	3525(11)	47(4)
C9	11242(19)	4210(20)	3187(12)	59(4)
C10	12601(18)	4680(20)	3273(13)	64(4)
C11	12400(20)	5930(30)	3742(15)	84(6)
C12	10813(17)	6905(18)	4074(10)	51(3)
C13	9470(17)	6502(17)	3958(10)	43(3)
C14	7588(17)	7304(18)	4241(11)	43(4)
C15	7314(15)	5876(14)	4955(10)	28(3)
C16	7472(14)	4677(15)	4546(9)	31(3)
C17	7254(16)	3271(16)	5092(11)	36(3)
C18	6862(16)	3145(16)	6001(11)	37(3)
C19	6378(16)	1885(15)	6577(10)	38(3)
C20	6098(17)	1724(15)	7497(9)	34(3)
C21	5997(16)	3051(17)	7919(10)	37(3)
C22	6276(15)	4444(15)	7364(11)	35(3)
C23	6688(15)	4509(15)	6411(10)	31(3)
C24	6956(16)	5882(15)	5877(11)	35(3)
C25	6790(20)	7170(20)	6367(13)	57(4)
C26	6276(18)	7227(18)	7245(10)	43(3)
C27	6160(16)	5787(16)	7788(10)	33(3)
C28	5723(17)	5683(17)	8758(11)	38(3)
C29	5397(16)	4418(16)	9281(10)	34(3)
C30	5600(15)	2920(17)	8890(11)	38(3)
C31	5244(15)	1619(14)	9545(10)	30(3)
C32	6637(15)	1078(16)	10469(9)	34(3)
C33	7931(18)	-530(20)	10846(12)	49(4)
C34	8990(20)	-910(20)	11659(13)	59(5)
C35	8742(19)	450(20)	12009(12)	55(4)
C36	7418(17)	2106(18)	11625(11)	47(3)
C37	6438(17)	2429(17)	10836(11)	37(3)
C38	4965(15)	4039(15)	10330(9)	35(3)
C39	3262(17)	3887(17)	10247(10)	40(3)
C40	1690(20)	4790(20)	10570(13)	64(5)

C41	230(20)	4460(20)	10441(15)	76(5)
C42	382(17)	3140(20)	10112(12)	67(4)
C43	1955(17)	2268(19)	9773(12)	60(4)
C44	3436(15)	2610(17)	9866(10)	42(3)
C1S	11620(20)	-940(30)	6483(15)	123(7)
C2S	11988(18)	272(18)	5863(11)	89(4)
C3S	11849(18)	1776(19)	6071(12)	105(5)
C4S	11259(15)	2205(17)	6927(11)	97(4)
C5S	10835(16)	1023(19)	7553(11)	106(4)
C6S	11090(20)	-530(20)	7346(15)	95(5)
C7S	10650(30)	-1860(30)	8010(17)	191(11)
C8S	12519(14)	-139(17)	4974(9)	86(4)
C9S	11038(17)	3854(18)	7110(13)	123(6)

Table S6. Anisotropic Displacement Parameters (Å^2×10^3). The Anisotropic displacement factor exponent takes the form: $-2\pi^2[h^2a^{*2}U_{11}+...+2hka\times b\times U_{12}]$.

Atom	U_{11}	U_{22}	U_{33}	U_{23}	U_{13}	U_{12}
Br1	91.1(10)	42.4(8)	43.4(10)	-21.0(8)	14.1(8)	-32.7(7)
Br2	92.1(10)	38.1(8)	43.3(10)	-18.6(7)	12.8(7)	-34.9(7)
C1	38(5)	36(5)	20(5)	-5(4)	3(4)	-15(4)
C2	46(5)	28(5)	36(6)	-9(4)	19(4)	-20(4)
C3	51(5)	31(5)	31(5)	-7(4)	13(4)	-18(4)
C4	47(6)	35(6)	38(6)	7(5)	-1(5)	-5(4)
C5	43(5)	57(7)	44(7)	5(6)	-8(5)	-8(5)
C6	58(6)	53(7)	49(7)	-16(6)	0(5)	-33(5)
C7	58(6)	43(6)	41(7)	-7(5)	-11(5)	-25(5)
C8	43(6)	45(6)	42(7)	-3(5)	6(5)	-13(5)
C9	54(6)	54(7)	48(7)	-6(6)	10(5)	-9(5)
C10	45(6)	65(7)	58(7)	0(6)	14(5)	-10(5)
C11	50(7)	98(9)	93(10)	10(7)	-6(6)	-41(6)
C12	59(6)	56(6)	36(6)	0(5)	10(5)	-30(5)
C13	49(6)	41(6)	33(6)	-10(5)	3(4)	-15(4)
C14	54(6)	44(7)	38(7)	-23(5)	12(5)	-24(5)
C15	47(5)	16(4)	25(5)	3(4)	7(4)	-21(4)
C16	34(5)	26(5)	27(6)	-3(4)	6(4)	-11(4)
C17	53(6)	24(5)	31(6)	-15(5)	8(5)	-13(4)
C18	46(5)	21(5)	46(7)	-4(5)	7(5)	-18(4)
C19	64(5)	24(5)	40(6)	-17(4)	12(4)	-26(4)
C20	67(6)	20(5)	18(5)	3(4)	9(4)	-26(4)
C21	42(5)	37(6)	27(6)	-10(5)	-2(4)	-12(4)
C22	46(5)	24(6)	35(6)	-12(5)	1(5)	-15(4)
C23	49(6)	21(5)	25(6)	2(4)	7(4)	-20(4)
C24	53(6)	20(5)	42(7)	-10(5)	11(5)	-25(4)

C25	79(7)	46(7)	63(9)	-25(6)	9(6)	-39(6)
C26	70(6)	36(5)	28(6)	-14(5)	8(4)	-25(4)
C27	47(5)	28(5)	26(6)	-10(5)	3(4)	-19(4)
C28	50(6)	37(6)	35(7)	-13(5)	-2(5)	-24(5)
C29	54(6)	24(5)	29(6)	-8(4)	1(4)	-20(4)
C30	36(5)	40(6)	36(7)	-11(5)	2(4)	-14(4)
C31	43(5)	22(5)	28(6)	3(4)	2(4)	-22(4)
C32	37(5)	38(5)	25(5)	-1(4)	-2(4)	-20(4)
C33	53(6)	42(6)	52(7)	-5(5)	4(5)	-23(5)
C34	54(6)	57(8)	50(8)	2(6)	2(5)	-17(6)
C35	59(6)	65(8)	42(7)	-3(6)	-11(5)	-35(6)
C36	55(6)	47(6)	32(6)	-7(5)	8(5)	-19(5)
C37	49(5)	34(5)	35(6)	-10(4)	14(4)	-25(4)
C38	52(5)	21(5)	27(5)	-7(4)	21(4)	-12(4)
C39	49(6)	32(5)	28(6)	3(4)	9(4)	-13(4)
C40	68(7)	52(7)	53(8)	-1(6)	23(6)	-15(5)
C41	48(6)	78(8)	76(8)	5(6)	20(6)	-16(6)
C42	40(6)	85(8)	56(7)	9(6)	0(5)	-22(5)
C43	51(6)	68(7)	62(8)	-2(6)	-13(5)	-35(5)
C44	40(5)	45(6)	40(6)	10(5)	3(4)	-27(4)
C1S	111(10)	125(11)	117(11)	-8(8)	-21(7)	-47(8)
C2S	79(7)	74(7)	94(8)	-18(7)	-16(6)	-18(5)
C3S	83(7)	109(8)	111(9)	-16(7)	-10(6)	-37(6)
C4S	70(6)	112(8)	95(8)	-17(7)	-17(5)	-30(6)
C5S	77(6)	138(9)	86(8)	-23(7)	-12(5)	-34(6)
C6S	82(7)	81(8)	103(9)	-17(7)	-26(6)	-21(6)
C7S	113(13)	230(20)	168(18)	56(15)	-58(12)	-74(14)
C8S	64(6)	97(8)	86(9)	-24(7)	7(5)	-24(5)
C9S	87(8)	121(12)	141(13)	-49(10)	-24(8)	-19(7)

Table S7. Bond Lengths.

Atom	Atom	Length/Å	Atom	Atom	Length/Å
Br1	C28	1.888(13)	C24	C25	1.450(17)
Br2	C17	1.937(12)	C25	C26	1.35(2)
C1	C2	1.400(17)	C26	C27	1.396(18)
C1	C6	1.452(17)	C27	C28	1.45(2)
C1	C7	1.578(18)	C28	C29	1.347(19)
C2	C3	1.400(17)	C29	C30	1.526(17)
C2	C14	1.403(18)	C29	C38	1.559(18)
C3	C4	1.402(18)	C30	C31	1.466(17)
C4	C5	1.40(2)	C31	C32	1.622(16)
C5	C6	1.38(2)	C31	C44	1.530(17)
C7	C8	1.562(19)	C32	C33	1.366(18)

C7	C16	1.49(2)	C32	C37	1.385(17)
C8	C9	1.420(19)	C33	C34	1.36(2)
C8	C13	1.433(19)	C34	C35	1.36(2)
C9	C10	1.40(2)	C35	C36	1.41(2)
C10	C11	1.40(2)	C36	C37	1.313(18)
C11	C12	1.40(2)	C37	C38	1.467(18)
C12	C13	1.345(19)	C38	C39	1.500(18)
C13	C14	1.529(18)	C39	C40	1.369(19)
C14	C15	1.555(18)	C39	C44	1.342(18)
C15	C16	1.308(17)	C40	C41	1.40(2)
C15	C24	1.372(19)	C41	C42	1.34(2)
C16	C17	1.414(19)	C42	C43	1.374(19)
C17	C18	1.35(2)	C43	C44	1.416(17)
C18	C19	1.451(17)	C1S	C2S	1.391(17)
C18	C23	1.438(17)	C1S	C6S	1.404(15)
C19	C20	1.341(18)	C2S	C3S	1.412(15)
C20	C21	1.437(17)	C2S	C8S	1.442(15)
C21	C22	1.435(19)	C3S	C4S	1.411(15)
C21	C30	1.437(19)	C4S	C5S	1.401(15)
C22	C23	1.419(8)	C4S	C9S	1.502(14)
C22	C27	1.448(16)	C5S	C6S	1.425(16)
C23	C24	1.406(17)	C6S	C7S	1.524(18)

Table S8. Bond Angles.

Atom	Atom	Atom	Angle/°	Atom	Atom	Atom	Angle/°
C2	C1	C6	123.2(12)	C26	C25	C24	126.6(16)
C2	C1	C7	111.3(11)	C25	C26	C27	116.4(13)
C6	C1	C7	124.8(12)	C26	C27	C22	120.8(13)
C1	C2	C3	117.0(12)	C26	C27	C28	120.8(12)
C1	C2	C14	113.5(12)	C28	C27	C22	118.0(13)
C3	C2	C14	129.5(12)	C27	C28	Br1	119.5(11)
C2	C3	C4	118.5(12)	C29	C28	Br1	116.8(11)
C5	C4	C3	125.4(13)	C29	C28	C27	123.5(12)
C6	C5	C4	116.8(13)	C28	C29	C30	120.6(13)
C5	C6	C1	118.7(14)	C28	C29	C38	131.7(12)
C8	C7	C1	99.4(11)	C30	C29	C38	107.4(11)
C16	C7	C1	105.5(11)	C21	C30	C29	115.3(13)
C16	C7	C8	107.3(11)	C21	C30	C31	129.9(13)
C9	C8	C7	125.5(15)	C31	C30	C29	114.7(12)
C9	C8	C13	121.0(14)	C30	C31	C32	102.4(10)
C13	C8	C7	113.3(12)	C30	C31	C44	104.5(10)
C10	C9	C8	115.5(16)	C44	C31	C32	104.0(11)
C9	C10	C11	121.0(14)	C33	C32	C31	124.6(11)

C10	C11	C12	123.7(15)
C13	C12	C11	115.5(15)
C8	C13	C14	108.6(12)
C12	C13	C8	123.0(13)
C12	C13	C14	128.5(14)
C2	C14	C13	108.6(12)
C2	C14	C15	109.3(11)
C13	C14	C15	107.2(11)
C16	C15	C14	110.0(12)
C16	C15	C24	125.3(12)
C24	C15	C14	124.7(11)
C15	C16	C7	118.0(12)
C15	C16	C17	117.7(12)
C17	C16	C7	124.2(11)
C16	C17	Br2	118.5(10)
C18	C17	Br2	118.9(11)
C18	C17	C16	122.6(12)
C17	C18	C19	126.8(12)
C17	C18	C23	117.2(13)
C23	C18	C19	115.5(13)
C20	C19	C18	125.7(12)
C19	C20	C21	117.8(12)
C22	C21	C20	119.5(12)
C22	C21	C30	122.9(13)
C30	C21	C20	117.6(13)
C21	C22	C27	119.4(14)
C23	C22	C21	121.0(8)
C23	C22	C27	119.6(10)
C22	C23	C18	119.6(9)
C24	C23	C18	120.2(14)
C24	C23	C22	120.3(9)
C15	C24	C23	116.9(12)
C15	C24	C25	127.5(13)
C23	C24	C25	115.5(14)
C33	C32	C37	122.0(12)
C37	C32	C31	113.4(11)
C34	C33	C32	121.1(14)
C35	C34	C33	115.2(16)
C34	C35	C36	124.0(14)
C37	C36	C35	119.0(15)
C32	C37	C38	113.2(12)
C36	C37	C32	118.1(14)
C36	C37	C38	128.2(13)
C37	C38	C29	106.5(10)
C37	C38	C39	112.2(11)
C39	C38	C29	103.9(11)
C40	C39	C38	127.8(14)
C44	C39	C38	112.3(11)
C44	C39	C40	119.7(14)
C39	C40	C41	120.3(18)
C42	C41	C40	121.2(16)
C41	C42	C43	117.5(15)
C42	C43	C44	121.7(15)
C39	C44	C31	117.1(11)
C39	C44	C43	118.9(13)
C43	C44	C31	123.9(13)
C2S	C1S	C6S	114(2)
C1S	C2S	C3S	123.7(18)
C1S	C2S	C8S	113.7(14)
C3S	C2S	C8S	122.6(16)
C4S	C3S	C2S	122.3(15)
C3S	C4S	C9S	121.3(15)
C5S	C4S	C3S	114.9(13)
C5S	C4S	C9S	123.7(15)
C4S	C5S	C6S	121.3(16)
C1S	C6S	C5S	124(2)
C1S	C6S	C7S	112.8(17)
C5S	C6S	C7S	123(2)

Table S9. Torsion Angles.

A	B	C	D	Angle/°
Br1	C28	C29	C30	-179.2(8)
Br1	C28	C29	C38	-6(2)
Br2	C17	C18	C19	-6.7(18)
Br2	C17	C18	C23	-178.4(8)
C1	C2	C3	C4	5.0(18)
C1	C2	C14	C13	58.8(15)

C1	C2	C14	C15	-57.8(14)
C1	C7	C8	C9	-125.0(15)
C1	C7	C8	C13	60.0(15)
C1	C7	C16	C15	-53.5(14)
C1	C7	C16	C17	129.1(12)
C2	C1	C6	C5	4(2)
C2	C1	C7	C8	-60.9(14)
C2	C1	C7	C16	50.1(14)
C2	C3	C4	C5	-3(2)
C2	C14	C15	C16	56.2(13)
C2	C14	C15	C24	-123.7(14)
C3	C2	C14	C13	-120.8(16)
C3	C2	C14	C15	122.6(15)
C3	C4	C5	C6	2(3)
C4	C5	C6	C1	-2(3)
C6	C1	C2	C3	-5.5(19)
C6	C1	C2	C14	174.8(13)
C6	C1	C7	C8	128.4(14)
C6	C1	C7	C16	-120.6(14)
C7	C1	C2	C3	-176.5(12)
C7	C1	C2	C14	3.9(16)
C7	C1	C6	C5	173.8(15)
C7	C8	C9	C10	-177.1(15)
C7	C8	C13	C12	175.0(14)
C7	C8	C13	C14	-5.0(18)
C7	C16	C17	Br2	-3.6(17)
C7	C16	C17	C18	178.6(12)
C8	C7	C16	C15	51.8(15)
C8	C7	C16	C17	-125.5(13)
C8	C9	C10	C11	5(3)
C8	C13	C14	C2	-58.0(16)
C8	C13	C14	C15	60.0(15)
C9	C8	C13	C12	0(2)
C9	C8	C13	C14	179.8(14)
C9	C10	C11	C12	-6(3)
C10	C11	C12	C13	3(3)
C11	C12	C13	C8	0(2)
C11	C12	C13	C14	179.9(14)
C12	C13	C14	C2	122.1(16)
C12	C13	C14	C15	-120.0(17)
C13	C8	C9	C10	-2(2)
C13	C14	C15	C16	-61.3(14)
C13	C14	C15	C24	118.8(13)
C14	C2	C3	C4	-175.4(15)
C14	C15	C16	C7	2.7(15)

C14	C15	C16	C17	-179.7(10)
C14	C15	C24	C23	177.9(11)
C14	C15	C24	C25	-1(2)
C15	C16	C17	Br2	179.0(9)
C15	C16	C17	C18	1.2(19)
C15	C24	C25	C26	173.5(15)
C16	C7	C8	C9	125.4(15)
C16	C7	C8	C13	-49.5(16)
C16	C15	C24	C23	-2(2)
C16	C15	C24	C25	179.3(13)
C16	C17	C18	C19	171.0(12)
C16	C17	C18	C23	-0.7(19)
C17	C18	C19	C20	175.8(14)
C17	C18	C23	C22	179.9(9)
C17	C18	C23	C24	-1.2(19)
C18	C19	C20	C21	10(2)
C18	C23	C24	C15	2.4(19)
C18	C23	C24	C25	-178.7(11)
C19	C18	C23	C22	7.3(13)
C19	C18	C23	C24	-173.8(12)
C19	C20	C21	C22	-2.8(18)
C19	C20	C21	C30	176.7(12)
C20	C21	C22	C23	-1.5(15)
C20	C21	C22	C27	179.5(10)
C20	C21	C30	C29	-176.4(10)
C20	C21	C30	C31	-0.9(19)
C21	C22	C23	C18	-1.1(10)
C21	C22	C23	C24	180.0(16)
C21	C22	C27	C26	-174.6(12)
C21	C22	C27	C28	-1.4(18)
C21	C30	C31	C32	127.4(14)
C21	C30	C31	C44	-124.4(14)
C22	C21	C30	C29	3.0(18)
C22	C21	C30	C31	178.5(11)
C22	C23	C24	C15	-178.7(9)
C22	C23	C24	C25	0.2(15)
C22	C27	C28	Br1	-177.3(8)
C22	C27	C28	C29	-1(2)
C23	C18	C19	C20	-12.4(19)
C23	C22	C27	C26	6.4(14)
C23	C22	C27	C28	179.6(9)
C23	C24	C25	C26	-5(2)
C24	C15	C16	C7	-177.3(13)
C24	C15	C16	C17	0.2(19)
C24	C25	C26	C27	10(2)

C25 C26 C27 C22	-10.5(19)
C25 C26 C27 C28	176.5(13)
C26 C27 C28 Br1	-4.1(16)
C26 C27 C28 C29	172.3(13)
C27 C22 C23 C18	177.9(14)
C27 C22 C23 C24	-1.0(10)
C27 C28 C29 C30	4(2)
C27 C28 C29 C38	178.0(12)
C28 C29 C30 C21	-5.2(18)
C28 C29 C30 C31	178.6(11)
C28 C29 C38 C37	-116.1(16)
C28 C29 C38 C39	125.4(15)
C29 C30 C31 C32	-57.0(11)
C29 C30 C31 C44	51.2(13)
C29 C38 C39 C40	-123.7(15)
C29 C38 C39 C44	61.5(15)
C30 C21 C22 C23	179.1(9)
C30 C21 C22 C27	0.1(19)
C30 C29 C38 C37	58.2(13)
C30 C29 C38 C39	-60.3(12)
C30 C31 C32 C33	-120.9(15)
C30 C31 C32 C37	57.0(13)
C30 C31 C44 C39	-54.9(16)
C30 C31 C44 C43	124.3(15)
C31 C32 C33 C34	-176.0(14)
C31 C32 C37 C36	175.3(12)
C31 C32 C37 C38	2.3(16)
C32 C31 C44 C39	52.0(15)
C32 C31 C44 C43	-128.7(14)
C32 C33 C34 C35	-5(2)
C32 C37 C38 C29	-61.1(14)
C32 C37 C38 C39	51.9(16)
C33 C32 C37 C36	-7(2)
C33 C32 C37 C38	-179.8(14)
C33 C34 C35 C36	5(3)
C34 C35 C36 C37	-6(3)
C35 C36 C37 C32	6(2)
C35 C36 C37 C38	178.1(15)
C36 C37 C38 C29	126.8(15)
C36 C37 C38 C39	-120.2(16)
C37 C32 C33 C34	6(2)
C37 C38 C39 C40	121.6(16)
C37 C38 C39 C44	-53.2(17)
C38 C29 C30 C21	179.7(11)
C38 C29 C30 C31	3.5(14)

C38	C39	C40	C41	-179.1(16)
C38	C39	C44	C31	-3.0(18)
C38	C39	C44	C43	177.7(13)
C39	C40	C41	C42	8(3)
C40	C39	C44	C31	-178.2(12)
C40	C39	C44	C43	2(2)
C40	C41	C42	C43	-9(3)
C41	C42	C43	C44	7(2)
C42	C43	C44	C31	177.0(13)
C42	C43	C44	C39	-4(2)
C44	C31	C32	C33	130.6(15)
C44	C31	C32	C37	-51.5(13)
C44	C39	C40	C41	-5(2)
C1S	C2S	C3S	C4S	-2(2)
C2S	C1S	C6S	C5S	4(2)
C2S	C1S	C6S	C7S	179.1(19)
C2S	C3S	C4S	C5S	0.4(18)
C2S	C3S	C4S	C9S	-177.0(12)
C3S	C4S	C5S	C6S	3.3(17)
C4S	C5S	C6S	C1S	-5.8(19)
C4S	C5S	C6S	C7S	179.6(14)
C6S	C1S	C2S	C3S	0(2)
C6S	C1S	C2S	C8S	-179.5(10)
C8S	C2S	C3S	C4S	177.3(12)
C9S	C4S	C5S	C6S	-179.5(11)

Table S10. Hydrogen Atom Coordinates (Å×10^4^) and Isotropic Displacement Parameters (Å^2^×10^3^).

Atom	*x*	*y*	*z*	U(eq)
H3	5000	10470	3252	45
H4	3066	10929	1981	57
H5	3264	8851	1244	67
H6	5419	6075	1904	60
H7	8046	3911	3281	57
H9	11383	3312	2925	71
H10	13655	4162	3015	77
H11	13381	6135	3839	100
H12	10695	7770	4356	61
H14	7434	8226	4535	51
H19	6252	1123	6282	46
H20	5973	784	7849	41
H25	7054	8036	6044	68
H26	6015	8177	7475	52
H31	5330	677	9286	36

H33	8096	-1378	10542	59
H34	9811	-2006	11953	71
H35	9496	259	12534	65
H36	7241	2963	11926	56
H38	4823	4959	10624	42
H40	1591	5618	10876	77
H41	-874	5178	10588	91
H42	-540	2830	10111	80
H43	2050	1428	9476	72
H1S	11708	-1926	6340	148
H3S	12157	2510	5629	126
H5S	10380	1255	8116	127
H7SA	10301	-1516	8586	287
H7SB	11686	-2932	8157	287
H7SC	9706	-1955	7704	287
H8SA	12740	751	4577	129
H8SB	11590	-253	4658	129
H8SC	13580	-1189	5094	129
H9SA	11411	4460	6589	184

Table S11. Crystal data and structure refinement for 3• $C_6H_3(CH_3)_3$

$C_{44}H_{24}Br_2$, C_9H_{12} Chemical_formula_sum	C53 H36 Br
Chemical_formula_weight	832.64
Chemical_absolute_configuration	unk
Space_group_crystal_system	triclinic
Space_group_IT_number	1
Space_group_name	P 1
Space_group_symop_operation_xyz	1 'x, y, z'
Cell_length_a	8.3886(7)
Cell_length_b	9.0069(8)
Cell_length_c	14.5283(13)
Cell_angle_alpha	76.634(8)
Cell_angle_beta	89.729(7)

Cell_angle_gamma	64.661(8)
Cell_volume	959.66(14)
Cell_formula_units_Z	1
Cell_measurement_reflns_used	2053
Cell_measurement_temperature	295(2)
Cell_measurement_theta_max	25.6900
Cell_measurement_theta_min	2.5810
Exptl_absorpt_coefficient_mu	2.150
Exptl_absorpt_correction_T_max	1.00000
Exptl_absorpt_correction_T_min	0.74231
Exptl_absorpt_correction_type	multi-scan
Exptl_crystal_colour	light yellow
Exptl_crystal_colour_modifier	light
Exptl_crystal_colour_primary	yellow
Exptl_crystal_density_diffrn	1.441
Exptl_crystal_description	prism
Exptl_crystal_F_000	424
Crystallisation from 2,4,6-trimethylbenzene	
Exptl_crystal_size_max	0.25
Exptl_crystal_size_mid	0.2
Exptl_crystal_size_min	0.15

Table S12. Crystal data and structure refinement for 3• $C_6H_3(CH_3)_3$

Bond precision:	C-C = 0.0207 A	Wavelength=0.71070	
Cell:	a=8.3886(7)	b=9.0069(8)	c=14.5283(13)
alpha=76.634(8)	beta=89.729(7)	gamma=64.661(8)	
Temperature:	295 K		
	Calculated	Reported	
Volume	959.66(17)	959.66(14)	
Space group	P 1	P 1	
Hall group	P 1	P 1	
Moiety formula	C44 H24 Br2, C9 H12	C44 H24 Br2, C9 H12	
Sum formula	C53 H36 Br2	C53 H36 Br2	
Mr	832.62	832.64	
Dx,g cm-3	1.441	1.441	
Z	1	1	
Mu (mm-1)	2.150	2.150	
F000	424.0	424.0	
F000'	423.57		
h,k,lmax	10,11,18	10,11,18	
Nref	7864[3932]	5001	
Tmin,Tmax	0.603,0.724	0.742,1.000	
Tmin'	0.578		
Correction method= # Reported T Limits: Tmin=0.742 Tmax=1.000 AbsCorr = MULTI-SCAN			
Data completeness= 1.27/0.64	Theta(max)= 26.370		
R(reflections)= 0.0509(3714)	wR2(reflections)= 0.1536(5001)		
S = 1.006	Npar= 497		

CrysAlisPro, Agilent Technologies, Version 1.171.36.32 (release 02-08-2013 CrysAlis171 .NET) (compiled Aug 2 2013,16:46:58)

References

1 Clark, R. C.; Reid, J. S. *Acta Cryst*. **1995**, *A51*, 887-897
2 O. V. Dolomanov, L. J. Bourhis, R. J. Gildea, J. A. K. Howard and H. Puschmann, OLEX2: a complete structure solution, refinement and analysis program. J. Appl. Cryst. (2009). 42, 339-341.
3 olex2.solve (L.J. Bourhis, O.V. Dolomanov, R.J. Gildea, J.A.K. Howard, H. Puschmann, in preparation, 2011)
4 SHELXL, G.M. Sheldrick, Acta Cryst. (2008). A64, 112-122